Université de Montréal

Un criblage ciblant de nouveaux facteurs impliqués dans l'assemblage mitotique des chromosomes dans le nématode *C. elegans*

Par Rajesh Ranjan

Programmes de biologie moléculaire
Faculté de médecine

Thèse présentée à la Faculté de médecine en vue de l'obtention du grade de doctorat en biologie moléculaire option biologie des systèmes

Avril_2014

Résumé

La division cellulaire est un processus fondamental des êtres vivants. À chaque division cellulaire, le matériel génétique d'une cellule mère est dupliqué et ségrégé pour produire deux cellules filles identiques; un processus nommé la mitose. Tout d'abord, la cellule doit condenser le matériel génétique pour être en mesure de séparer mécaniquement et également le matériel génétique. Une erreur dans le niveau de compaction ou dans la dynamique de la mitose occasionne une transmission inégale du matériel génétique. Il est suggéré dans la littérature que ces phénomènes pourraient causé la transformation des cellules cancéreuses. Par contre, le mécanisme moléculaire générant la coordination des changements de haut niveau de la condensation des chromosomes est encore incompris.

Dans les dernières décennies, plusieurs approches expérimentales ont identifié quelques protéines conservées dans ce processus. Pour déterminer le rôle de ces facteurs dans la compaction des chromosomes, j'ai effectué un criblage par ARNi couplé à de l'imagerie à haute-résolution en temps réel chez l'embryon de *C. elegans*. Grâce à cette technique, j'ai découvert sept nouvelles protéines requises pour l'assemblage des chromosomes mitotiques, incluant la Ribonucléotide réductase (RNR) et Topoisomérase II (topo-II). Dans cette thèse, je décrirai le rôle structural de topo-II dans l'assemblage des chromosomes mitotiques et ces mécanismes moléculaires. Lors de la condensation des chromosomes, topo-II agit indépendamment comme un facteur d'assemblage local menant par la suite à la formation d'un axe de condensation tout au long du chromosome. Cette localisation est à l'opposé de la position des autres facteurs connus qui sont impliqués dans la condensation des chromosomes. Ceci représente un nouveau mécanisme pour l'assemblage des chromosomes chez *C. elegans*. De plus, j'ai découvert un rôle non-enzymatique à la protéine RNR lors de l'assemblage des chromosomes. Lors de ce processus, RNR est impliqué dans la stabilité des nucléosomes et alors, permet la

compaction de haut niveau de la chromatine. Dans cette thèse, je rapporte également des résultats préliminaires concernant d'autres nouveaux facteurs découverts lors du criblage ARNi. Le plus important est que mon analyse révèle que la déplétion des nouvelles protéines montre des phénotypes distincts, indiquant la fonction de celles-ci lors de l'assemblage des chromosomes. Somme toute, je conclus que les chromosomes en métaphase sont assemblés par trois protéines ayant des activités différentes d'échafaudage: topoisomérase II, les complexes condensines et les protéines centromériques. En conclusion, ces études prouvent le mécanisme moléculaire de certaines protéines qui contribuent à la formation des chromosomes mitotiques.

Mots clés - division cellulaire, condensation des chromosomes, Ribonucléotide réductase (RNR) et Topoisomérase II (topo-II).

Abstract

Cell division is a fundamental process that continuously happens in all living organisms. In each cell division, genetic material of the parent cell duplicates and segregates to produce genetically identical daughter cells in a process called mitosis. Cells need to condense their genetic material to be able to partition them equally. Any subtle defects, either timing or compaction level, could lead to the unequal inheritance of genetic material, a phenomenon that is believed to be the leading cause of cancerous transformation. However, the precise molecular mechanisms underlying the coordinated changes of higher-order chromosome structure are poorly understood.

In the last two decades, various approaches have identified several conserved factors required for chromosome condensation. To define the roles of known and novel factors in this process, I performed an RNAi based screen using high-resolution live imaging of the *C. elegans* one-cell embryo. Importantly, using an *in vivo* approach, I discovered seven novel factors required for mitotic chromosome assembly, including Ribonulceotide reducatase (RNR) and DNA topoisomerase II (topo-II). In this thesis, I report a structural role for topo-II in mitotic chromosome assembly and underlying molecular mechanisms. During chromosome condensation process, topo-II acts independently as a local assembly factor leading to global chromosome axis formation, contradicting models that chromosomes organize around preassembled scaffolds, thus representing a novel pathway for chromosome assembly in *C. elegans*. Furthermore, I also discovered a non-enzymatic role of RNR in the mitotic chromosome assembly process. During this process, RNR is involved in nucleosome stability, and thereby, it allows higher-order chromatin assembly. In this thesis, I also report preliminary data for other novel factors that I discovered in the RNAi based screen for factors involved in chromosome condensation. Importantly, my analyses revealed that the depletion of several proteins results in distinct chromosome

condensation phenotypes, indicating that they function in discrete events during mitotic chromosome assembly. In sum, I conclude that metaphase chromosomes are built by the distinct scaffolding activities of three proteins: DNA topoisomerase II, condensin complexes and centromere proteins. Taken together, these studies provide underlying molecular mechanisms contributing to the mitotic chromosome formation.

Key words – Cell division, Chromosome condensation, topoisomerase II (topo-II), ribonucleotide reductage (RNR).

Acknowledgment

I really do not know how to thank everyone who has assisted me along the way. I have worked with a number of people whose contributions in assorted ways to the research and the making of the thesis deserve special mention. It is a pleasure to convey my gratitude to all of them in my humble acknowledgment.

Words cannot adequately express my indebtedness and gratitude to my Ph.D. supervisor, Dr. Paul S. Maddox, with whom I started my scientific career. Throughout my Ph.D., he provided untiring encouragement, sound advices, liberty to think and execute experiments and excellent tips about scientific writing and presentation. I am especially thankful to him for constant encouragement, friendly attitude and motivating me to do excellent cutting edge research. Above all, as a person he is a great human being; always treated me as a family member. I always feel proud and grateful to be associated with you, Paul. I will cherish the Maddox lab culture throughout my life.

I would like to give a big thank to my Ph.D committee members Dr. Damien D'Amours, Dr. Alain Verreault, Dr. Alisa Piekny and Dr. Pascal Chartrand for giving me valuable and constructive comments on my projects. I express my sincere thanks to Dr. Amy S. Maddox and Dr. Jean-Claude Labbé for providing encouragement and giving invaluable suggestions. I thank to Vivianne Jodoin and Pascale Le Thérizien for providing all the assistance over the years.

I would like to thank all past and present members of the Maddox lab, at the UNC and at the UdeM, for many fruitful discussions on both scientific and non-scientific ideas over the years. A big thank to Joel, Jonas, Valerie, Abbas, Jayshree, Anne-Marie, Ben, Karine, Carlos, Anaick, Lily, Jack, Ines, Ian, Vincent, Abby, and Patrick for too many things that are too long to list here. Thanks to members from Labbé lab, Rana,

Alexia, Forum, Laura, Vincent, Nicolas, and Marianne for making light moments and sharing thought on different issues. Thanks to my friends, Rahul, Yogita, Dhanaraman, Roshan, Ramraj, Prabhash, Shashi, and Shuchi for all their love and support.

Thanks to Institut de recherche en immunologie et en cancérologie (IRIC) for hosting me during my Ph.D studies. Thanks to Département de pathologie et de biologie cellulaire, Université de Montréal, for providing Ph.D in molecular biology program. Thanks to the awards provided from the molecular biology program. I am very grateful for the international fee waiver award provided from the Université de Montréal. Thanks to the Canadian Institutes of Health Research (CIHR) for financial support for my project.

Last but not the least, I would like to express my deepest gratitude to my family, Dad and Mom for supporting me from far distance. The journey would not have been completed without the blessings of my loving Mom, Dad, brother, sister and all family members. Their unconditional love, support and motivation to pursue my higher studies helped me to reach this platform.

Thank you everyone….

Table of contents

List of Figures

List of Tables

List of abbreviations

2-AP	2-aminopurine
A.A	amino acids
ABCX	ABC (ATP-binding cassette) transporter
APC	Anaphase promoting complex
Asf1	Anti-silencing factor 1
ATP	adenosine triphosphate
ATPase	ATP-hydrolysis
BSA	Bovine serum albumin
CAF-1	chromatin assembly factor 1
CAP-D3	Chromosome associated protein D3
CAP-E	chromosome associated protein
CAP-H	chromosome associated protein H
CatC	Premitotic catenated plasmids
CatC$^{\#}$	Mitotic catenated plasmids
Cdc20	cell-division cycle protein 20
CENP-A	CENtromere Protein A
CIN-4	Chromosome Instability – 4
DAPI	4',6-diamidino-2-phenylindole
DNA	deoxyribonucleic acid
dNTP	deoxyribonucleotide
dsRNA	double stranded RNA
FACT	facilitate chromatin transcription
G2	Gap 2
GFP	green fluorescence protein
H2B	histone H2B
H3	histone H3

H4	histone H4
HU	hydroxyurea
ICRF-187	dexrazoxane
ICRF-193	bisdioxopiperazine
Kb	kilobase
kDa	kilodalton
kDNA	kinetoplast DNA
KIF4	chromosome-associated kinesin
MMS	methyl methane sulfonate
MUG	mitosis with an unreplicated genome
Nap1	nucleosome assembly protein 1
NASP	nuclear autoantigenic spern protein
NASP	nuclear envelope break down
PCC	prophase chromosome condensation
PCNA	proliferating cell nuclear antigen
PCR	polymerase chain reaction
RNA	ribonucleotide reductase
RNAi	RNA interference
RNR	ribonucleotide reductase
RPA-1	replication protein A-1
SAR	scaffold associated region
SC-I	scaffold protein I

SC-II	scaffold protein II
SDS-PAGE	sodium dodecyl sulfate-polyacrylamide gel electrophoresis
SEM	standard error of the mean
SMC	structure maintenance of chromosome
Topo-II	topoisomerase II
UV	ultra violet
VM-26	teniposide (Vumon)
VP-16	etoposide
WT	wild-type

Contribution of authors

Chapter I.2 - DNA Topoisomerase II scaffold function in mitotic chromosome assembly: an overview.

Rajesh Ranjan, Joel Ryan, and Paul S. Maddox.

PSM and RR designed and wrote the manuscript. RR and JR made the figures.

Chapter II - DNA Topoisomerase II acts in both structural and enzymatic capacities during mitotic chromosome assembly in *C. elegans.*

Rajesh Ranjan, Jonas F. Dorn, Amy S. Maddox, and Paul S. Maddox.

PSM and RR designed the project. RR carried out all the experiments and prepared all the figures and movies as shown in the manuscript, except, JFD generated a computational simulation of chromosome condensation, and prepared simulation figures and movies. PSM and RR prepared the manuscript, and ASM and JFD oversaw the manuscript.

Chapter III - Ribonucleotide reductase is involved in nucleosome stability.

Rajesh Ranjan, and Paul S. Maddox. The manuscript is in preparation.

PSM and RR designed the project. RR carried out all the experiments and prepared all the figures and movies as shown in the manuscript. PSM and RR prepared the manuscript.

Supplementary Chapter I - A candidate screen for novel factors involved in mitotic chromosome assembly in *C. elegans.*

PSM and RR designed the screen. RR carried out all the experiments and prepared all the figures as shown in the chapter.

Dedicated to my father and late mother

Chapter I

Introduction

I.1 Mitotic chromosome condensation: an overview

I.1.1 Abstract

One of the most visually dynamic processes in cell biology is the dramatic reorganization of interphase chromatin to form cytologically distinct X-shaped structures known as mitotic chromosomes; this process is often referred to as mitotic chromosome condensation. Upon entry into mitosis, chromosomes undergo dynamic conformational changes. These conformational changes are critical to ensure the faithful segregation of sister chromatids in anaphase (Swedlow and Hirano, 2003). Mechanistically, two fundamental processes must operate in order to separate sister chromatids faithfully. First, protein-mediated compaction of the DNA must occur (i.e., condensation), as well as the complete removal of sister DNA entanglement generated during DNA replication (i.e., decatenation). These two processes must be coordinated as supported by evidence from both prokaryotes and eukaryotes (Baxter et al., 2011; Charbin et al., 2014; Hayama et al., 2013; Hayama and Marians, 2010; Hirano, 2010; Li et al., 2010). Independent investigations have co-discovered many proteins involved in mitotic chromosome compaction. Here, I discuss how these factors coordinate to form mitotic chromosomes during the cell cycle.

I.1.2 Introduction

Chromosomes have been characterized as inheritable genetic material that duplicates and segregates into daughter cells in each cell division. In order to segregate faithfully, chromatin, a complex of DNA and proteins, must condense over a thousand fold in each mitotic division. Walter Flemming first described chromosomes with drawings of mitosis in his watershed comprehensive book “Zellsubstanze, Kern und Zelltheilung” in 1882. Based on his observations, he drew chromosomes, centromeres and the spindle during mitosis, with accuracy similar to what we observe today with modern technology (Paweletz, 2001). While we have known about chromosomes for over 100 years, our molecular understanding of mechanisms regulating chromosome assembly is poor.

During the 1970s, the discovery of histones as a part of a chromosome-building unit was the first step in understanding the molecular basis of chromosome assembly. Electron microscopy of thin sections of metaphase chromosomes revealed that the chromosomes are composed of knobby fibers of about 20-30nm in diameter (DuPraw, 1970; Ris, 1975). Another study showed that the core histones contribute to the short-range organization of the DNA helix in chromatin; with a repeating structural unit called the nucleosome (Kornberg, 1974; Kornberg and Thomas, 1974; Oudet et al., 1975). Nucleosomes form bead-like structures, that can be observed under electron microscopy as thin “beads on a string” fibers with a diameter of about ~10-11nm (Olins and Olins, 1974) (Woodcock, 1973). Later, many models have been proposed based on the folding and coiling of chromatin fibers, such as how beads on a string could form into a solenoidal structure (Finch and Klug, 1976), or could form “super bead” with units consisting of 6-10 nucleosome clusters (Hozier et al., 1977). These studies and observations were critical to understanding the role of histones in chromatin organization in higher order structures (Hizume et al., 2005; Kepert et al., 2005; Robinson and Rhodes, 2006).

Considerable progress has been made in the last five decades in understanding mitotic chromosome condensation with the discovery of several chromatin

organization factors; such as histones (Akey and Luger, 2003; Robinson and Rhodes, 2006; Schalch et al., 2005), the condensin complex (Hirano and Mitchison, 1994; Thadani et al., 2012) (2012), the cohesin complex (Haering et al., 2008; Nasmyth, 2011), topoisomerase II (Depew et al., 1978; Earnshaw and Heck, 1985; Wang, 1971), Kif-4 (Samejima et al., 2012), and centromere proteins (Maddox et al., 2007; Maddox et al., 2006).

Mechanistically, metaphase chromosome formation would involves at least two different processes: axial compaction and lateral compaction of the sister chromatids. A shorter and thicker chromatid would be generated with axial compaction whereas lateral compaction would generate longer and thinner chromatids. Here, I discuss how known condensation factors coordinate for faithful chromosome assembly during each cell division.

I.1.3 Known chromosome condensation factors

Multiple approaches, including biochemistry, genetics and microscopy, have been used to advance our understanding of chromosome formation in mitosis and the factors involved. These proteins function independently, in space and time, in a coordinated fashion, and play a major role in chromosome formation.

I.1.3.1 Histones

Histones are the most abundant chromosomal proteins that package DNA into structural units. They are evolutionarily highly conserved proteins and play a pivotal role in the maintenance of genome integrity and chromosome condensation through mitosis. Two copies of each of the four core histone molecules (H2A, H2B, H3 and H4) form an octameric complex called the nucleosome, on which 147 base pair of helical DNA wraps (Kornberg, 1974; Kornberg and Thomas, 1974; Oudet et al., 1975) (Figure I.1.1).

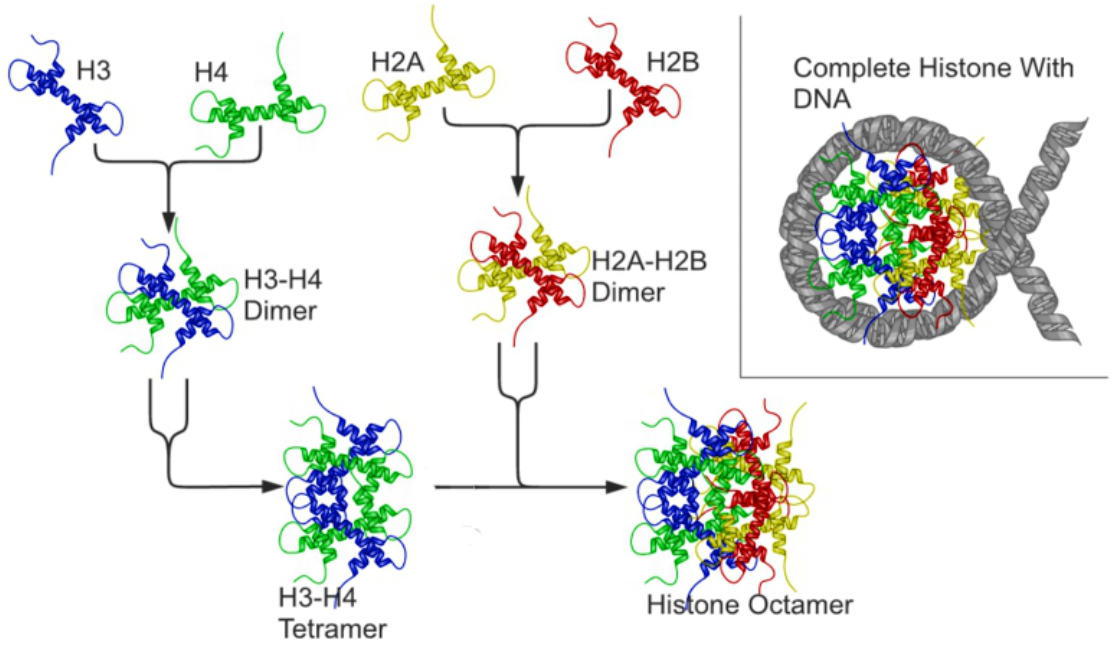

Figure I.1.1 – Nucleosome assembly. Nucleosome composed of two copies of each of the core histones H2A, H2B, H3 and H4. A histone $(H3\text{-}H4)_2$ tetramer and two histone H2A-H2B dimers assemble to form a histone octamer. Around 147 base pairs of DNA wrapped around a histone octamer to form "nucleosome." Adapted from wikipedia.org.

Without histones, unwrapped DNA fibers would be too long to fit into the nucleus. For instance, in each human cell, the combined DNA fiber length is about 2m, but it reduced to 90μm when wrapped on histone octamers (Redon et al., 2002). Nucleosomes function as the building units of chromosomes. Additionally, histone H1, known as the "linker histone," which is not part of the nucleosome, binds to nucleosomes and linker DNA regions to stabilize a higher order structure, known as the 30nm fiber (Hizume et al., 2005; Kepert et al., 2005; Robinson and Rhodes, 2006). However, this 30nm structure has never been observed in cellular conditions.

I.1.3.2 Condensins

Scaffold protein (Sc-II) was identified in a biochemical assay and it was found to be abundant in the chromosome scaffold (Lewis and Laemmli, 1982). Later, Sc-II was identified as SMC-4, a condensin core subunit (Earnshaw et al., 1985; Gasser et al., 1986; Hirano and Mitchison, 1994; Saitoh et al., 1994). Condensin is an evolutionarily conserved multi-protein complex that plays an important role in the structural maintenance of chromosomes and genome integrity through mitosis. The condensin complex was found to be a major non-histone pentameric protein complex required for chromosome condensation. Loss of condensin or mutation results in massive chromatin disorganization in mitosis. Condensin consists of two SMC (Structural Maintenance of Chromosomes) family subunits, SMC-2 and SMC-4, and three non-SMC subunits. SMC-2 and SMC-4 subunits have ATPase activity that regulates opening and closing of the ring in an ATP-hydrolysis dependent manner (Hirano and Mitchison, 1994; Thadani et al., 2012) (Figure I.1.2).

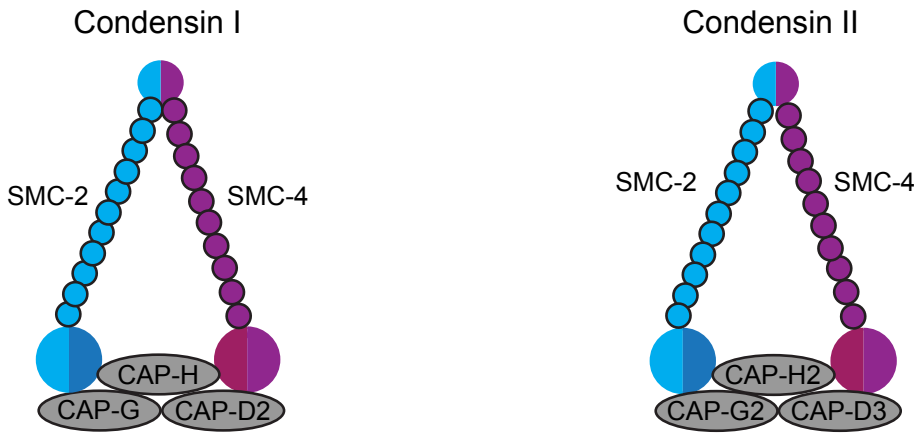

Figure I.1.2 – Eukaryotic condensin complexes. Each condensin complex is composed of SMC-2 and SMC-4 dimer and three non-SMC subunits. Condensin I and II differ from each other by their non-SMC subunits.

Condensin forms a scaffold axis, which is defined as a linear protein structure on metaphase chromosomes. It exists in two forms in higher eukaryotes, condensin I and II, which differ in their localization and protein components. Condensin II is nuclear, whereas condensin I is cytoplasmic and only localizes at the chromosomes after nuclear envelope break down (NEBD) (Gerlich et al., 2006; Hirota et al., 2004; Ono et al., 2004). Biochemical and microscopic analyses showed that the condensin complex forms a ring structure (Anderson et al., 2002) that entraps DNA strands and holds them together (Cuylen et al., 2011). Recently, it has been shown that condensin II is required for primary chromatin organization during S phase and for sister chromatid resolution, (Ono et al., 2013). Additionally, it plays a role in the lateral and axial compaction of chromosomes (Samejima et al., 2012; Shintomi and Hirano, 2011).

I.1.3.3. DNA Topoisomerases

DNA Topoisomerase was discovered in the 1970s in *E. coli* as a protein capable of introducing transient breaks in DNA strands (Liu et al., 1976; Wang, 1971). DNA topoisomerase is an evolutionarily conserved protein that plays a critical role in chromatin organization and genome integrity throughout mitosis. DNA Topoisomerases are divided into two classes, type I and II, based on the number of strands cut in one round of action. Type I topoisomerase cuts one strand of DNA, whereas Type II topoisomerase cuts both strands of DNA and reseals them. Both types of topoisomerase could release DNA stress and tension across the nucleus. However, type II Topoisomerase could decatenate sister chromatid catenanes, generated with very high frequency in S-phase (Figure I.1.3).

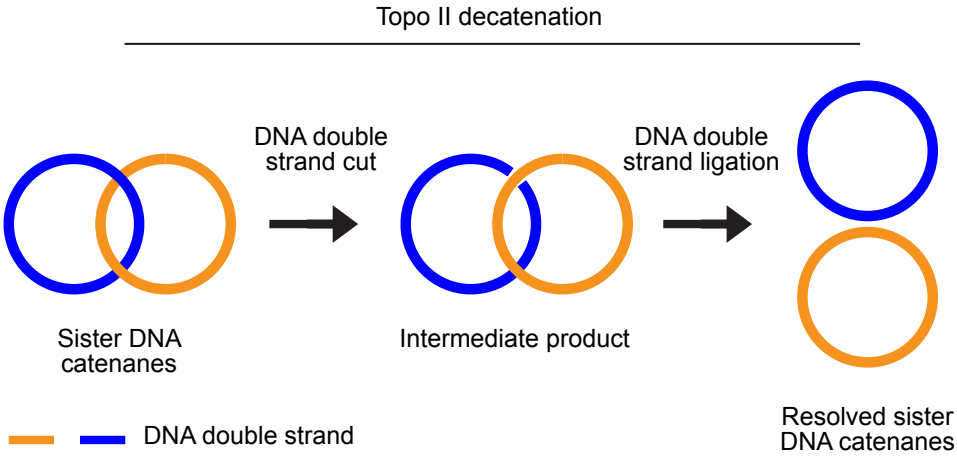

Figure I.1.3 – Topoisomerase II enzymatic function. Schematic diagram shows sister DNA catenanes, DNA replication results in sister DNA catenanes with high frequency, generated during S phase. Sister DNA catenanes resolution is essentially required for faithful chromosome segregation in anaphase. Topo-II enzymatic activity cuts both the strands of one DNA molecule, passes other DNA through it and then reseals it. This decatenates sister DNA catenanes in order to resolve them.

Therefore, topo-II is required for primary chromatin organization, for chromosome condensation in mitosis and faithful chromosome segregation in anaphase. Also, Topo-II plays important roles in various cellular process such as replication, transcription and recombination with its catalytic capacity (Wang, 2002).

I.1.3.4 Kinesins

Kinesins are molecular motors that generate microtubule-based forces for various cellular processes. The chromokinesins are a type of kinesin that act in chromosome condensation (Mazumdar et al., 2004), metaphase alignment (Levesque and Compton, 2001; Theurkauf and Hawley, 1992), chromosome segregation (Kwon et al., 2004) and cytokinesis (Kurasawa et al., 2004; Mazumdar et al., 2004). The chromokinesin family is divided into two distinct subfamilies; kinesin-4 and kinesin-10. In humans, Kinesin-4 has two different genes, KIF4A and KIF4B (Ha et al., 2000; Oh et al., 2000). KIF4A is a highly conserved dimeric plus-end directed microtubule based motor. Human KIF4 has several conserved motifs including an N-terminal motor domain, a central coiled coil region, a nuclear localization signal, a DNA binding motif and a cysteine rich Zn finger motif. In contrast to other kinesins, chromokinesins contain a nuclear localization signal, and are nuclear during interphase, but relocates during mitosis to mitotic structures, such as chromosome axes, the spindle, spindle midzone, and midbody (Antonio et al., 2000; Lee and Kim, 2003; Sekine et al., 1994; Vernos and Karsenti, 1996; Wang and Adler, 1995; Zhang et al., 1990). Antibody staining shows that it associates along the entire arms of condensed chromosomes during mitosis. Cells lacking KIF4 frequently exhibit lagging chromosomes, defective cytokinesis, and cleavage furrow defects.

I.1.4 Mitotic chromosome condensation: functional interplay among the factors

I.1.4.1 Functional interplay between condensin I and II in mitotic chromosomes condensation

Most eukaryotes have two condensin complexes, condensin I and II; Condensin II is nuclear and bound to chromatin during interphase, whereas condensin I is cytoplasmic and has access to chromatin after nuclear envelope break down (Gerlich et al., 2006; Hirota et al., 2004; Ono et al., 2004). Notably, some species, including yeast, possess only condensin I, which is nuclear during interphase (Hirano, 2005). Condensins have been known for two decades, but distinct roles of condensin I and II have remained elusive (Hirano and Mitchison, 1994). Therefore, to decipher relative roles of condensin I and II in mitotic chromosome assembly, Green et al. created a chicken DT40 conditional knockouts for the condensin I-specific subunit CAP-H and condensin II-specific subunit CAP-D3. To understand how mitotic chromosomes are affected by depletion of condensin I and II, they immunostained chromosome spreads of both CAP-$H^{ON/OFF}$ (condensin $I^{ON/OFF}$) and CAP-$D3^{ON/OFF}$ (condensin $II^{ON/OFF}$) cells with antibodies recognizing the scaffold protein KIF4A (Green et al., 2012). Results revealed distinct chromosome morphologies; chromosomes become short with CAP-H^{OFF} (condensin I^{OFF}), whereas chromosomes were long with CAP-$D3^{OFF}$ (condensin II^{OFF}). These morphologies are broadly consistent with previous chromosome spread in vertebrates (Abe et al., 2011; Ono et al., 2003) and *in vitro* analysis on assembled chromosomes using Xenopus egg extracts (Shintomi and Hirano, 2011).

To understand the nature of the morphological defect more closely, they used 3D structured illumination microscopy (SIM), a technique that generates significantly high-resolution images (Green et al., 2012). Results showed that CAP-H^{OFF} chromosomes displayed a wider and shorter KIF4A signal than that of untreated cells. Strikingly, KIF4A signal appeared to join together and crossover from one chromatid to another along the axis in CAP-$D3^{OFF}$, which is due to twisting and bending of chromatid pairs as a result of CAP-D3 depletion. This result suggests that the key role

of condensin II is to keep the chromatid axes straight and distinct.

Previous studies estimated the relative ratios of condensin I and II to be 5:1 in Xenopus egg extracts (Shintomi and Hirano, 2011), 1:1 in nuclear extracts from HeLa cells (Ono et al., 2003), and 10:1 in chicken DT40 cells on condensed chromosomes (Green et al., 2012). To evaluate how the relative abundance of condensin I and II might contribute to the assembly of mitotic chromosomes, Shintomi et al. developed protocols in which their levels are precisely changed in the cell-free system derived from Xenopus egg extracts to recapitulate cell cycle regulated chromosomal events. In this assay, sperm chromatin was induced to replicate by incubating with an interphase extract, and converted into metaphase chromosomes by adding a nondegradable Xenopus cyclin B. To investigate chromosome shape, chromatin was isolated at various time points after cyclin B addition and analyzed by immunofluorescence with the condensin I and II specific antibodies. Immunostaining showed that condensin I and II formed axis-like structures within each chromatid, however, condensin I was more continuous and robust than condensin II. To evaluate the role of condensin I and II in metaphase chromosome assembly; immunodepletion experiments were conducted in the Xenopus system. When both condensin I and II were depleted, unorganized masses of chromatin formed and individual chromosomes did not appear. Slightly ordered masses of chromatin formed when condensin I was depleted. In striking contrast, an extract depleted of condensin II produced individual chromosomes (Shintomi and Hirano, 2011). Therefore, the functional contribution of condensin II is much smaller than that of condensin I in this cell-free system, unlike HeLa cells where the functional contribution of condensin I is smaller (Ono et al., 2003). The relative ratio of condensin I and II, 5:1 (Xenopus egg extracts) to 1:1 (nuclear extract of HeLa cells), explains the differential contribution of condensin I and II to chromosome condensation.

Therefore, to test what would happen if the ratio of condensin I to II in the egg extracts were changed; egg extracts with different relative ratios were used (Shintomi and Hirano, 2011). Chromosomes assembled in the 1:1 extract were shorter than

chromosomes assembled in the 5:1 extract. Quantitative analysis showed that the average lengths of the chromosomes assembled the 5:1 and 1:1 extracts were 13.3 ± 4.9 mm and 9.3 ± 3.3 mm (± standard deviation), respectively. The width of the chromosomes assembled in the 1:1 extract was greater than that of the 5:1 extract. However, one could argue that thick and short chromosomes are because of reduced absolute levels of condensin I in the 1:1 extract rather than the relative ratio of condensin I and II. To test this possibility, another extract was prepared with reduced absolute levels of both condensin I and II to 20% of the original level, keeping their relative ratio at 5:1. Results revealed that chromosomes assembled similar to those assembled in the original 5:1 extract. In sum, these results demonstrated that the relative ratio of condensin I to II is one of the critical determinants in shaping metaphase chromosomes.

To test the effect of different levels of condensin I on chromosome morphology in the absence of condensin II; condensin II was depleted from the 5:1 and 1:1 egg extracts (Shintomi and Hirano, 2011). Results revealed little difference in the chromosome length when condensin II was depleted (the 5:0 extract, 13.1 ± 4.6mm) from the standard extract (the 5:1 extract, 13.3 ± 4.7mm). However, in contrast, the length of assembled chromosomes were similar to control (11.0 ± 3.4 mm). When condensin II was depleted from the 1:1 extract in which short chromosomes were assembled (8.6 ± 2.9 mm). In sum, these results suggest that condensin II contributes to the axial compaction of the chromosomes, which is the shortening of chromosome length. The action of condensin II remains rather cryptic when the action of condensin I is predominant under normal conditions. This is consistent with previous observations, where Lai et al. showed that cleavage of a condensin I resulted in short and thick chromosome formation in metaphase-arrested cells (Lai et al., 2011).

To know whether there is a functional interaction between condensin I and II; a single-chromatid assembly assay was conducted (Shintomi and Hirano, 2011). To produce single chromatids, without DNA replication, sperm chromatin was incubated with metaphase-arrested egg extracts. Unexpectedly, a far larger amount of

condensin II loaded on to the single-chromatids compared to replicated chromatids, whereas the amount of condensin I was comparable on the both types of chromosomes. Surprisingly, no individual chromatids assembled in the 1:1 extract, rather, masses of entangled chromatin formed (table I.1). Interestingly, when condensin II was depleted from the 1:1 extract the phenotype was partially rescued and individual chromatids formed (table I.1).

***Xenopus* egg extract (condensin I : II)**	**Chromosome condensation phenotype**	**Immunostaining with anti-condensin I and II antibodies**
5 : 1 (control)	Chromosomes condensed and chromatids formed	Condensin I and II stain chromosomes
0 : 1	Mass of entangled chromatin forms and no chromatids formed	Condensin II stains chromosomes
0 : 0	Mass of entangled chromatin forms and no chromatids formed	Condensin I and II do not stain chromosomes
1 : 1	Mass of entangled chromatin forms and no chromatids formed	Condensin I and II stain chromosomes
1 : 0	Phenotype partially rescued and chromatids formed	Condensin I stains chromosomes

Table I.1 – Functional interaction between condensin I and II (Shintomi and Hirano, 2011).

These observations suggest that the functional balance between the two condensins in the 1:1 extract shifted towards condensin II, and as a consequence, the action of condensin I was compromised. Whereas, balance was restored towards condensin I

when condensin II was depleted from the 1:1 extract, thereby partially rescuing the phenotype (table 1). These results suggest that, the functional balance between the two condensins is critical for chromosome individualization and mitotic chromosome assembly.

In sum, Shintomi et al. showed that the primary actions of condensin I and II are distinct; condensin I mediates lateral compaction, while, condensin II mediates axial shortening of mitotic chromosomes.

I.1.4.2 Functional interplay among condensin, topo-II, and KIF4 in mitotic chromosome condensation

Earlier studies showed that KIF-4 and condensin physically interact (Geiman et al., 2004; Mazumdar et al., 2004), and it has been hypothesized that KIF-4 acts as a spacer for the condensin complex (Mazumdar and Misteli, 2005). Other studies in prokaryotic systems showed that condensin physically interacts with topo-II (Hayama et al., 2013; Hayama and Marians, 2010; Li et al., 2010). Therefore, interdependency of chromosomal localization of KIF-4, condensin, and topo-II has been quantified. GFP-KIF4 is localized on chromatid axes in control cells; however, the chromosomal signal is strongly reduced after SMC2 depletion. In KIF-4 depleted cell SMC4-GFP signal is reduced by 56% on chromatid axes and 32% at the kinetochore. The kinetochore is a large protein complex assembled on chromatids where spindle fibers attach during cell division. Total condensin I localization is reduced along the chromatid axes, however, in contrast, condensin II localization is much less affected by KIF4 depletion. It has been observed that KIF4 is required for SMC2 localization on the chromatid axes (Mazumdar et al., 2004; Samejima et al., 2012). Whereas, in contrast, KIF4 localization is strongly reduced on the chromosomes in $SMC4^{OFF}$ cells, and the remaining protein is diffused.

Immunoprecipitation with anti-KIF4 antibody from nuclear extracts (MRC-5 or HeLa cells) specifically pulled down condensin subunits hCAP-E, -G, and –G2 (Hudson et al., 2003; Samejima et al., 2012). Immunofluorescence showed that hKIF4A partially colocalized with the condensin I and II subunits hCAP-E, -G and -G2. Chromosomes lacked the axial localization of hCAP-E, -G and –G2 in KIF4A RNAi treated cells and appeared diffusely distributed. Topo-II localization was diffused and only faintly detectable on chromosomes in $SMC2^{OFF}$ cells (Hudson et al., 2003; Samejima et al., 2012), however, its localization was normal on chromosomes in KIF4 depleted cells. KIF4 and SMC2 localization were normally located on chromosomes after topo-II depletion. These results suggest that KIF4 and topo-II localization on the chromatid axes are SMC2 dependent.

Quantitative mass spectrometry analysis of chromosomes also revealed that condensin I was significantly decreased in KIF4 depletion; however, condensin II subunits were less affected. KIF4 and condensin have been shown to interact physically (Geiman et al., 2004; Mazumdar et al., 2004). In reciprocal experiments, KIF4 was strongly affected after SMC2 depletion. In contrast, it has been observed that topo-II was little affected in the KIF4 or SMC4 depleted cells.

KIF4 depletion induces hypercondensation of chromosome leading to shorter and wider chromosomes. $KIF4^{ON/OFF}$ cells were also used to measure chromosome dimension and analysis showed that $KIF4^{OFF}$ chromosomes were shorter and slightly wider than $KIF4^{ON}$ chromosomes. Quantitative analysis showed that the average length of control chromosomes were 4.88μm and their average width was 0.68μm, whereas, in contrast, chromosomes were on average 3μm long and 1.2μm wide in KIF4 depleted cells. KIF4 depleted chromosomes resembled those depleted of condensin I rather than condensin II (Green et al., 2012). These results suggested that KIF4 is required for structural integrity of the mitotic chromosome and provides proper chromosome architecture.

Chromosomes adopt a characteristic morphology, short and thick, if cells are arrested in mitosis with colcemid for prolonged periods of time. In topo-II depleted cells,

chromosomes were longer and thinner than non-treated cell (Sakaguchi and Kikuchi, 2004; Samejima et al., 2012; Spence et al., 2007). Surprisingly, the chromatids did not shorten further if topo-II depleted cells were arrested for prolonged periods in mitosis with colcemid. This clearly demonstrates that topo-II has a specific function in axial compaction of mitotic chromosomes.

Chromosomes doubly depleted of KIF4 and SMC2 yielded more severe phenotypes than that seen with either single depletion; chromosomes were highly disorganized (Samejima et al., 2012). Interestingly, double depletion of either of KIF4 and topo-II or SMC2 and topo-II partially or completely rescued chromosome morphology defects seen with the single depletions. Chromosomes doubly depleted of topo-II and KIF4 were indistinguishable from wild type. Similarly, chromosomes from SMC2 and topo-II depleted cells were significantly less expanded with sharper outlines than chromosomes of only SMC2 depleted.

Unexpectedly, a striking result was observed with chromosomes triply depleted of topo-II, KIF4 and SMC2 from DT40 cells. Although the double depletion of KIF4 and SMC2 resulted in complete loss of mitotic chromosome morphology, however, additional depletion of topo-II substantially rescued chromosome morphology. Triply depleted chromosomes appeared to be more compact and had more defined outlines than chromosomes doubly depleted of KIF4 and SMC2 (Samejima et al., 2012).

In sum, these results suggest that KIF4 and SMC2 function in parallel, whereas topo-II acts in an opposing manner to condensin (SMC-2). This is consistent with a previous study that showed topo-II and condensin have opposite functions in regulating centromeric chromatin (Ribeiro et al., 2009; Spence et al., 2007).

I.1.4.3 Functional Interplay among the mitotic spindles, condensin, and topo-II in mitotic chromosome condensation.

Topo-II is a catalytic enzyme, which is required to remove DNA catenation before DNA segregation in anaphase. It has been shown that topo-II efficiently removes DNA positive supercoiling (Baxter et al., 2011). Many factors have been shown to induce positive supercoiling in DNA such as condensin, the mitotic spindle force and kif-4, however, the underlying molecular mechanism is poorly understood (Baxter et al., 2011; Hayama and Marians, 2010; Hirano, 2010; Li et al., 2010).

The mitotic spindle-kinetochore attachment has been shown to be required to complete sister chromatid decatenation generated during DNA replication (Holm et al., 1985). It has been proposed in prokaryotes that decatenation is promoted by supercoiling, suggesting that DNA topology could be a driving force for decatenation (Hardy et al., 2004; Martinez-Robles et al., 2009; Zechiedrich et al., 1997). To test this in eukaryotes, Baxter et al. have done an *in vivo* analysis with circular plasmids in yeast that have topological information (Baxter et al., 2011). These small plasmids contain yeast-origins of replication and centromeric sequences and their segregation behavior mimics that of endogenous chromosomes.

Replication in the absence of topo-II converted the plasmids into a concatenated plasmid dimer, and both were negatively supercoiled. Concatenated plasmids were in the premitotic form (CatC) and mitotic form ($CatC^{\#}$). The CatC to $CatC^{\#}$ transition occured in cells arrested in metaphase by depleting the APC activator Cdc20. In contrast, the CatC to $CatC^{\#}$ transition did not occur in cells arrested in metaphase with nocodazole, a microtubule depolymerizing drug (Baxter et al., 2011). These results suggest that CatC to $CatC^{\#}$ transition occurs before anaphase onset and mitotic spindle-kinetochore attachments are required.

To analyze the effect of the spindle on the supercoiling of plasmids, they were isolated from nocodazole treated cells (without spindle) and from nocodazole wash-off cells (with spindle). Results revealed that spindle formation shifted the distribution of supercoiling from a negative state to more positive state (Baxter et al., 2011). Therefore, a potent positive supercoiling activity is induced on plasmids during mitosis.

It has been observed that kinetochore-mitotic spindle attachment is required to complete topo-II mediated sister chromatid decatenation during mitosis, one reason behind this could be the positive supercoiling induced by mitotic spindle force (Holm et al., 1985; Uemura et al., 1987). Also, in prokaryotes, it has been observed that intrachromosomal supercoiling induces decatenation (Hardy et al., 2004; Martinez-Robles et al., 2009; Zechiedrich et al., 1997). Therefore, it could be possible that mitotic positive supercoiling is a prerequisite for topo-II mediated decatenation. Baxter et al. tested this hypothesis; using purified recombinant topoisomerase II. Their analysis revealed that negatively supercoiled plasmids required relatively high enzyme concentration (>20 units), whereas positively supercoiled plasmids required low topo-II concentration (one order of magnitude) to resolve catenanes completely.

Studies also showed that condensin (smc2), similar to mitotic spindle force, is required for the positive supercoiling of decatenated plasmids (Hirano et al., 2001; Hirano and Hirano, 2002). Formation of the mitotic spindle generates a high level of positive supercoiling in monomer plasmids in topo-II mutant strain with wild-type Smc2. However, in contrast, positive supercoiling was not observed once Smc2 function was inhibited (Baxter et al., 2011). These results show Smc2 function to generate positive supercoiling.

Prokaryotes also contain a condensin homolog, MukB-D, which function as a homodimer and shares five domains common to all SMC family members of eukaryotes (Cobbe and Heck, 2004; Hirano, 1999; Niki et al., 1991; Anderson et al., 2002; Haering et al., 2002; Hirano et al., 2001; Hirano and Hirano, 2002; Hirano and Mitchison, 1994; Hopfner et al., 2002; Melby et al., 1998; Niki et al., 1992; Yoshimura et al., 2002). It has been shown, using pull down experiments and mass spectrometry, that ParC, one of the two subunits of bacterial type II topoisomerase, is a binding partner of Muk B-D (Cristea et al., 2005; Li et al., 2010; Corbett and Berger, 2004; Levine et al., 1998).

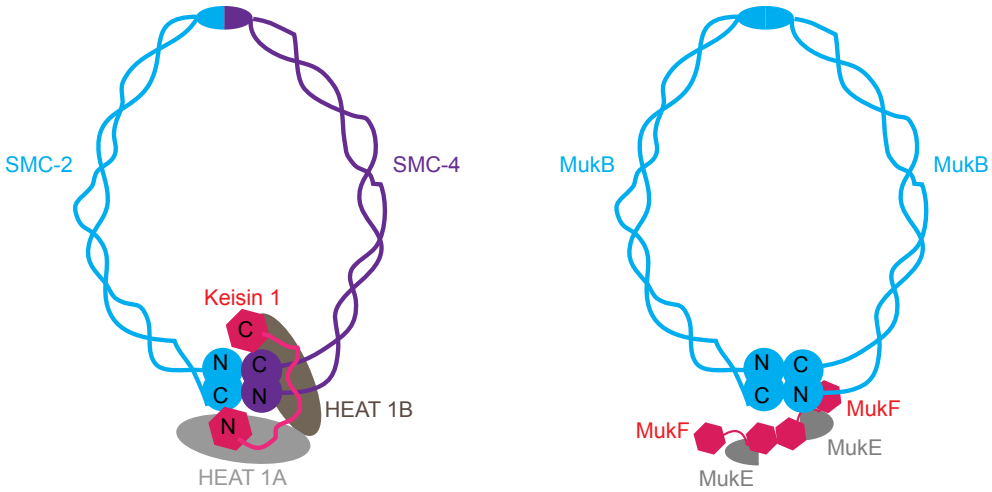

Figure I.1.4 – Molecular architecture of eukaryotic and prokaryotic condensins. The eukaryotic (left) and prokaryotic (right) condensins are composed of core SMC dimer, SMC2-SMC-4 and MukB-MukB (SMC-like) ATPases, respectively. In both, core subunits dimerization form hinge at one end and catalytic head domain at the other. The core dimers are closed into the rings by non-SMC subunits.

To test the effect of MukB on the activity of *E. coli* topo-II, DNA relaxation and decatenation assays were performed. Results revealed that the fraction of topoisomers increased with increasing concentrations of MukB at constant topo-II concentration. This showed that MukB functions in a dose dependent manner to the relaxation activity of topo-II (Englund, 1978; Miller et al., 1981). These results suggest that the functional interaction of topo-II and condensin is conserved.

In sum, condensin and mitotic spindles forces generate extensive positive supercoils in chromatin, which topo-II decatenates efficiently.

I.1.5 Discussion

In the last two decades, many factors have been shown to be involved in mitotic chromosome assembly. These factors have been shown to function independently, in

time and space, but also in a coordinated manner to make it feasible to assemble mitotic chromosome faithfully.

The two condensin complexes play distinct roles in mitotic chromosome structure in which the primary actions of condensin I and II are to provide lateral compaction and axial shortening, respectively, and that their intricate balance acts as one of the critical determinants in shaping mitotic chromosomes. Also, condensin II alone can provide mitotic chromosome rigidity, whereas condensin I is not able to do so.

Topo-II is essential for axial compaction of chromosomes and acts independently and in opposition to both KIF4 and condensin. KIF4 and condensin independently and additively contribute to the lateral compaction of chromosomes, whereas topo-II decatenates sister chromatids catenanes and the loops in steps required for the axial compaction of chromosomes.

Condensin and mitotic spindle force generate a topology, positive supercoiling, on catenated chromosomes that maximize topoisomerase II decatenation activity. Once the sister chromatids are fully decatenated, topoisomerase II rapidly relaxes the positive supercoiling and allows for higher order chromatin organization.

Still, the mechanism of mitotic chromosome assembly at the molecular level remains elusive, and requires further study. The development of technologies, such as super-resolution microscopy and genetic tools, should allow us to look at chromosome structure at the molecular level.

I.2 DNA Topoisomerase II scaffold function in mitotic chromosome assembly: an overview

I.2 DNA Topoisomerase II scaffold function in mitotic chromosome assembly: an overview

Rajesh Ranjan[1, 2], Joel Ryan[2] and Paul S. Maddox[1-5]

[1]Systems biology option in the graduate program in Molecular Biology, Université de Montréal

[2]Institute for Research in Immunology and Cancer (IRIC), Université de Montréal

[3]Department of Pathology and Cell Biology, Université de Montréal

[4]Current Address: Department of Biology, University of North Carolina at Chapel Hill

[5]To whom correspondence should be addressed

Paul S. Maddox

Department of Biology, University of North Carolina at Chapel Hill

Campus Box #3280

Chapel Hill, NC 27599-3280

USA

I.2.1 Abstract

Chromosome condensation is a highly dynamic and tightly regulated process in mitosis. Histones and non-histone proteins have been shown to be involved in mitotic chromosome assembly. DNA Topoisomerase II (Topo II) is one of the non-histone proteins that are involved in chromosome assembly via its enzymatic activity. While several pieces of evidence suggest that topo-II has a scaffolding role in mitotic chromosome assembly, this function is still poorly understood. Here I discuss the scaffolding role of topo-II in mitotic chromosome assembly.

I.2.2 Introduction

In the last 4-5 decades the development of high-resolution optical and electron microscopy coupled to advanced genetic and biochemical techniques has helped to understand chromatin condensation process both *in vivo* and *in vitro*, and gave us modern insight to chromosome condensation process. These various approaches have discovered many factors involved in the mitotic chromosome assembly process and its underlying molecular mechanisms.

Originally histones were thought to play a vital role in giving the characteristic X-shape morphology to mitotic chromosomes. However, later, it was observed that histone-depleted chromosomes have normal X-shape morphology, held by a protein-based scaffold, resulting in the proposed non-histone “scaffold protein model” (Adolph et al., 1977; Adolphs et al., 1977; Paulson and Laemmli, 1977). The chromosome scaffold was later found to be enriched with topo-II and the condensin complex, (Lewis and Laemmli, 1982; Gasser et al., 1986; Hirano and Mitchison, 1994; Saitoh et al., 1994; Earnshaw et al., 1985). Topo-II has long been known as an enzyme that resolves DNA catenanes (Figure I.1.3). A topo-II non-enzymatic role in chromosome scaffolding has been both supported and discredited by disparate reports, leaving a key unanswered question in chromosome assembly. Here, I discuss mounting evidences for a topo-II scaffold role in mitotic chromosome assembly.

I.2.3 Topoisomerase II as a scaffold protein in mitotic chromosome assembly.

I.2.3.1 Evidence that supports topoisomerase II scaffold function.

During the 1970s, histones were discovered to be the only known structural proteins involved in mitotic chromosome assembly (Finch and Klug, 1976; Kornberg and Thomas, 1974; Olins and Olins, 1974; Oudet et al., 1975; Ris and Kubai, 1970). It was also shown that chromosomes contain a large number of non-histone proteins (Adolph et al., 1977), but their roles remained largely unknown. To reduce confusion in the complex topology of mitotic chromosomes, a method was developed to remove histone proteins from metaphase chromosomes allowing the study of chromosome structure without histones (Adolph et al., 1977; Adolphs et al., 1977; Paulson and Laemmli, 1977).

Chromosomes isolated from metaphase arrested HeLa cells (Wray and Stubblefield, 1970) can be treated with dextran sulphate and heparin to remove more than 99% of their histones. The histone-depleted chromosomes are unstable after treatment with proteases, whereas RNAase treatment does not affect their structure. The conclusion from these experiments is that non-histone protein structural elements are required to maintain chromosome morphology. Although these experiments were performed in the absence of histones, it is very likely that the same structural requirement is present in normal metaphase chromosomes.

Electron microscopy studies of histone-depleted metaphase chromosomes showed that the shape of chromosome scaffolds is similar to that of X-shape metaphase chromosomes (Adolph et al., 1977; Adolphs et al., 1977; Paulson and Laemmli, 1977). The majority of DNA in these histone-depleted chromosomes exists in loops on average 10-30 μm long (30-90 kb) extending outward from the scaffold axis. DNA loops with similar size have been observed in bacteria, however, it is unclear if these are fixation artifacts or structures that actually exist in living cells (Kavenoff and Ryder, 1976). In any case, a chromosome scaffold has not been observed or, for that matter,

proposed to exist in bacteria. In support of non-histone proteins stabilizing chromosomes with a structural scaffold, histone-depleted chromosomes are stable in 2 M NaCl for long periods of time. This suggests that non-histone scaffold proteins stabilize metaphase chromosome structure. Biochemical analysis revealed that two high molecular weight proteins were most abundant (Sc-I (170 KDa) and Sc-II (135 KDa) (Lewis and Laemmli, 1982)) and it has been hypothesized that these two proteins have scaffold function.

Comparative analysis of isolated metaphase chromosomes treated with nucleases revealed that the scaffold protein composition of chicken and human chromosomes are similar (Lewis and Laemmli, 1982). A high molecular weight polypeptide, Sc-I (Mr 170 KDa) was identified as topo-II (Earnshaw et al., 1985). Quantitative analysis of cell fractionations showed that at least 72% of topo-II is associated with the structure that was originally termed the chromosome scaffold. These results suggest that topo-II is a scaffold protein component of mitotic chromosomes and could play a structural role in mitotic chromosome assembly.

At the beginning of the 1990s, the topo-II scaffold model became a hot topic in the condensation field. To understand the molecular mechanism of topo-II as a scaffold, Adachi et. al. took an innovative approach. HeLa cell nuclei or Chicken erythrocyte nuclei were incubated in topo-II depleted *Xenopus laevis* egg extracts. Confoundingly, HeLa chromosomes condensed normally, whereas chicken erythrocyte derived chromatin did not condense. It was known that HeLa nuclei contain high levels of endogenous topo II, whereas Chicken erythrocyte nuclei contain very low levels. Therefore, it was concluded that, in HeLa cells, chromosomes condensed due to endogenous topo II, whereas, in chicken erythrocyte nuclei, chromosomes did not condense due to lack of endogenous topo II. In support of this line of reasoning, addition of purified topo-II (from yeast) added to chicken nuclei supported chromosome condensation in a dose-dependent manner. Dose-dependent topo-II function is consistent with a structural role, as opposed to a catalytic function.

Andreassen et. al. blocked topo-II catalytic activity using a small molecule inhibitor, VM-26, to dissect enzymatic versus structural roles of topo II. VM-26 inhibits topo-II catalytic activity by blocking the DNA strand passage step, wherein the enzyme forms a covalent intermediate with cleaved double strand DNA (Chen et al., 1984). This forms a stable DNA-VM-26-topo-II complex and induces G2 arrest in mammalian cells due to double strand breaks (Charron and Hancock, 1990; Misra and Roberts, 1975). G2 arrested cells could be induced to enter mitosis using 2-aminopurine (2-AP) that activates p32-cdc2 kinase (Norbury and Nurse, 1992). It has been observed that chromosomes condense and form nicely in cells induced with 2-AP mediated override of G2 arrest (Andreassen et al., 1997). To test chromosome condensation in detail, chromosome spreads were prepared from cells treated with VM-26 and 2-AP revealing that condensed chromosomes form with apparently normal morphology (Figure I.2.1A-B). However, 2-AP induced mitosis after S-phase arrest with hydroxylurea (HU) resulted in severe fragmentation of chromosomes. To understand chromosome formation in this condition, five hours after release from HU, chromosomes were exposed to VM-26 for three hours and then treated with 2-AP in the presence of VM-26. Interestingly, results showed that chromosomes form with normal appearance after brief exposure to VM-26. In sum, these results showed that normal chromosomes can form in the presence of VM-26 and 2-AP despite the presence of fragmented DNA and argues that topo-II catalytic activity is not required for generation of morphologically correct metaphase chromosomes.

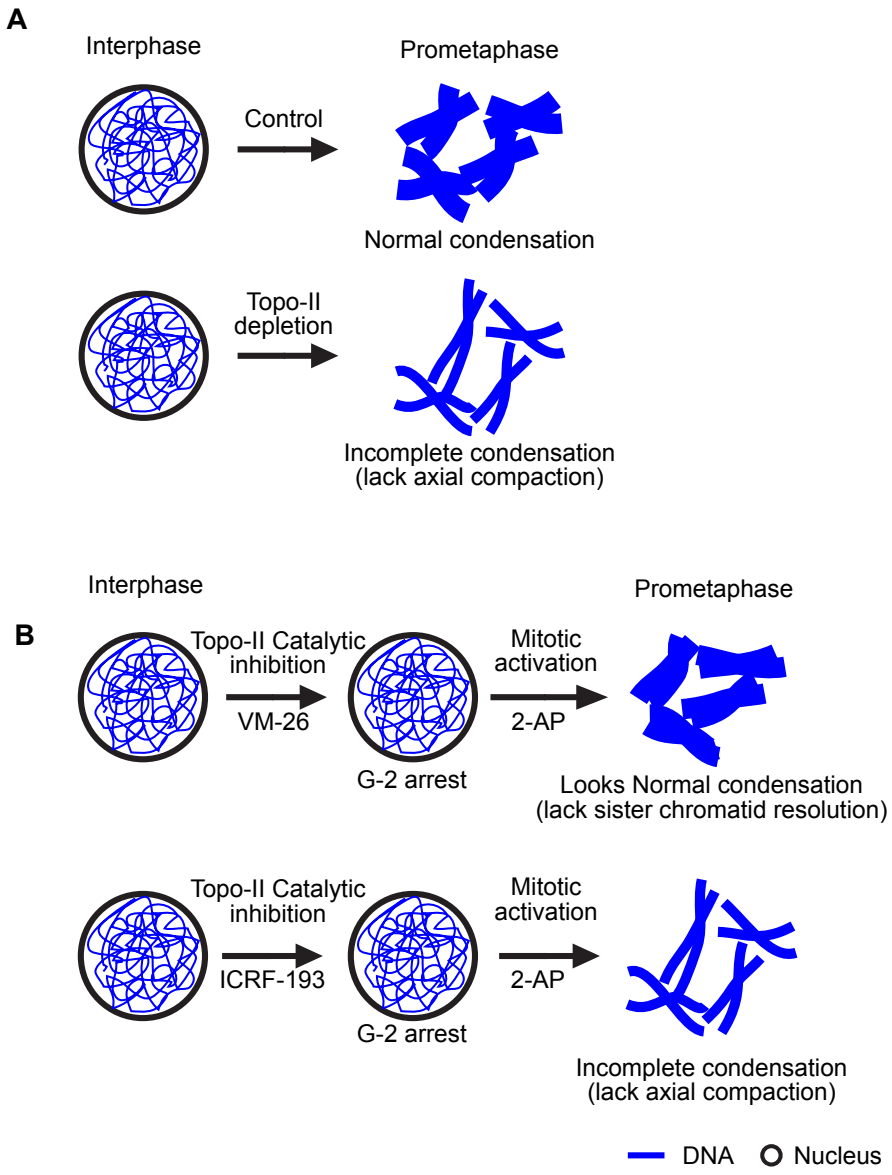

Figure I.2.1 - Chromosome condensation dynamics in topo-II depletion and topo-II catalytic inhibition. (A) Schematic diagram shows chromosome condensation in control and topo-II depletion. Topo-II depletion results in a lack of axial compaction of chromosomes leading to abnormally long chromosomes. **(B)** Schematic diagram shows chromosome condensation in topo-II catalytic inhibition using two different drugs, VM-26 and ICRF-193, having different molecular mechanisms of inhibition. Topo-II catalytic inhibition results in G2 cell cycle arrest. VM-26 mediated topo-II catalytic inhibition, where VM-26 forms a stable complex with DNA breaks, followed by mitotic activation with 2-AP results in condensed chromosomes that look normal but lack sister chromatid resolution. ICRF-193 mediated

topo-II catalytic inhibition, where ICRF-193 binds to N-terminus ATPase domain and locks enzyme in a closed conformation that might not be bound to DNA, followed by mitotic activation with 2-AP result in axially elongated chromosomes.

Topo-II catalytic activity can also be inhibited by a small molecule ICRF-193, via a different molecular mechanism; it inhibits reaction pathways at an earlier step than VM-26. ICRF-193 binds to the N-terminal ATPase domain and locks the enzyme in a closed-clamp conformation before DNA cleavage (Roca et al., 1994; Tanabe et al., 1991). ICRF-193 also induces an effective G2 block, however, it does not induce DNA fragmentation, unlike VM-26. In contrast to VM-26, after mitotic induction with 2-AP in the presence of ICRF-193, chromosomes condense incompletely with elongated chromatin arms (Figure I.2.1A-B). Incomplete chromosome condensation in ICRF-193, unlike VM-26, suggests that complete chromosome condensation requires the non-enzymatic function of topo II. In sum, catalytic inhibition experiments reveal two characteristics of topo-II activity; (i) chromosomes are generally able to form without topo-II enzymatic function, consistent with a topo-II scaffold model, while (ii) Topo-II enzymatic activity is required for complete and proper condensation.

Kohzi et al. took an *in vitro* approach using chromatin reconstitution assays combined with atomic force microscopy and fluorescence microscopy analysis to understand the molecular mechanism of topo-II scaffold function. Nucleosomal plasmids (26kb) did not exhibit a structural change after various amounts of topo-II addition (Figure I.2.2). Interestingly, when histone H1 was added, it resulted in the formation of 30nm chromatin fibers. Topo-II addition to 30 nm fibers induced large complex formation in the absence of ATP (Figure I.2.2). These results suggest that topo-II induce chromatin compaction in higher order structures in a histone H1 dependent manner independently of ATP. In support of this hypothesis, topo-II is able to clamp two DNA strands together independently of ATP, suggesting that its structural role could be distinct from its catalytic function.

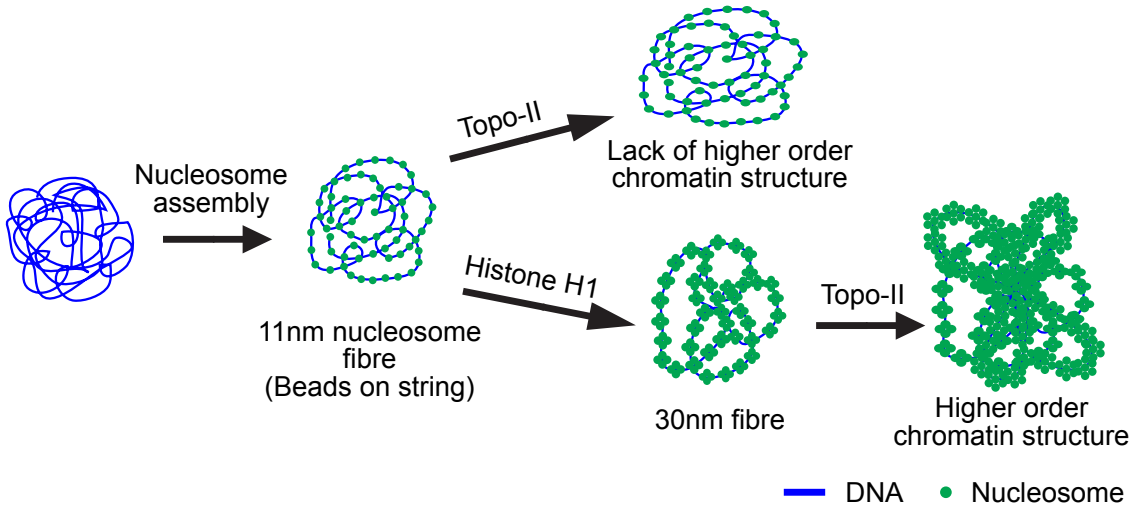

Figure I.2.2 - Topo-II mediated chromatin assembly in higher order structure. Chromatin assembly has been studied *in vitro* using pBR322 plasmid that allows nucleosome assembly. After nucleosome assembly, it has been treated with either topo-II or histone H1. Figure shows histone H1 treatment allows 11nm fiber, "beads on a string," to assemble into 30nm fiber. However, topo-II treatment does not facilitate chromatin assembly in higher order structure. When topo-II is added to the 30nm fiber after addition of histone H1 the chromatin assembles in higher order structure.

In sum, the biochemical extraction of topo-II from scaffold fractions, catalytic inhibition of topo II, *in vitro* chromatin reconstitution assays and studies in cell lines suggest that topo-II has a distinct structural role to scaffold chromatin in higher order structures as well as an enzymatic role to decatenate sister chromatids.

I.2.3.2 Evidence that does not support topo-II scaffold function

The topo-II scaffold model was a hotly investigated subject during the early 1990s in the chromosome condensation field. Several pieces of contradictory evidence did not

support the topo-II scaffold model. Hirano et al. concluded that topo-II does not play a scaffolding role in mitotic chromosome assembly in *Xenopus laevis* egg extracts. In controls, sperm chromatin incubated in mitotic *Xenopus* egg extract rapidly swells and then undergoes mitotic chromosome condensation. In topo-II depleted extracts, however, highly compacted sperm chromatin rapidly swelled, but, condensation was completely blocked even after extended incubations. When purified Drosophila topo-II was added to the topo-II depleted extract, condensation activity was restored, suggesting that topo-II is required for chromosome assembly and condensation. However, topo-II is apparently dispensable for maintenance of chromosome condensation as topo-II depletion or VM-26 addition after complete condensation did not induce any detectable defects. Based on these observations Hirano et al. concluded that topo-II doesn't play a scaffold role in mitotic chromosome assembly in *Xenopus laevis*.

An *in vitro* experiment does not allow observation of temporal dynamics of a condensation protein. Therefore, to test *in vivo* dynamics, rhodamine-labeled purified topo-II was microinjected into Drosophila embryos during cycles 9-10 (Swedlow et al., 1993). At this stage, the embryos exist as a multinucleated syncytium with nearly synchronous mitotic divisions allowing for analysis of topo-II dynamics throughout many cells (Swedlow et al., 1993). Distribution of microinjected rhodamine-topo-II was monitored by time-lapse imaging. This revealed that topo-II distribution changed during the cell cycle and most of the topo-II associated to interphase chromatin leaves during mitosis. Nuclear topo-II increases gradually and reaches maximum levels in late interphase. Topo-II concentration decreases gradually throughout prophase and prometaphase. Correspondingly, the cytoplasmic concentration increases suggesting that the loss of nuclear topo-II is due to the diffusion from the nucleus into the cytoplasm. Chromatin-associated topo-II further decreases during metaphase, but at a reduced rate, and decreases again during anaphase. Overall, the decrease in topo-II concentration is ~60 % during prophase and prometaphase and a further decrease by ~10% during anaphase. However, ~25% of the topo-II pool remains associated to chromosomes throughout the cell cycle. These data suggest

that there are at least three dynamic populations of topo II; (i) dissociated from chromosomes after prophase, (ii) dissociates from chromosomes after metaphase, and (iii) remains associated with chromosomes throughout mitosis. Since the bulk of topo-II is dynamic, where ~70% topo-II dissociates from chromosome, these data undermine a scaffold model for topo-II function.

In cultured tissue culture cells, topo-IIα localizes along the central axis of each chromatid arm during prometaphase and metaphase (Earnshaw and Heck, 1985; Gorbsky, 1994; Rattner et al., 1996). In late anaphase and telophase, cytoplasmic topo-IIα levels increase, as observed in fly embryos. A topo-II scaffold might be expected to be quite stable, however, fluorescence recovery after photobleaching of the majority of GFP-tagged topo-II occurred rapidly at kinetochores and chromosome arms. The extent of recovery at kinetochores was ~62%, whereas, on chromosome arms it was ~76%, arguing that stable populations do exist (Christensen et al., 2002). However other studies have found that nearly 100% of GFP topo-II is dynamic in other cell types, indicating that this could be experimental or biological variation (Tavormina et al., 2002). When topo-II was bleached in a small area in the cytoplasm, loss of GFP-topo-II occurred on unbleached chromosomes. This suggests that topo-II mobility is not regionally confined and that chromosome associated topo-II exchanges with the cytoplasm. When topo-II catalytic activity was inhibited by addition of ICRF-187 in mitotic cells, only a minimal recovery of EGFP-topo-II was detected in the bleached areas. These results suggest that the bulk of topo-II is dynamically associated with chromosomes in a manner that requires its catalytic activity.

In sum, *in vivo* studies show that the bulk of topo-II rapidly exchanges from chromatin-bound to cytosolic in mitosis. These data are generally inconsistent with a “static scaffold” model and may indicate that how the scaffold is conceived itself is incorrect.

I.2.4 Discussion

Chromosome condensation is a highly dynamic process that occurs at each round of mitosis. Biochemical and *in vitro* assays do not allow us to stop the condensation process once it has started; therefore it has been difficult to understand spatio-temporal functions of topo II. Decatenase activity, being required for global nuclear function, makes it even more difficult to dissect possible topo-II structural roles in chromosome condensation. A solution to this problem has been to use *in vivo* studies to investigate topo-II spatial and temporal requirement through mitosis.

In vivo studies with fluorescently tagged topo-II revealed that the bulk of topo-II is dynamic (Swedlow et al., 1993; Christensen et al., 2002; Tavormina et al., 2002); which is not in line with a scaffold function as defined in earlier works. Nevertheless, this interpretation could be misleading for the following reasons; (i) A subpopulation of topo-II still remains stably associated with chromosomes (Tavormina et al., 2002), (ii) Fluorescently tagged topo-II does not represent endogenous topo II, and (iii) Topo-II scaffold function could be one step in generating a “scaffold” that is not required to maintain it. Swedlow et al. showed that there are multiple populations of topo-II that dissociate at different stages of mitosis, supporting a temporal requirement hypothesis. Possibly, a fraction of topo-II that shows the dynamic behavior could be carrying out catalytic functions, whereas, other less dynamic populations could be acting as a scaffold.

It has been shown that, after topo-II depletion, chromosomes are abnormally long and lack axial compaction (Figure I.2.2) (Samejima et al., 2012; Andreassen et al., 1997; Sakaguchi and Kikuchi, 2004; Spence et al., 2007). Samejima et al., reasoned that topo-II enzymatic function is required for chromosome axial compaction. Depletion of topo-II removes almost all topo-II protein, and in such conditions it is difficult to say whether the lack of axial compaction is due to loss of catenase activity or scaffold function or both. Accordingly, a topo-II scaffold function may well be partly required for the axial compaction of the chromosomes.

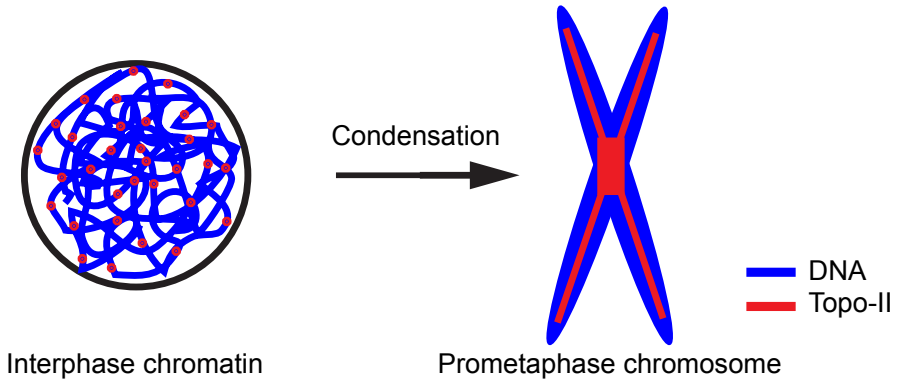

Figure I.2.3 – Topo-II chromosomal localization. Topo-II localization is punctate in interphase. Parallel to chromosome condensation in prophase, topo-II assembles to form a linear chromosome axis on metaphase chromosomes. Topo-II localizes more at the centromere than chromosome arms.

Topo-II has punctate localization in interphase (Figure I.2.3) (Earnshaw and Heck, 1985), suggesting that it has high affinity regions in the genome. It has been shown that topo-II preferentially binds to scaffold associated regions (SAR) with high affinity (Figure I.2.4) (Adachi et al., 1989), a feature that could facilitate future mitotic scaffold function. SARs are sequences present on the DNA of eukaryotic chromosomes where the nuclear matrix attaches, and mediates the structural reorganization of the chromatin (Mirkovitch et al., 1984). Whereas, in prometaphase, topo-II is enriched at the chromosome axis (Figure I.2.3) (Samejima et al., 2012). Topo-II high affinity regions in the genome could potentially explain a mechanism of topo-II scaffolding; wherein, a local scaffold extends to form a global scaffold axis parallel to the prophase chromosome assembly process. This activity could potentially bring an axial compaction of the chromosome (Figure I.2.4).

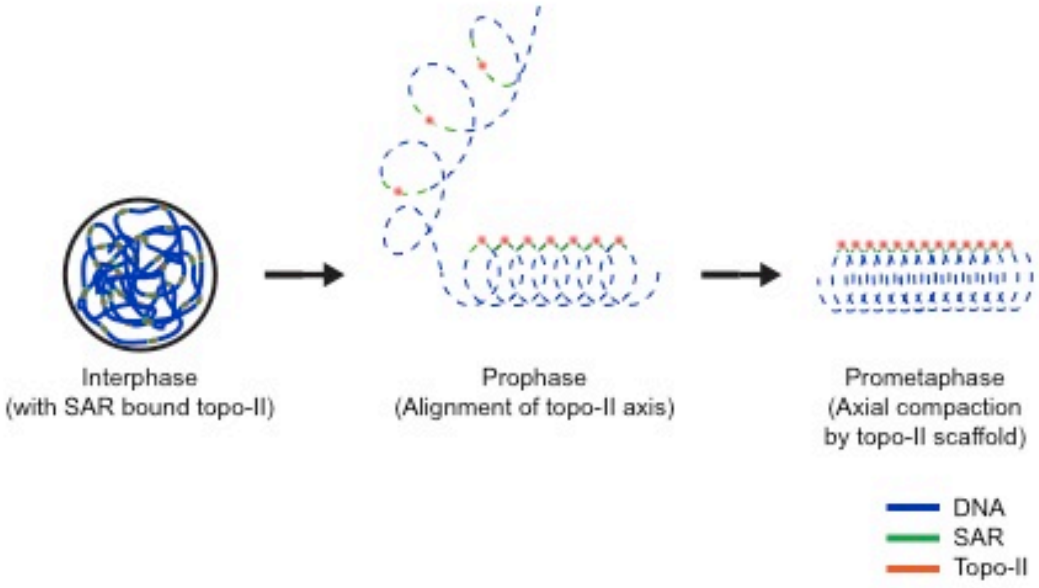

Figure I.2.4 - Topo-II scaffold model. Schematic diagram shows topo-II is punctate in interphase; probably at the Scaffold Associated Region (SAR, green). Parallel to chromosome condensation, SAR bound topo-II aligns and assembles, thereby contributing to axial compaction of the chromosome, to form a linear scaffold axis. In topo-II depletion and catalytic inhibition, chromosome lack topo-II scaffold axis and, therefore, lacks axial compaction. Red = topo-II and green = SAR.

In order to understand a possible topo-II scaffold role, more work needs to be done, and the following questions need to be addressed. (i) How can one distinguish catalytic and scaffold functions *in vivo*? (ii) How does topo-II contribute to the axial compaction of chromosomes; what are the underlying molecular mechanisms? (iii) How does it coordinate with other condensation factors to form mitotic chromosomes and what other proteins interact with topo II? The outcomes of these studies would certainly give more insight to understand the scaffold role of topo-II, as well as new condensation mechanisms and pathways.

Chapter II

A candidate screen for novel factors involved in mitotic chromosome assembly in *C. elegans*

II.1 Abstract

Despite many decades of study, mitotic chromosome structure remains incompletely characterized with respect to their composition and underlying molecular mechanisms. Quantitative analysis shows mitotic chromosomes contain roughly equal amounts of DNA and histones, which comprise 60% of the protein mass. The remaining 40% of the protein mass consists of non-histone components (Ohta et al., 2010b). While several studies have identified multiple non-histone proteins involved in chromosome assembly, it is highly probable that unidentified proteins play important roles. To identify additional proteins required for chromosome assembly, I used RNAi based screening of genes required for early development of *C. elegans* embryos, combined with high-resolution time-lapse imaging and quantitative analysis. With this approach, I have identified seven non-histone proteins involved in mitotic chromosome assembly, which function in temporally distinct manners during mitosis. I conclude from these results that mitotic chromosome assembly is temporally regulated by many independent factors.

II.2 Introduction

As cells enter mitosis, chromosomes undergo remarkable structural transformations to form metaphase chromosomes. Mitotic chromosome structure and condensation mechanisms can only be fully understood once all of the components have been identified and their functional relationships and interdependencies determined. Our understanding of the molecular mechanisms underlying chromosome condensation and the involved molecular players is still poor.

Many attempts have been made to identify mitotic chromosome proteins including studies focused on the mitotic chromosome scaffold fraction, and studies of isolated intact chromosomes from human cells. Biochemical fractionation of mitotic chromosomes identified approximately 200 polypeptides with highly purified chromosomes (Gassmann et al., 2005; Morrison et al., 2002; Takata et al., 2007; Uchiyama et al., 2005; Takata et al., 2007; Hirano et al., 1997; Hirano and Mitchison, 1991, 1994; Porter et al., 2007; Takata et al., 2007; Uchiyama et al., 2005; Dejardin and Kingston, 2009; Schirmer et al., 2003; Foster et al., 2003; Andersen et al., 2003; Ohta et al., 2010a; Ong et al., 2002).

Despite all of these efforts, all available reports lack to identify genuine mitotic chromosome components and their functional characterization. Therefore, I took an *in vivo* approach to understand how do mitotic chromosomes form and what are the factors involved. To find novel factors, first I pre-screen candidates (~100) from *C. elegans* genome databases, and I depleted them using RNAi followed by high-resolution time-lapse imaging in *C. elegans* early embryos. I choose the *C. elegans* early embryo as a model system for the following reasons. First, it has small number of chromosomes (n=6), which allows tracking of individual chromosomes using fluorescently tagged histones. Second, cell cycle events are highly reproducible in space and time. Third, condensation factors are conserved allowing translation into other organisms. Fourth, it allows efficient depletion of the target protein using RNAi. My *in vivo* approach, using these methods, lead to the discovery of seven novel condensation factors including topo-II, CIN-4, CDL-1, RNR-2, RPA-1, ABCX-1 and

W02D9.2.

My main objective was to understand how do mitotic chromosomes form in mitosis. To decipher molecular mechanism, I focus on two of my hits topo-II and RNR-2, because, depletion of either gives a distinct phenotype than known condensation factor depletion.

II.3 Materials and Methods

II.3.1 Candidate protein selection

C. elegans databases mainly comprise annotated results from whole genome RNAi screens. To select candidate proteins, I reasoned that proteins required for chromosome assembly would be required for embryonic viability early in development; therefore I first excluded proteins that are not required for the first two embryonic divisions. Multiple whole genome RNAi screens have identified a set of 661 genes as necessary for the first two mitotic divisions. A set of approximately 100 proteins whose phenotypes were consistent with condensation defects was chosen for RNAi screening. Strain TH32 was used for live cell imaging, which co-expresses GFP-histone H2B and GFP-γ-tubulin. GFP-histone H2B accumulates at the nucleosome and acts as a chromosome marker, whereas, GFP-γ-tubulin accumulates at the spindle poles as mitosis proceeds, and, acts as an indicator of cell cycle progression. The time-lapse movies of chromosome condensation (using strain TH-32) were acquired after introducing RNAi targeting expression of each of these candidate proteins using high-resolution swept-field confocal microscopy. These time-lapse movies were further analyzed for condensation using our fluorescence area based assay (see below).

II.3.2 RNA interference

RNA interference (RNAi) was performed as described previously in the chapter II (see materials and methods).

II.3.3 Live imaging

C. elegans early embryos were live imaged as described earlier in the chapter II (see materials and methods).

II.3.4 Quantitative area intensity assay

Previously described fluorescence intensity based assay was used for quantitative analysis of chromosome condensation in time-lapse images (Chapter II, see materials and methods) (Maddox et al., 2006).

II.3.5 Lethality test

Young adult worms were incubated on dsRNA expressing bacterial plates for 24 hours, and then transferred on to second dsRNA expressing bacterial plates for the next 24 hours; thereafter, adult worms were killed and laid embryos were counted. After 24 hours, non-viable embryos and larvae were counted on second plates. The percentage of non-viable embryos was calculated (Table 2.1).

II.4 Results

II.4.1 Depletion of candidate proteins results in quantitatively distinct phenotypes

A protein required for condensation would be expected to be required for first two embryonic divisions. Furthermore, depletion of these proteins would be expected to show a visible condensation defect in early embryos. To test this hypothesis, I individually depleted each candidate protein using RNAi and observed condensation by time-lapse imaging. I analyzed these time-lapse movies by both visual subjective and quantitative analysis. Visual analysis of time-lapse movies revealed that the depletion of 7, out of 100 candidate proteins showed chromosome condensation defects. Quantitative analysis using an area based assay (see methods) revealed distinct results indicating that these candidate proteins may function in different condensation pathways (Figure II.1, II.3 and table II.1).

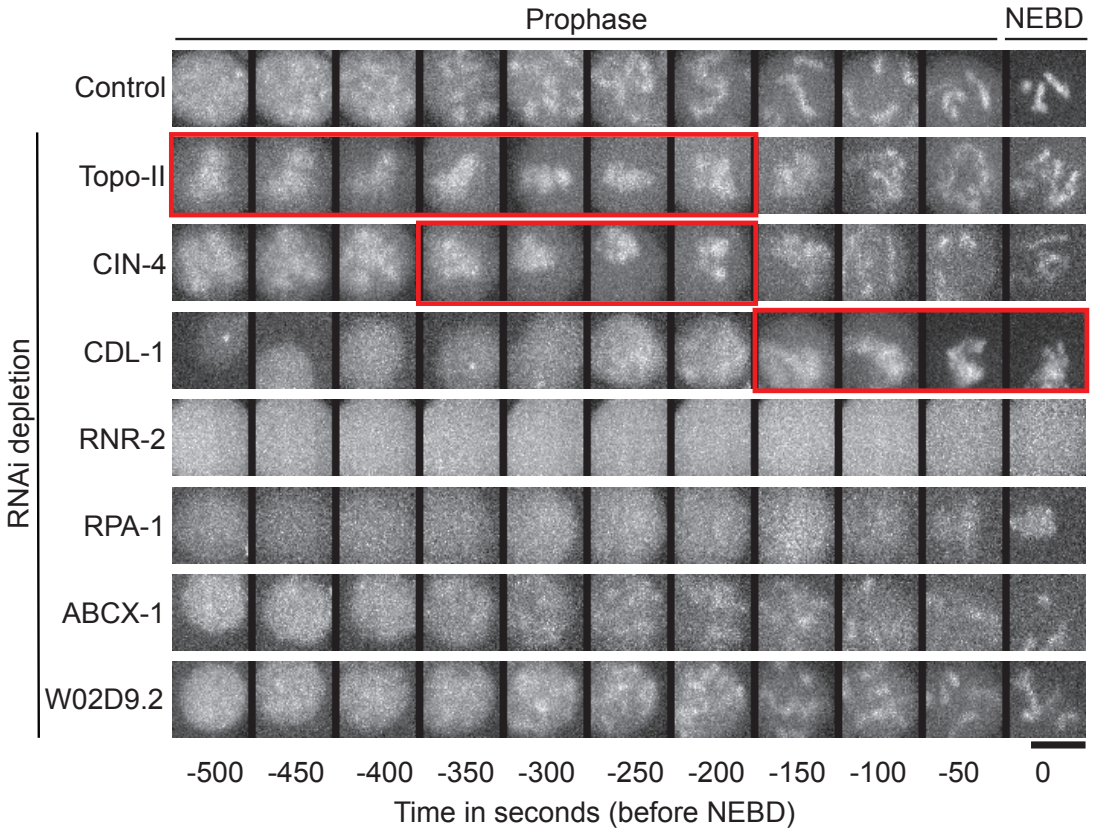

Figure II.1 – Candidate protein depletion results in defective chromosome condensation. The TH32 *C. elegans* early embryo (One-cell embryo), co-expressing GFP-Histone H2B and GFP-γ tubulin, were used for time-lapse imaging. A 50x50 pixel square region was selected encompassing the male pronucleus at 50-second intervals before nuclear envelope break down (NEBD, 0 sec). Montages show chromosome condensation in the control as well as TOPO-II, CIN-4, CDL-1, RNR-2, RPA-1, ABCX-1 and W02D9.2 depletions at different mitotic stages; prophase (-500s to -50s) and prometaphase (0s, NEBD). Red-rectangle boxes in the montage show PCC (prophase chromosome collapse) duration in mitosis; montage shows early-prophase (TOPO-II), mid-prophase (CIN-4) and late-prophase (CDL-1) chromosome collapse (PCC). Scale bar = 5μm.

II.4.2 Grouping of newly discovered candidate proteins

The proteins identified in the screen were grouped into three different categories based on their depletion phenotype, temporal requirement, and molecular mechanism (table II.1).

	Gene number	Gene name	% Lethality	Condensation defects
1	Control		3.57	Normal, chromosomes gradually condense and form
2	C03C10.3	*rnr-2*	100	Severe, diffused histones H2B and chromatin.
3	F18A1.5	*rpa-1*	100	Severe, diffused chromatin
4	K12D12.1	*top-2*	97.2	Severe, chromosome collapsed in early-prophase
5	ZK1127.7	*cin-4*	100	Severe, chromosome collapsed in mid-prophase
6	R06F6.1	*cdl-1*	100	Severe, chromosome collapsed in late-prophase
7	C56E6.1	*abcx-1*	96.96	Minor, delayed condensation
8	W02D9.2	Uncharacterized	23.65	Minor, delayed condensation

Table II.1 – Embryonic lethality of candidate protein depletion and condensation defects. Candidate proteins were depleted individually for 48 hours using RNAi and the percentage of non-viable embryos were calculated. The table shows the percentage of lethality for individual protein depletion and associated condensation defects.

(i) **Primary chromatin organizing factor** – Ribonucleotide reductase (RNR) and Replication protein A 1 (RPA-1). RNR is a catalytic enzyme, which catalyzes the formation of deoxyribonucleotides (dNTPs) from ribonucleotides, which is the raw material for DNA biosynthesis. Whereas,

RPA-1 is single stranded DNA binding protein, which is required to facilitate DNA replication.

(ii) **Chromosome axis formation** – TOPOisomerase II (TOPO-II), Chromosome INstability 4 (CIN-4) and Cell Death Lethal (CDL-1). Topo-II is a catalytic enzyme, which is required to decatenate sister DNA catenanes generated during DNA replication. *cin-4* encodes a homolog of *C. elegans* topo-II (with ~93% identity), but CIN-4 lacks ~700 amino acid at the C-terminus, including the catalytic tyrosine residue. CIN-4 is largely uncharacterized in *C. elegans*. *cdl-1* encodes a homolog of human hairpin binding protein (HBP), with ~37% identity that promotes histone mRNA processing and is required for high levels of histone gene expression. The CDL-1 is largely uncharacterized in *C. elegans*.

(iii) **Condensation delay** – ABC transporter eXtended (ABCX-1) and W02D9.2 (uncharacterized). ABCX-1 is a homolog of the human ABC transporter (with ~55% identity), which uses the hydrolysis of ATP to translocate a variety of compounds across membranes. ABCX-1 is largely uncharacterized in *C. elegans*. Whereas, W02D9.2 is a homolog of human YIPF6 (with ~75% identity), which is a multi-pass membrane protein required for the biogenesis of ER derived transport vesicles. W02D9.2 is largely uncharacterized in *C. elegans*.

When I depleted RNR-2 or RPA-1, I observed that the chromatin remained diffuse, throughout the prophase and there was very little signal at the chromosomes in metaphase (Figure IV.3). These data could indicate that these proteins function during nucleosome assembly in an unknown way. Surprisingly, the RNR-2 depletion result shows that the GFP-H2B signal goes to the background level after NEBD. This is interesting phenotype, and I choose it to study in detail. When I depleted proteins

from the second group; TOPO-II, CIN-4 and CDL-1, I observed that the prophase chromosome collapsed (PCC) at the center of the nucleus and chromosomes failed to segregate in anaphase (Figure II.1). PCC was temporally distinct in the different treated chromosomes collapsed in early-prophase in TOPO-II, in mid-prophase in CIN-4, and in late-prophase in CDL-1 depletion. This data indicates that this group of proteins is required to form mitotic chromosomes in a temporally independent fashion. When I depleted the third group of proteins (ABCX-1 or W02D9.2), I did not see any visual condensation defects, rather I observed delayed chromosome condensation (Figure II.1, II.2 and II.3). These results indicate that this group of proteins is required for timely chromosome condensation.

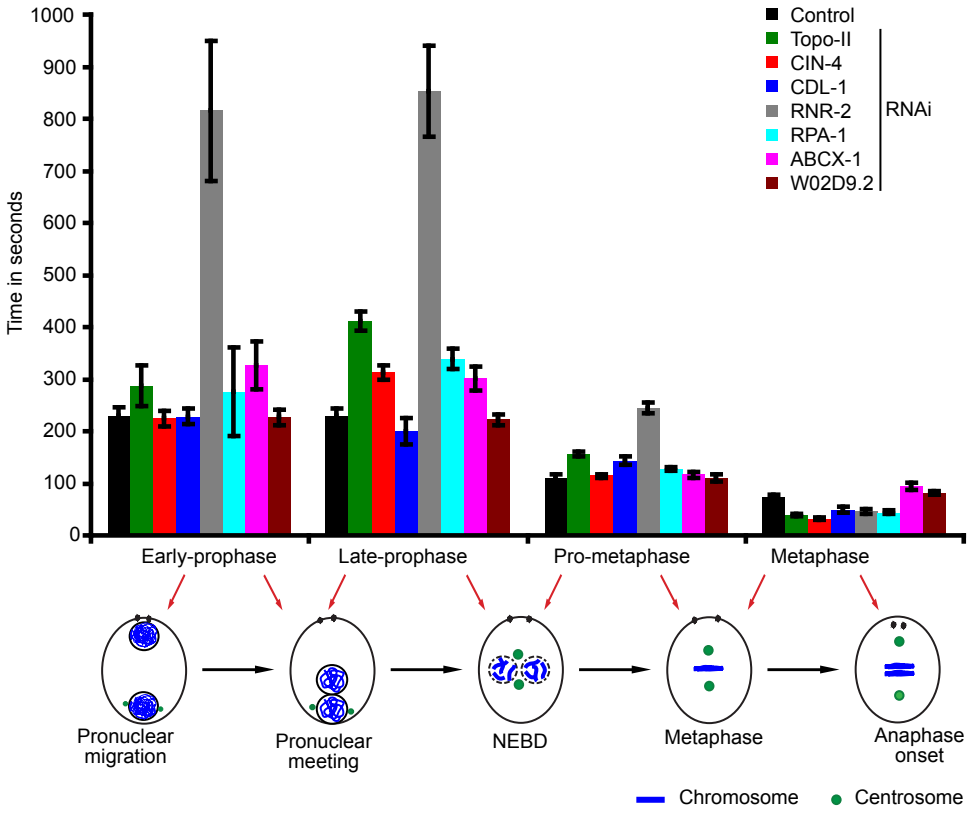

Figure II.2 – Candidate protein depletion results in cell cycle delay. Candidate proteins depleted individually for 48 hours using RNAi. The graph shows mitotic delay at different mitotic stages, early-

prophase, late-prophase, prometaphase and metaphase. Schematic representation shows different mitotic events, pronuclear migration, pronuclear meeting, NEBD, metaphase and anaphase onset, in *C. elegans* early embryos. Time required between two events is calculated as the duration of mitosis as indicated by the red arrow. Error bar = standard error of the mean; n, control = 20, CIN-4 = 17, CDL-1 = 10, TOPO-II = 20, RNR-2 = 19, RPA-1 = 11, ABCX-1 = 9, and W02D9.2 = 17.

II.4.3 Quantitative analysis of time-lapse movies

To test if the candidate proteins gave significantly distinct phenotypes, I used a quantitative fluorescence area based assay. This assay gives a percentage of area occupied by the chromosomes within the region of interest at each time point, which I term as a condensation parameter (Maddox et al., 2006).

As expected from visual inspection, quantitative analysis showed similar trends of condensation defects. Specifically, a flat graph was observed in RNR-2 and RPA-1 depletion throughout prophase showing diffuse chromatin (Figure II.3A). A peak in the profile was observed in Topo-II, CIN-4 or CDL-1 depletion in prophase showing prophase chromosome collapse (PCC) (Figure II.3B). Topo-II and CIN-4 were dispensable in late-prophase, where the chromosomes formed after early- and mid-prophase chromosome collapse, respectively, during a recovery phase (Figure II.3B). This quantitative analysis also further characterized delayed condensation in ABCX-1 and W02D9.2 depletion. In this case, condensation was delayed in early-prophase, which recovered and followed normal condensation in late-prophase (Figure II.3C).

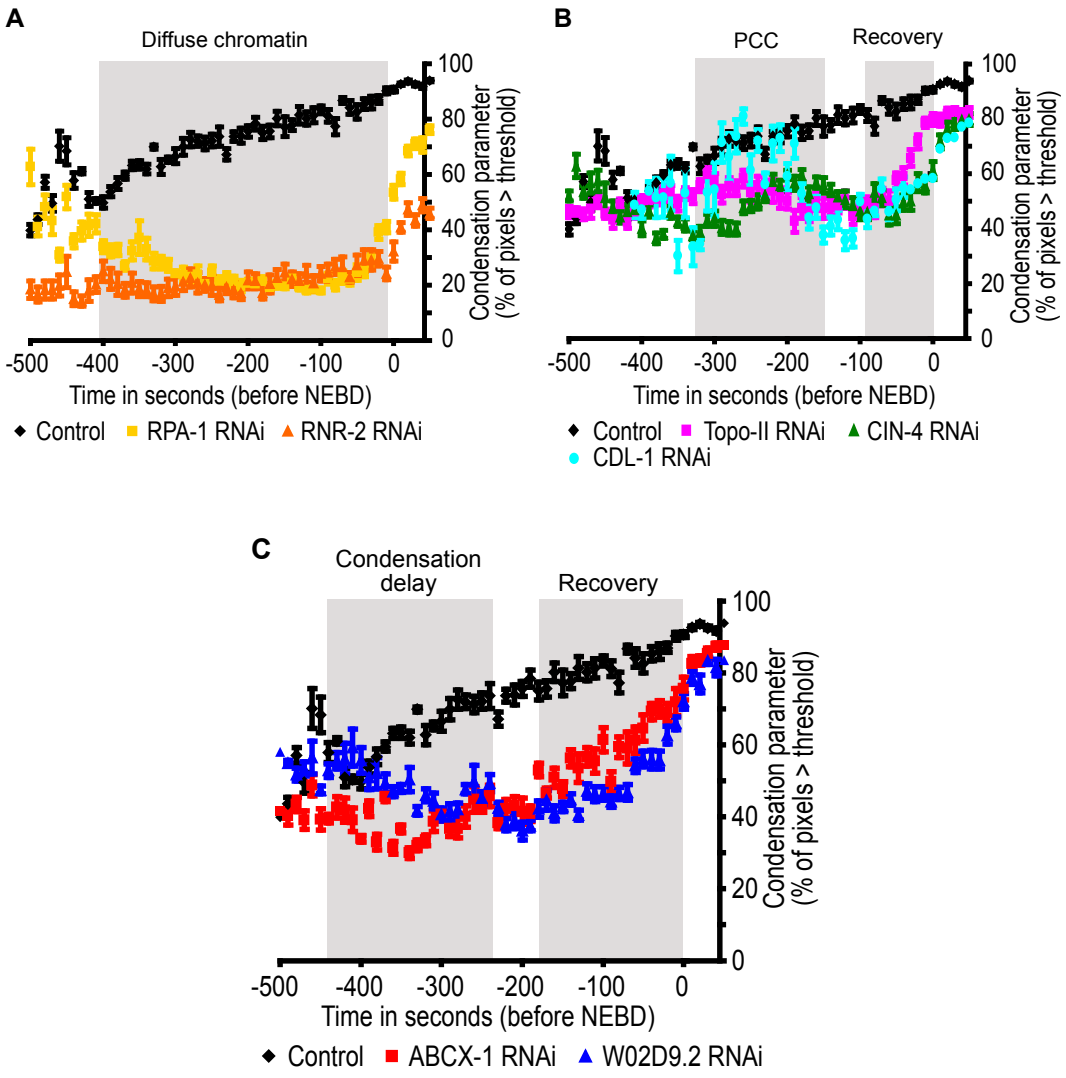

Figure II.3 – Candidate protein depletion results in a quantitatively different phenotype. The TH32 *C. elegans* early embryo (One-cell embryo), co-expressing GFP-Histone H2B and GFP-γ tubulin, is used for time-lapse imaging. Quantitative analysis of chromosome condensation in prophase (-500s to 0s) using a fluorescence area based assay (Maddox et al., 2006), in candidate protein depletion. **(A)** Graph is made for the control (black), RNR-2 depletion (orange) and RPA-1 depletion (yellow). A flat graph, the shaded region, in RNR-2 and RPA-1 depletion in prophase shows chromatin remains diffuse. Condensation parameter is the percentage of pixels below 35% threshold intensity. Error bar is the standard error of the mean; n, control = 10, RNR-2 = 19, and RPA-1 = 11. **(B)** Graph is made for the control (black), topo-II depletion (pink), CIN-4 (green) and CDL-1 (cyan). A peak at -300s

(topo-II), -250s (CDL-1) and -180s (CIN-4) shows prophase chromosome collapse (PCC), the shaded region. After chromosome collapse (PCC), chromosomes form in late prophase, a recovery phase, shaded region. Condensation parameter is the percentage of pixels below 35% threshold intensity. Error bar is the standard error of the mean; n, control = 10, topo-II = 19, CIN-4 = 17 and CDL-1 = 10. **(C)** Graph is made for the control (black), ABCX-1 (red) and W02D9.2 depletion (blue). Shaded region shows a condensation delay phase in early-prophase and a recovery phase in late-prophase. Condensation parameter is the percentage of pixels below 35% threshold intensity. Error bar is the standard error of the mean; n, control = 10, ABCX-1 = 12, and W02D9.2 = 17.

II.5 Discussion

My *in vivo* approach, protein depletion combined with high-resolution time-lapse imaging, in *C. elegans* offers a powerful tool to identify novel functional proteins of mitotic chromosome assembly. Further studies would give the full range of chromosome-associated function and the basis for the development of high-resolution structural maps.

In sum, so far I have discovered seven novel condensation factors in *C. elegans*. These newly discovered proteins belong to different protein families and based on preliminary analysis seem to function in a temporally independent manner with distinct molecular mechanisms.

Chapter III

DNA Topoisomerase II acts in both structural and enzymatic capacities during mitotic chromosome assembly in *C. elegans*

DNA Topoisomerase II acts in both structural and enzymatic capacities during mitotic chromosome assembly in *C. elegans*

Rajesh Ranjan[1, 2], Jonas F. Dorn[2], Amy S. Maddox[1-4] and Paul S. Maddox[1-5]

[1]Systems biology option in the graduate program in Molecular Biology, Université de Montréal

[2]Institute for Research in Immunology and Cancer (IRIC), Université de Montréal

[3]Department of Pathology and Cell Biology, Université de Montréal

[4]Current Address: Department of Biology, University of North Carolina at Chapel Hill

[5]To whom correspondence should be addressed

Paul S. Maddox

Department of Biology, University of North Carolina at Chapel Hill

Campus Box #3280

Chapel Hill, NC 27599-3280

USA

III.1 Abstract

The linear dimensions of the average human chromosome (~5cm) require that, in order to be segregated within the confines of a cell during mitosis (~0.003cm), chromosomes condense several orders of magnitude (Gassmann et al., 2004; Hirano, 2006; Huang et al., 2005; Nasmyth and Haering, 2005). The physical nature of chromosome compaction is largely unknown, however, non-histone protein components have long been proposed to play critical roles in organizing metaphase chromosome architecture (Adolph et al., 1977; Adolphs et al., 1977; Paulson and Laemmli, 1977). Topoisomerase II (Topo-II) is a DNA-binding and modifying enzyme that has been variously proposed as, and excluded from a role as, a chromosome scaffolding protein (Adachi et al., 1991; Andreassen et al., 1997; Earnshaw et al., 1985; Hizume et al., 2007, Christensen et al., 2002; Hirano and Mitchison, 1993; Tavormina et al., 2002). Here I use quantitative high-resolution live cell imaging assays in the *C. elegans* one-cell embryo to demonstrate that topo-II plays a distinct role in mitotic chromosome condensation. Localization and RNAi based protein depletion studies demonstrate that topo-II acts as a structural protein in conjunction with centromeric chromatin to organize compaction during mitotic entry. Small molecule inhibitors generated disparate phenotypes that were alleviated by removal of topo-II protein indicating a structural function distinct from enzymatic activity. Thus, my results are consistent with both enzymatic and structural hypotheses for topo-II in mitotic chromosome compaction and help to clarify the function of this conserved chromatin-binding protein during cell division.

III.2 Introduction

Chromatin is assembled into mitotic chromosomes just prior to cell division. Due to the transient nature and complex structure of chromosomes, the physical mechanism of condensation is largely unknown, and only a few proteins are known to be critical for chromosome assembly. Histones are basally required for the organization of DNA at all times throughout the cell cycle, transforming linear DNA into compacted structures (Akey and Luger, 2003; Robinson and Rhodes, 2006; Schalch et al., 2005). Histone-mediated structures observed *in vitro* by atomic force and electron microscopy includes the so-called “beads-on-a-string” structure of nucleosomal DNA and the “30nm fiber” formed by histone H1 mediated nucleosome stacking. Interestingly, the “30nm fiber” has not been directly observed in cells (Eltsov et al., 2008; Fussner et al., 2011; Joti et al., 2012; Maeshima et al., 2010; Tremethick, 2007). The condensin complex, a five-protein ATPase holoenzyme, is proposed to generate closed loops of DNA and thus actuate the “compaction” of mitotic chromatin (Cuylen et al.; Hirano; Hirano et al., 1997; Hirano and Mitchison, 1994). In addition, for holocentric chromosomes, on which the centromere runs the entire length of each chromosome, the centromere plays a role in chromosome condensation (Maddox et al., 2007; Maddox et al., 2006). Importantly, condensation must proceed beyond the proposed 30nm fiber stage in order to generate mitotic chromosomes (Hizume et al., 2005; Kepert et al., 2005; Robinson and Rhodes, 2006), but no higher-order structural intermediates, nor the responsible protein scaffolds, have been identified.

DNA topoisomerase II (topo-II) has been implicated via both biochemical and genetic approaches as an important factor for generating and maintaining mitotic chromosome structure (Christensen et al., 2002; Cuvier and Hirano, 2003; Earnshaw et al., 1985; Gasser et al., 1986; Uemura et al., 1987). Topo-II is a well-studied enzyme found throughout phylogeny that cleaves and then ligates, thus decatenating,

entangled double-stranded DNA molecules (Berger et al., 1996) and is thus thought to act late in chromosome segregation as sister chromatids release from one another. In support of this hypothesis, inhibition of topo-II activity by mutation or drug addition results in severe chromosome bridges during anaphase in metazoans (Murray and Szostak, 1985).

Topo-II is a major component of the “chromosome scaffold”, the structure remaining after biochemical extraction of histones and nuclease treatment of mitotic chromosomes (Adolph et al., 1977; Paulson and Laemmli, 1977; Earnshaw et al., 1985; Lewis and Laemmli, 1982). Thus, in addition to having catalytic roles in chromosome assembly, topo-II has been proposed to provide a structural framework for chromosome compaction (Adachi et al., 1991; Andreassen et al., 1997; Earnshaw et al., 1985; Hizume et al., 2007). These hypotheses have been debated for several decades, and data from various model systems has led to disparate conclusions. Recently, topo-II catalytic activity was shown to function in axial compaction of chromatids, indicating that supposed structural mechanisms could be accomplished by enzymatic activity (Samejima et al.; 2012). Additionally, interpretation of Topo-II loss-of-function studies have been confounded by cell cycle arrest (resulting from DNA replication errors) and disruption of topo-II based transcriptional regulation. In part because of these pleotropic defects, the role of topo-II in mitotic chromosome assembly remains unresolved.

Here I correlate quantitative imaging assays, small molecule inhibitors, and a computer based model to show that topo-II acts as both a structural protein and decatenase to ensure proper prophase chromosome assembly in the early *C. elegans* embryo. The one-cell embryo is transcriptionally silent and lacks DNA damage checkpoints (Hartman and Herman, 1982; Holway et al., 2005; Holway et al., 2006; Seydoux and Dunn, 1997), allowing direct interpretation of topo-II function in mitotic prophase chromosome condensation. I found that topo-II acts both structurally

and as a decatenase to ensure proper prophase chromosome assembly. Topo-II acts independently from centromeric chromatin to scaffold holocentric condensation. I propose that both topo-II and centromeric chromatin self-assemble during mitotic entry to general linear structural elements to promote chromosome assembly in *C. elegans.*

III.3 Materials and Methods

III.3.1 Antibodies and Antibodies labeling

A C-terminus fragment consisting of amino acids 1350-1470 from recombinant *Caenorhabditis elegans* Topoisomerase II was amplified with the primers 5'-GCGCGCCCATGGATGTTCGATTCGGACGATGAC-3' and 5'-GCGCGCCTCGAGTC

ATCTTGGAGCCACAACGAAGC-3'. This fragment was inserted into a bacterial expression vector (pGEX, GE Life Sciences) and expressed in Escherichia *coli* cells. Purified protein was then used for antibody production in rabbit (in IRIC core facility). A fraction of topo-II, SMC-4 and CENP-A antibodies were labeled with DyLight 499, 549 and 649 (DyLight Microscale Labeling kit; Thermo Fisher Scientific). Antibodies were used at concentrations of 10µg/ml and 0.33µg/ml for immunofluorescence and western blots, respectively.

III.3.2 RNA interference

In order to generate double-stranded RNA (dsRNA), 800-900 bp fragments of exons were amplified from genomic DNA using primers 5'-AATTAACCCTCACTAAAGGCCA

ACGAGTCGATGGTTATG-3' and 5'-TAATACGACTCACTATAGGTCTCCAACTTGCT

CGTATGC-3 for topo-II, and primers 5'-AATTAACCCTCACTAAAGGCGAGATGAGT

TGGGCGAAGAAG-3' and 5'-TAATACGACTCACTATAGGAGTCGCATCTGCTTGAT

TCG-3' for SMC-4. dsRNA fragments were transcribed *in vitro* using the Ambion High Yield Transcription kit. Co-depletion of topo-II along with other candidate proteins were performed by injecting dsRNA into the syncytial gonad of TH32 worms at L4, using an electronic micro-injector (Eppendorf), with a needle holder mounted to a Nikon Eclipse TE-2000-S microscope. Single depletions were achieved using bacterial feeding strains expressing dsRNA of individual genes.

III.3.3 Topoisomerase II graded depletion

Topoisomerase II was depleted to various extents using dsRNA injection or bacterial feeding for various time periods. To achieve high topo-II depletion (~95%), 1 mg/ml dsRNA was injected into L4 worms, which were then transferred to topo-II dsRNA expressing bacterial plates and incubated for 2 days at 20°C before imaging. To achieve medium topo-II depletion (~70%), L4 larvae were incubated on topo-II dsRNA expressing bacterial plates for 2 days at 20°C before imaging. To achieve low topo-II depletion (~25%), young adults were incubated on topo-II dsRNA expressing bacterial plates for 6.5 - 8 hours at 20°C before imaging. Depletion levels were quantified by western blot, using 90 worms (whole worm lysate) for each condition mentioned above.

III.3.4 Drugs

To inhibit catalytic activity of topo-II *in vivo*, the small molecules dexraxozane (ICRF-187) and etoposide (VP-16) were injected into young adult gonad of TH32 worms at 250 μM and 2 mM, respectively. Worms were then incubated for 60 minutes prior to imaging.

III.3.5 Worm strains

The TH32 *C. elegans* strain, which co-expresses GFP::histone H2B and GFP::γ-tubulin, was used for live and fixed-cell imaging. I have also used other GFP strains such as GFP::CAPG2, GFP::KNL2 and GFP::HCP3 for live and fixed-cell imaging. The N2 strain was used as a wild-type, and was used for biochemical assays as well as fixed-cell imaging.

III.3.6 Immunofluorescence

For immunofluorescence, control and RNAi-treated worms were dissected with a scalpel in M9 buffer on a polylysine bed, and then placed under a coverslip. The embryos were then incubated in liquid nitrogen for 5 minutes. The coverslip was then removed quickly in order to break the embryos eggshells, enabling the penetration of reagents. Embryos were then fixed in methanol at -20°C for 30-60 minutes, washed 3 times with PBS for 5 minutes each and blocked for 30 minutes with 4% BSA and 0.1% Triton X-100, in PBS. Primary antibodies were incubated at 10 µg/ml for 1.5 to 2 hours and secondary antibodies at 2 µg/ml for 45-60 minutes. Embryos were then washed 3 times with PBS and 3 times with PBST, for 5 minutes each. Embryos were transferred to mounting media containing DAPI for imaging.

III.3.7 Fixed Imaging

Fixed-cell imaging was performed on a wide-field epifluorescent microscope (Delta Vision, GE Health Care / Applied Precision) equipped with a CoolSnap HQ2 camera (Photometrics), using a 100X Olympus Plan Apo 1.4 NA objective. Softworx imaging software (GE Health Care / Applied Precision) was used for acquisition (with 1x1 binning, 0.2 µm z-steps) and deconvolution. Imaris software (Bitplane) was used to generate 3-D reconstructed images from deconvolved z-stacks.

III.3.8 Live Imaging

For live-cell imaging, worms were dissected in M9 buffer with a scalpel**,** and embryos were collected using a mouth pipette. Embryos were then placed on a thin 2% agarose pad, and covered with a coverslip prior to imaging. All live-cell imaging was performed on Swept Field Confocal (Prairie Instruments) microscope (Nikon Eclipse TE2000-E) equipped with a CoolSnap HQ2 camera (Photometrics), using a 60X Nikon objective (1.4 NA), 1.5 x optivar magnification, and 60µm pinhole setting. NIS-Elements AR 3.10 software (Nikon) was used for acquisition (with 2x2 binning, 0.75/1.0 µm z-steps).

III.3.9 Quantitative area intensity assay

In this study, a previously described fluorescence intensity based assay was used for quantitative analysis of chromosome condensation in time-lapse images(Maddox et al., 2006). Maximum intensity projections of z-stacks of nine images were generated for each time point, and a square of 50x50 pixels fitting to the male pronucleus was selected as the region of interest (ROI). Then, a threshold of 35% of the maximum pixel intensity was applied to the projections. The percentage of pixels below the threshold within the ROI was plotted over time, which serves as a quantitative readout of condensation kinetics over time.

III.3.10 Quantitative assay to measure chromosome axial compaction

For quantitative analysis of chromosome axial compaction, topo-II was depleted to various extents (low ≈ 25% and high ≈ 70%) using RNAi as described above. Lengths of individual, horizontally oriented chromosomes were measured in each condition just prior to NEBD using ImageJ software by line scanning.

III.3.11 Super resolution analysis method to measure distance

For quantitative analysis of the distance between axes, I used a super-resolution analysis method modified from the SHREC (single molecule high resolution colocalization) technique (Churchman et al., 2005). In this method, I generated intensity linescans of different fluorophores, and then measured the distance between the intensity peaks of different wavelengths, using imageJ (NIH). Embryos were fixed in methanol and stained with fluorophore-labeled antibodies and then imaged on a wide-field epifluorescent microscope (Delta Vision, GE Health Care / Applied Precision) as described above. Softworx imaging software was used for acquisition and deconvolution. Imaris software (Bitplane) was used to generate reconstructed images from single deconvolved focal plane.

III.3.12 Illustrative simulation of chromosome condensation

Chromosomes were simulated as freely jointed chains consisting of solid balls and massless sticks to allow disentanglement of adjacent chromosomes. The motion of the balls was governed by the discretized Langevin equation, which includes a randomly oriented force that reflects random thermal motion, as well as forces arising from collisions between balls and from the bonds between balls. Chromosome conformations were initialized similar to (Wong et al., 2012): The chromosomes started out in a fully stretched conformation surrounded by an accordingly large nucleus, which was slowly shrunk to its initial size. Once that initial size was reached, the initialization continued until the thermal motion of all balls, as well as overall characteristics of the chromosomes, such as radius of gyration plateaued. Following initialization, a combined angular and torsional force (Bulacu and van der Giessen, 2007) was gradually turned on in succession. Both angular and torsional force arose from narrow Gaussian-shaped potentials, such that the force was strong close to the ideal conformation, but that movement remained unconstrained when the conformation was far from ideal. Thus, I reflected the assumption that the constraints imposed on the DNA via condensation-related proteins were not only local, but also short-ranged.

III.4 Results

III.4.1 Topo-II catalytic activity is necessary for proper chromosome condensation

In metazoans, the majority of chromosome compaction occurs prior to nuclear envelope breakdown (NEBD). Previously we showed that in the one-cell *C. elegans* zygote, chromosome assembly begins about 5 minutes prior to NEBD and completes to over 90% of full compaction just before NEBD (Maddox et al., 2006). Depletion of the condensin complex resulted in nearly complete loss of prophase chromosome assembly as would be expected; however, disruption of centromeric chromatin also caused a major and quantitatively unique defect in chromosome assembly (Maddox et al., 2007; Maddox et al., 2006). Given that in either case chromosomes form to some extent just prior to NEBD, I reasoned that additional factors have a strong influence on chromosome assembly.

As introduced earlier, topo-II is a leading candidate for an additional factor in mitotic chromosome assembly. To test if topo-II activity is critical for chromosome condensation in *C. elegans*, I used small molecule inhibitors. There are several specific inhibitors of topo-II enzymatic activity effective over a very broad phylogenetic range from prokaryotes to human cells. The mechanism of action of various inhibitors is known, and sequence alignment suggested that two, ICRF-187 and VP-16 should inhibit the *C. elegans* DNA topoisomerase IIα isoform (Top-2) (Figure III.1).

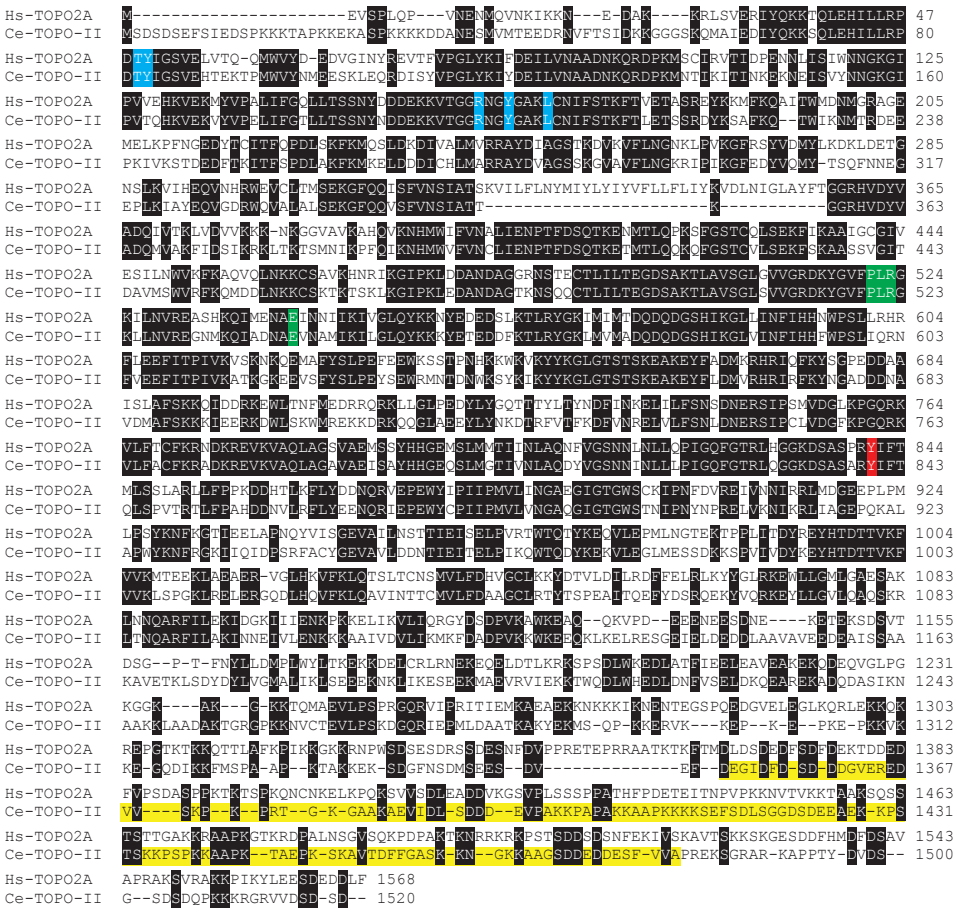

Figure III.1 - Topo-II key residues are conserved in *C. elegans*. Amino acid sequences alignment of human DNA Topoisomerase II (DNA Topoisomerase II alpha/Hs-TOPO2A) and *C. elegans* DNA Topoisomerase II (K12D12.1/Ce-TOP-2). Amino acid identity is indicated in black background boxes. The yellow background boxes show C-terminus epitope used to develop anti-topo-II antibody. The red background box shows conserved tyrosine in the active site. The cyan background boxes show conserved ICRF-187 binding residues and green background boxes show conserved VP-16 binding residues(Classen et al., 2003; Wu et al.).

Treatment of *C. elegans* embryos with either topo-II inhibitor generated a strong phenotype. First, the cell cycle was delayed relative to controls, likely due to defects in DNA replication (Figure III.2).

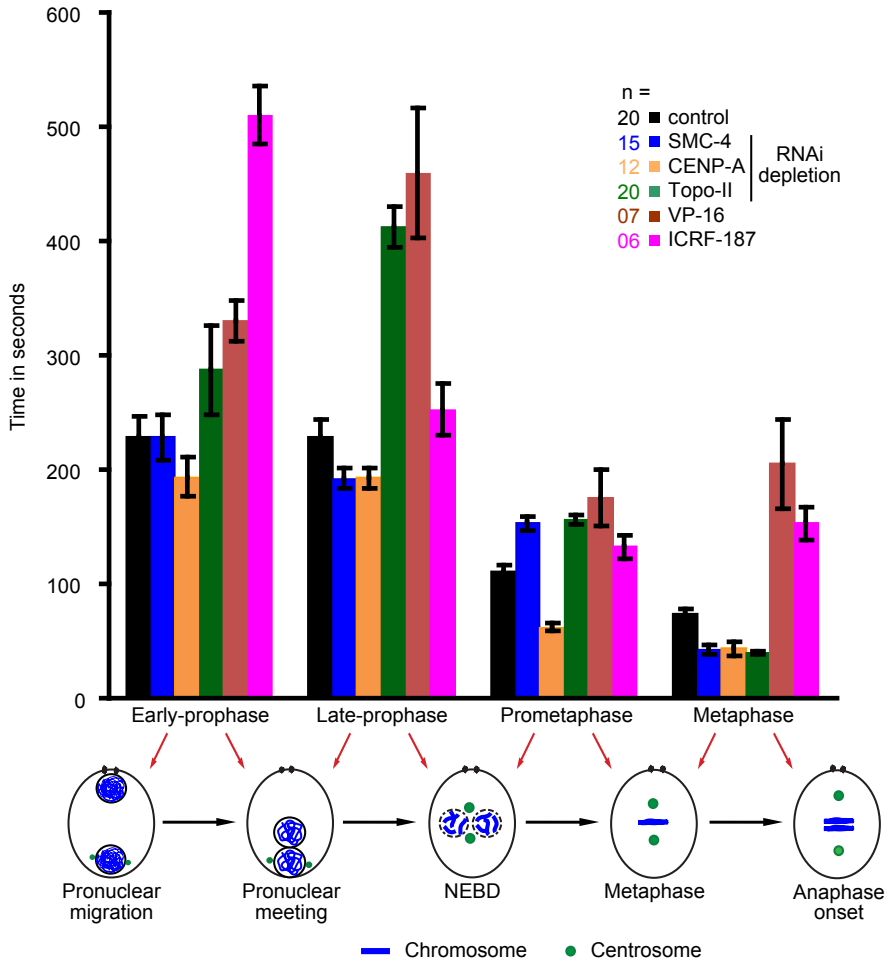

Figure III.2 - Topo-II depletion and catalytic inhibition result in cell cycle delay. Topo-II, SMC-4 and CENP-A are depleted individually for 48 hours using RNAi method and topo-II catalytic activity is inhibited with ICRF-187 and VP-16. Graph shows mitotic delay at different mitotic stages, early-prophase, late-prophase, prometaphase and anaphase. Schematic representation shows different mitotic events, pronuclear migration, pronuclear meeting, NEBD, metaphase and anaphase onset, in *C. elegans* early embryos. Time required between two events is analyzed to calculate the duration of mitosis as indicated by the red arrow. Error bar = standard error of mean; n, control = 20, SMC-4 = 15, CENP-A = 12, topo-II = 20, VP-16 = 7 and ICRF-187 = 6.

Second, chromosomes failed to condense in a manner quantitatively similar (as determined by our live cell condensation assay) to that seen after condensin depletion (Figure III.3 A-C). This was unexpected as catalytic inhibition of topo-II in other model systems did not grossly inhibit chromosome condensation (Andreassen et al., 1997). Finally, chromosome segregation was disrupted resulting in severe chromatin bridging in anaphase as observed in various other model systems (Figure III.3A). Importantly, the defects I observe are not due to meiotic defects as both the sperm and oocyte chromatin exhibit the same phenotype. The sperm in *C. elegans* are formed in the L4 larval stage, at least 24 hours prior to treatment with inhibitors.

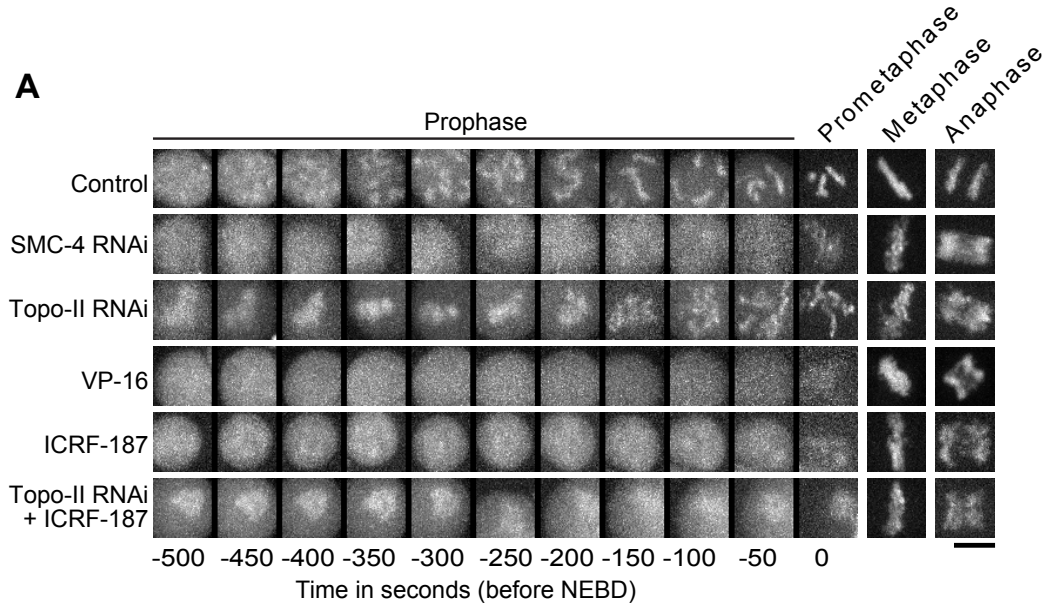

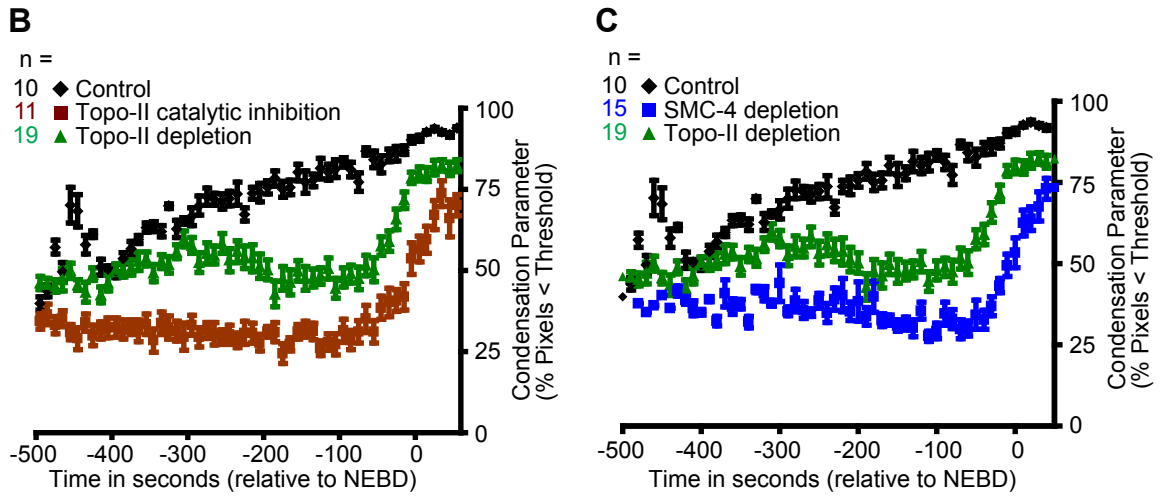

Figure III.3 - Topo-II depletion results in a different phenotype compared to catalytic inhibition. The TH32 *C. elegans* early embryo (One-cell embryo), co-expressing GFP-Histone H2B and GFP-γ tubulin, is used for time-lapse imaging. **(A)** A 50x50 pixel square region is cut from male pronucleus time-lapse movies at 50-second intervals before nuclear envelope break down (NEBD, 0 sec). A montage is made for the control, condensin depletion (SMC-4), topo-II depletion, topo-II catalytic inhibition (by VP-16 and ICRF-187) and topo-II depletion followed by catalytic inhibition. Montages show chromosome condensation profiles at different mitotic stages; prophase (-500s to -50s), prometaphase (0s), metaphase and anaphase. Scale bar = 5μm. **(B)** Quantitative analysis of chromosome condensation in prophase (-500s to 0s) using a fluorescence area based assay(Maddox et al., 2006), in topo-II depletion and topo-II catalytic inhibition. The graph is made for the control (black), topo-II depletion (green) and topo-II catalytic inhibition (brown). A flat graph in topo-II catalytic inhibition in prophase shows chromatin remains diffuse. Condensation parameter is the percentage of pixels below 35% threshold intensity. Error bar is standard error of the mean; n, control = 10, topo-II = 19, and Catalytic inhibition (ICRF-187) = 11. **(C)** Quantitative analysis of chromosome condensation in prophase (-500s to 0s), using fluorescence area based assay, in topo-II and SMC-4 depletion. The graph is made for the control (black), topo-II depletion (green) and condensin depletion (blue). A peak at -300s in topo-II depletion shows prophase chromosome collapse (PCC). Condensation parameter is the percentage of pixels below 35% threshold intensity. Error bar is standard error of the mean; n, control = 10, topo-II = 19, condensin = 15 and Catalytic inhibition (ICRF-187) = 11.

The fact that similar results were observed with both inhibitors is somewhat surprising given that their mechanism of inhibition is different. ICRF-187 acts by blocking the ATPase activity, whereas VP-16 results in blocking the DNA religation step. Therefore, I conclude that chromosome condensation defects are independent of where in the enzymatic cycle topo-II is inhibited. As mentioned above, the one-cell zygote lacks cell cycle check-points, therefore, DNA replication would undoubtedly generate errors that would propagate to mitosis and contribute to the phenotypes observed. This is clear from the measured delay in mitotic onset. However, RNAi of DNA replication proteins does not result in a severe mitotic chromosome condensation phenotype in prophase. Therefore, it is unlikely that replication errors are solely responsible for lack of condensation in prophase following enzymatic inhibition of topo-III. Altogether, these data are consistent with topo-II decatenase activity being required for global DNA metabolism including mitotic chromosome condensation.

III.4.2 Topo-II plays a structural role in chromosome condensation

Inhibition of topo-II enzymatic activity does not remove the protein (Figure IV.6) and, therefore, does not test non-enzymatic roles in chromosome assembly. I therefore depleted topo-II by RNA interference (RNAi) to determine if there were non-catalytic roles in mitosis. After depleting topo-II, I observed a cell cycle delay in the first division similar to small molecule inhibition (Figure III.2). However, visual and quantitative analysis revealed a dramatic difference in prophase chromosome assembly; specifically topo-II RNAi resulted in prophase chromosome aggregation towards the center of the nucleus (Figure III.3A-C). Aggregation occurred about 600 second prior to NEBD and lasted, seemingly unchanged, until about 150 seconds prior to NEBD when the chromosomes separated from the collapsed mass and

individualized into abnormally long chromosomes (Figure III.3A). It is important to note that, while chromosomes individualized during prophase, the overall progress of condensation was highly aberrant in a manner that was unique compared to other perturbations. The appearance of chromosomes late in prophase implies that additional mechanisms function in the absence of topo-II to generate linearly distinct chromosomes. This is not surprising given the important roles of both condensin II and centromere proteins in holocentric chromosome condensation.

At NEBD after topo-II depletion, the chromosomes interacted with microtubules of the mitotic spindle and aligned at the metaphase plate. This phenotype was grossly similar to condensin depletion and likely due to the activity of centromere proteins in driving chromosome assembly (Maddox et al., 2007; Maddox et al., 2006). The fact that chromosomes assembled in the absence of condensin or topo-II form a metaphase plate indicates that kinetochore assembly was unperturbed (although likely improperly organized). As seen in topo-II enzymatic inhibition, chromosome segregation failed due to severe anaphase bridging (Figure III.3A). Overall, topo-II depletion was phenotypically distinct from that of catalytic inhibition (by either of two drug additions), indicating a possible structural as well as an enzymatic role for topo-II in chromosome assembly.

While it is possible that the phenotype observed after small molecule inhibition of topo-II is due to off-target effects, this is less likely the case as multiple inhibitors with different molecular mechanisms yielded similar phenotypes. Nonetheless, to confirm that inhibitors were acting specifically, I treated topo-II depleted animals with inhibitors. Interestingly, RNAi depletion in combination with small molecule addition resulted in a similar phenotype to RNAi alone (Figure III.3A). This suggested that the defects seen after small molecule addition can be relieved by removal of topo-II; a result consistent with topo-II being the relevant target of the inhibitors. In sum, this

data supports the hypothesis that topo-II has an important non-catalytic role in *C. elegans* chromosome assembly.

III.4.3 Topo-II, centromeres and the condensin complex function independently in chromosome formation.

As mentioned above, *C. elegans* are holocentric and we previously showed that both centromere proteins and the condensin complex independently contribute to chromosome formation (Maddox et al., 2006). As topo-II depleted embryos eventually formed curvilinear individualized chromosomes after prophase collapse (Fig III.3A), I hypothesized this could be mediated by either centromere or condensin function. To test this hypothesis, I co-depleted CENP-A (centromeres) and topo-II or SMC-4 (condensin complex) and topo-III. Co-depletion in either combination resulted in failure of chromosome individualization prior to NEBD (Figure III.4A). These results suggested that chromosome formation in the absence of topo-II 150s prior to NEBD could be due to the action of alternative protein based chromosome axes. If centromere axis formation were a contributor, I would expect that sister centromere resolution (the point in prophase where the two sister centromeres are visually separated) would occur concomitant with chromosome individualization in topo-II depleted animals (approximately 150s prior to NEBD). Consistent with this hypothesis, centromere resolution (as measure by in GFP-centromere proteins) temporally coincided with chromosome individualization in topo-II depleted animals (Figure III.4B) supporting the hypothesis that, in *C. elegans* holocentric chromosomes, centromeres form a structural axis.

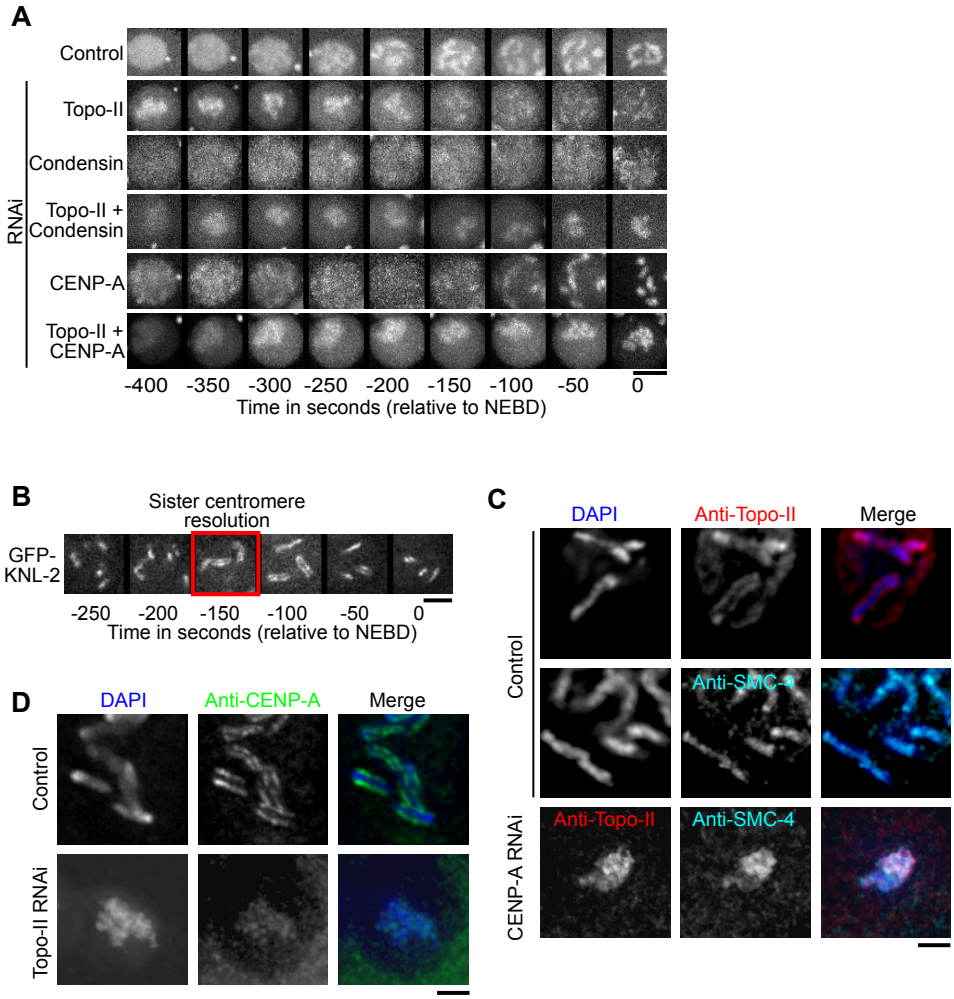

Figure III.4 - Topo-II, centromeres and the condensin complex function independently in chromosome formation. (A) The TH32 *C. elegans* early embryo (One-cell embryo), co-expressing GFP-Histone H2B and GFP-γ tubulin, is used for time-lapse imaging. A 50x50 pixel square region is cut from male pronucleus time-lapse movies at 50-second intervals before NEBD. Montages depict control, condensin depletion (SMC-4), topo-II depletion, CENP-A depletion and co-depletion of topo-II and condensin or topo-II and CENP-A. Scale bar = 5μm. **(B)** Montage made from the time-lapse movies of GFP-KNL-2 (kinetochore) expressing embryo at 50-second intervals before NEBD. Montage shows the sister centromere resolution occurs about 150 sec prior to NEBD (red box). Scale bar = 5μm. **(C-D)** Fixed embryos are immunostained with anti-topo-II, anti-CENP-A and anti-SMC-4 antibody in wild-type worms (N2) after RNAi depletion of one condensation factor at a time (topo-II, SMC-4 and CENP-A) and stained with other two. **(C)** Immunofluorescence image shows SMC-4 staining and topo-II staining after CENP-A depletion and in control. **(D)** Immunofluorescence image shows CENP-A

staining after topo-II depletion and in control. Scale bar = 2μm; blue = DAPI, Red = topo-II, cyan = condensin, green = centromere.

If topo-II, centromeres and condensin function as independent chromosomal elements, then I would expect these factors to localize independently. To test this hypothesis, I sequentially depleted one factor and probed the other two (Figure III.4C-D). Immunofluorescence and GFP-based data previously concluded that centromere proteins and the condensin complex are localized independently (Figure III.4C) (Maddox et al., 2006). Analysis of centromere proteins after topo-II depletion revealed no gross defects in metaphase localization (Figure III.4D). Generally, depletion of condensin resulted in massive chromosome disorganization precluding proper evaluation of topo-II localization (data not shown). Overall, these results are consistent with the conclusion that topo-II, centromeres, and the condensin complex act as independent chromosome structural elements in holocentric organisms.

III.4.4 Endogenous topo-II localizes linearly on mitotic chromosomes.

Based on the above results and previous works, it is reasonable to posit that the non-enzymatic role of topo-II is manifested as a chromosome structural protein. A protein acting as a chromosomal structural element would be expected to localize in a linear fashion along the length of mitotic chromosomes. In other systems, topo-II localizes to chromosome arms with a concentration as centromere regions. To test if topo-II localized in a manner consistent with a structural element in *C. elegans*, I generated an affinity purified polyclonal antibody directed against *C. elegans* topo-II (Top-2) (Figure III.5). Immunofluorescence staining with this antibody revealed linear

localization along prometaphase chromosomes, as expected for a structural protein (Figure III.5).

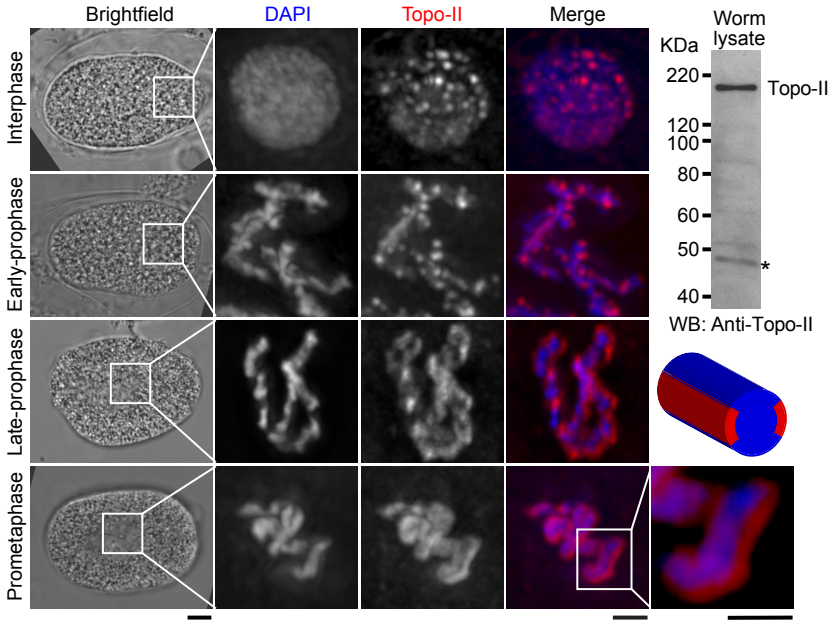

Figure III.5 - Endogenous topo-II localizes linearly on mitotic chromosomes consistent with a structural function. One-cell early embryos are fixed in methanol, stained with anti-topo-II antibody and DAPI, and then imaged at different mitotic stages; interphase, early-prophase, late-prophase, and prometaphase chromosomes. Imaris software was used to reconstruct 3-D images from deconvolved Z-stacks (see materials and methods). Inset shows zoom-in image of a single prometaphase chromosome. Schematic of single prometaphase chromosome shows a 3-D view of spatial organization of the topo-II axis. Blue = chromosome and red = topo-II. Scale bar: 1μM in fluorescence images and 5μM in brightfield images. Anti-topo-II antibody is tested on western blot using a whole worm lysate. Asterisk (*) indicates a band that is unaffected by topo-II RNAi.

It is possible that the linear localization pattern was due to problems with antibody penetrance in to chromatin. Attempts to generate a GFP version of topo-II failed, possibly reflecting a dominant phenotype of tagged topo-II in *C. elegans*. Other

antibodies generated by the same methods and used to stain chromosomes using the same protocol are able to penetrate into chromosomes (Oegema et al., 2000), therefore, I do not believe the localization to be due to epitope accessibility problems. Importantly, staining failed after RNAi of topo-II indicating that the specificity of the staining pattern (Figure III.6).

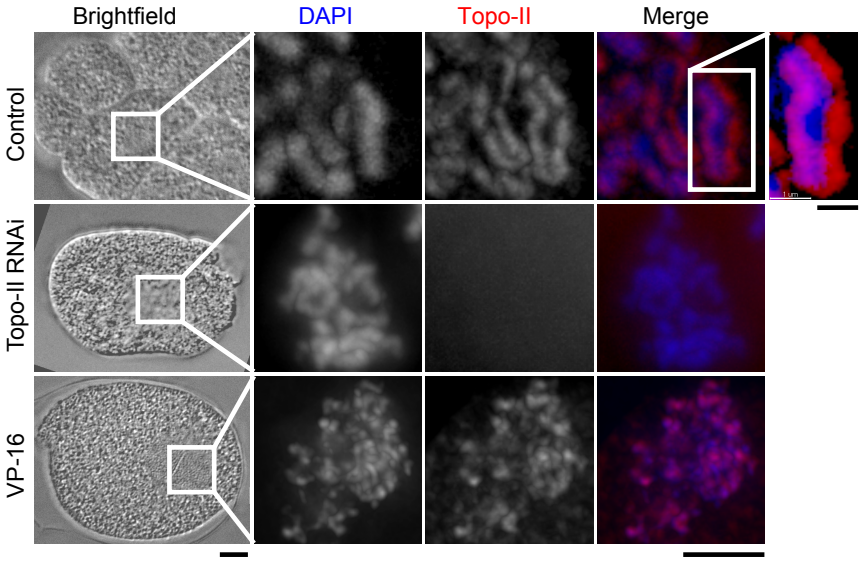

Figure III.6 - Topo-II catalytic inhibition does not remove topo-II protein. Wild-type (N2) embryos are immunostained with anti-topo-II antibody. Immunofluorescence image shows topo-II staining in control, topo-II depletion and topo-II catalytic inhibition (with VP-16). Inset shows zoom-in view of a single prometaphase chromosome with two topo-II axes. Blue = DAPI and Red = topo-II. Scale bar, brightfield images = 5μm and fluorescence images = 2μm .

During early prophase topo-II staining was punctate, only forming an obvious axis after completion of pronuclear migration, approximately the same time as centromere resolution (Fig III.4B and III.5). As with centromeres, the punctate to linear localization

pattern is not consistent with a pre-assembled chromosome scaffold, however, indicates that axis formation is the result of local assembly leading to eventual global axis formation. I hypothesize that chromosome structural elements could be co-assembled with chromosomes during prophase, as opposed to chromatin organization around preassembled scaffolds.

III.4.5 Topo-II, condensin and centromere axes are physically distinct.

My RNAi and localization results suggest that topo-II is physically separated from centromeres on condensed chromosomes. To test this hypothesis, I co-stained centromeres and topo-II. Prior to observable chromosome condensation, topo-II and centromeres display non-overlapping punctate staining patterns. During prophase, both centromere and topo-II puncta became somewhat larger, however, remained spatially independent throughout the remainder of mitosis. As best observed by cross-sectional views of prometaphase chromosomes, it is clear that topo-II localizes to superficial chromosome regions and seems to be excluded at centromeres (Figure III.7). It should be noted that, as is the case for centromeres, I never observed topo-II localization at chromosome interior regions. This could be due to incomplete antigen access, however, antibodies to other proteins located interior to centromeres (e.g. condensin or inner centromere proteins) generated and applied using the same protocols do not have antigen access problems (as discussed above).

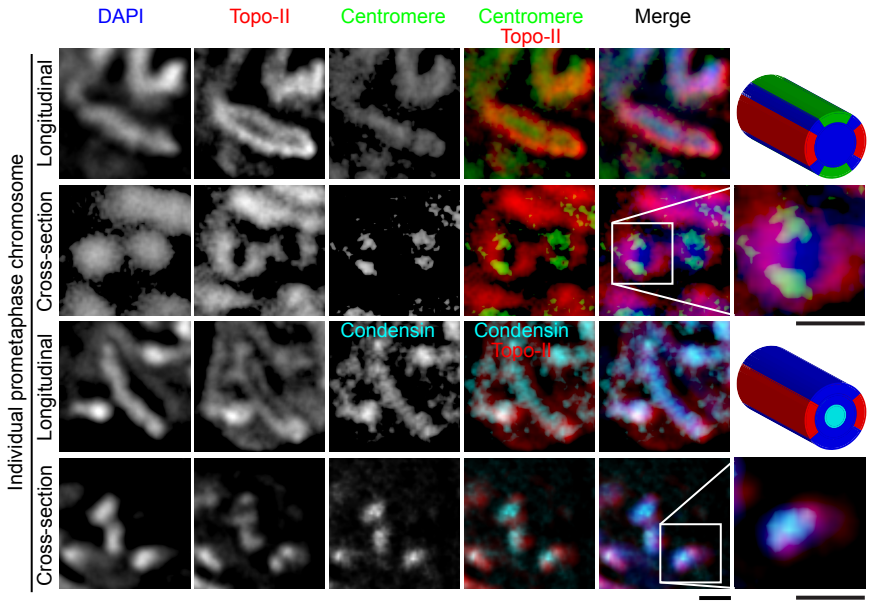

Figure III.7 - Topo-II, condensin and centromere axes are spatially distinct. One-cell early embryos were fixed in methanol and immunostained for prometaphase chromosomes with anti-topo-II antibody in GFP-KNL-2 expressing embryos. Imaris software was used to reconstruct 3-D images from deconvolved Z-stacks (see materials and methods). Montage shows a longitudinal view of a single prometaphase chromosome (first row) and cross-sectional view of a chromosome, a randomly occurring event, (second row). Inset shows zoom-in cross-section view of a chromosome. Prometaphase chromosomes are immunostained with anti-topo-II antibody in GFP-condensin (GFP-CAPG-2) expressing embryos. Montage shows a longitudinal view of a single prometaphase chromosome (third row) and cross-section view of a chromosome (fourth row). Inset shows zoom-in cross-section view of a chromosome. Schematic of single prometaphase chromosome shows a 3-D view of spatial organization of the topo-II, centromere and condensin axes. Blue = DNA, red = topo-II, green = centromere protein and cyan = condensin, scale bar = 1μm.

The condensin complex forms an axis adjacent to or slightly overlapping with centromeres. Analysis of GFP-condensin showed that the timing of condensin axis formation was similar to that of topo-II and centromeres (data not shown). However, I know from previous studies that centromere axis formation is independent from

condensin function (Maddox et al., 2006), indicating that despite the temporal and spatial similarities, these axes are not physically associated. Using a super-resolution analysis method modified from the SHREC technique (Churchman et al., 2005), I determined that the topo-II axis was spatially distinct by 200-300 nm from either centromeres or condensin in metaphase, as expected based on RNAi phenotypic data (Figure III.8A-C).

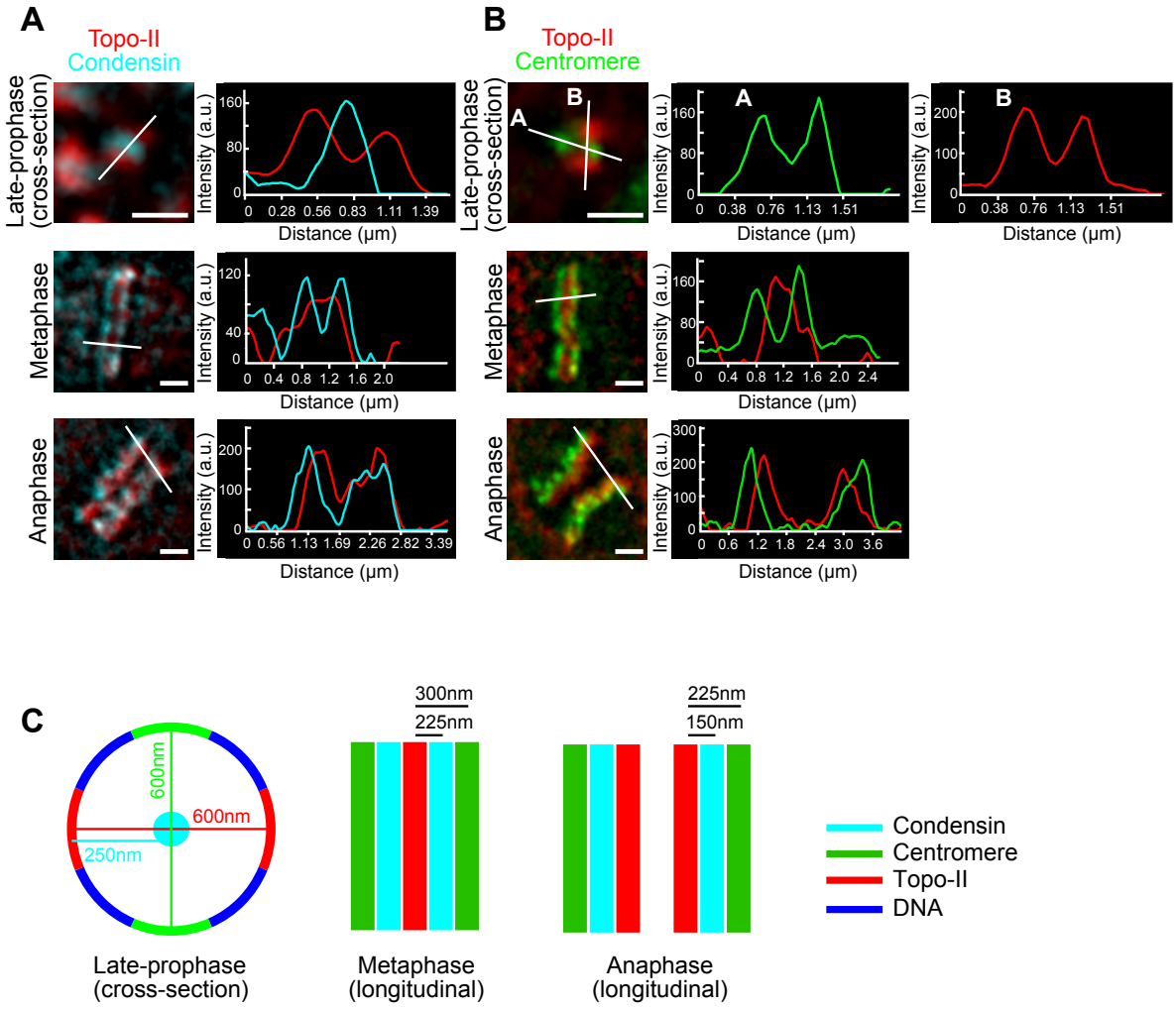

Figure III.8 - Topo-II, condensin and centromere axes are physically distinct. Embryos are immunostained with anti-topo-II antibody in GFP-KNL-2 (late-prophase and metaphase) GFP-CENP-A

(anaphase) and GFP-Condensin (GFP-CAPG-2) expressing worms. A super-resolution analysis method (modified from SHREC, see materials and methods) used to measure the distance between the intensity peaks on the intensity linescans. **(A)** Immunofluorescence of late-prophase chromosome in cross-section view reveals the condensin localizes interior to the chromosome and topo-II localizes 254±11 nm outside (relative to the chromosomes) of the condensin. In metaphase and in anaphase the condensin localizes 224±28 nm and 152±34 nm outside (relative to the chromosomes) of the topo-II, respectively. The n=44 (late-prophase), n=22 (metaphase), n=6 (anaphase). **(B)** Immunofluorescence of late-prophase chromosome reveals the distance between the topo-II-to-topo-II axes and centromere-to-centromere axes are 591±27 and 604±26 nm in cross-section view, respectively. In metaphase and in anaphase the centromere localizes 306±18 nm and 232±25 nm outside (relative to the chromosomes) of the topo-II, respectively. The n=9 (between topo-II axes, late-prophase), n=20 (between centromere axes, late-prophase), n=58 (metaphase), n=19 (anaphase). **(C)** Schematic representation of relative spacing and spatial localization of axes on the chromosome during the mitotic phase; late-prophase (cross-section view) and metaphase and anaphase (longitudinal view). Scale bar = 1μm; the distance = mean ± standard error of the mean.

Therefore, at least three spatially independent protein-based axes act together to mediate mitotic chromosome formation in *C. elegans*.

III.4.6 Graded topo-II depletion shows that topo-II is required stoichiometrically and contributes to axial chromosome compaction.

The role of chromosome axes could be to provide a “ruler”, limiting the dimensions of chromosomes in mitosis. A structural protein (as opposed to an enzyme) would likely be stoichiometrically required for a ruler function. Thus, graded depletion of ruler proteins might generate intermediate phenotypes manifested in abnormal chromosome lengths. By treating animals with RNAi for shorter periods of time, I was able to reproducibly deplete varying amounts of topo-II (Figure III.9).

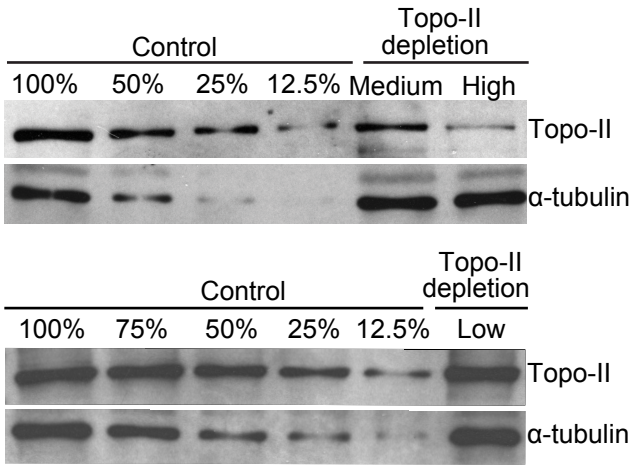

Figure III.9 - Graded topo-II depletion. Topo-II is depleted to various levels (low ~25%, medium ~70% and high ~95% depletion) using the RNAi method (see materials and methods). Depletions are quantified by western blot using anti-topo-II antibody.

Interestingly, the phenotypic outcome correlated strongly with the level of topo-II depletion. Using our chromosome condensation assay, I was able to show that the length of time for prophase aggregation varied consistently with the level of topo-II depletion, possibly indicating a stoichiometric function for topo-II (Figure III.10A-10B). Furthermore, in the medium (70% depleted) and low (25% depleted) topo-II depletion, the chromosomes were 225% and 125% longer, respectively than that of controls just prior to NEBD (Figure III.10C).

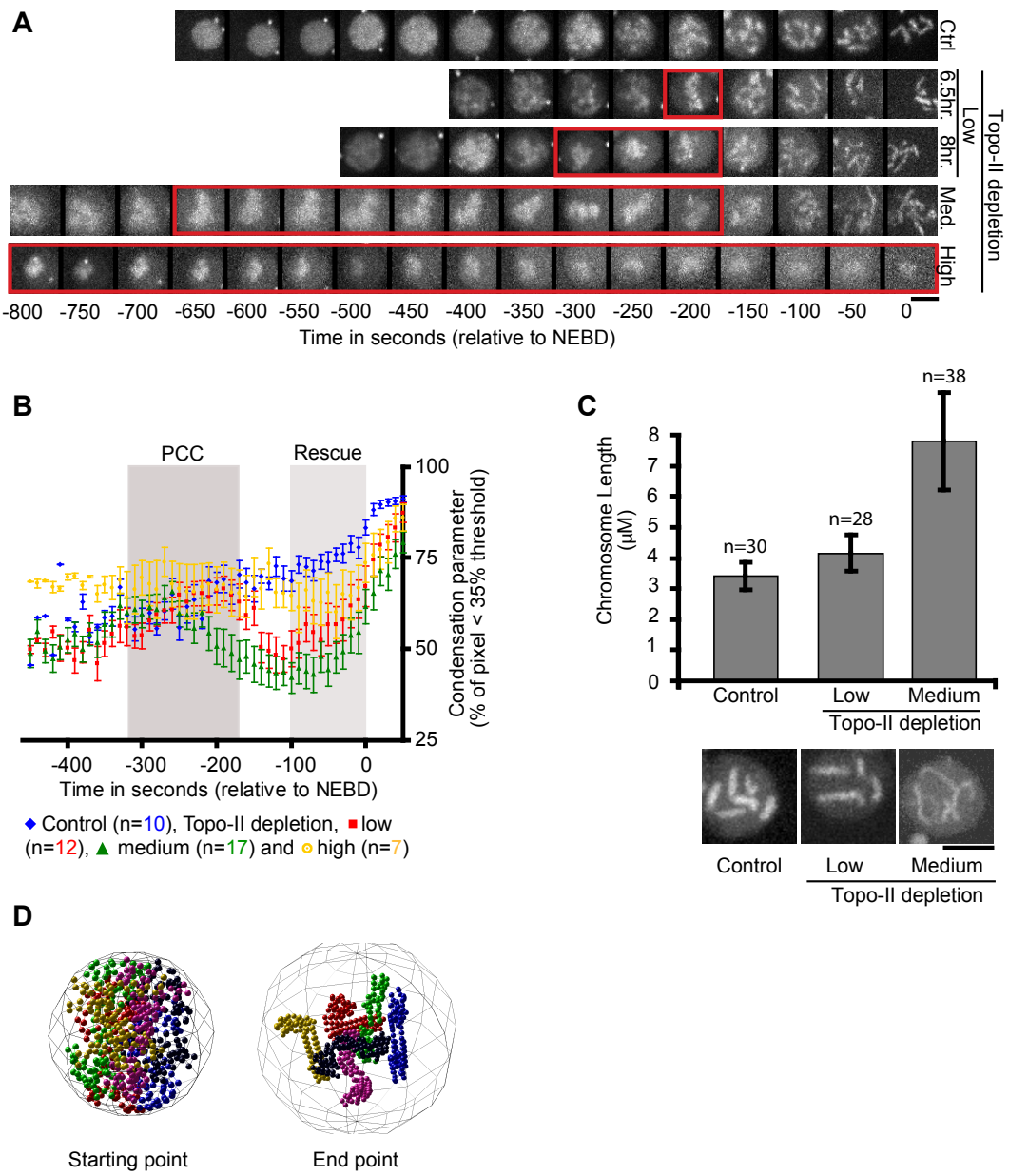

Figure III.10 - Graded topo-II depletion shows that topo-II is required stoichiometrically and contributes to axial chromosome compaction. (A) topo-II is depleted to various levels using RNAi method (see materials and methods), and then imaged; montage is made from the time-lapse movie of control, and graded topo-II depletion (low ≈ 25%, medium ≈ 70% and high ≈ 95% depleted). Red-rectangle boxes in the montage show PCC (prophase chromosome collapse) duration in mitosis;

montage shows higher the topo-II depletion longer the PCC. Scale bar = 5μm. **(B)** Quantitative analysis of graded topo-II depletion using a fluorescence area based assay. The graph is made from low (6.5 and 8 hours depletion), medium and high topo-II depletion. Two shaded regions in the graph are labeled as PCC, from -310s to 180s, and Rescue, from -100s to 0s. The PCC region indicates when chromosome collapse peaks occur, at -250s for medium topo-II depletion (green) and at -200s for low topo-II depletion (red). The Rescue region indicates when chromosomes form after PCC. On high topo-II depletion chromosome remains collapse through the mitosis. N, control = 10, topo-II depletion, low = 12, medium = 17 and high = 7. **(C)** Chromosome axial compaction as determined by measuring the chromosome length in control, low and medium topo-II depletion just prior to NEBD. The graph shows chromosome length in control and in graded topo-II depletion (low and medium). Montage is made from time-lapse images just prior to NEBD, and shows chromosomes in control and low and medium topo-II depletion. Scale bar = 5μm. N, control = 30, topo-II depletion, low = 28, and medium = 38. **(D)** The images show starting point and end point of chromosome simulation of condensation, using two simple local rules as described in the text. Different colors indicate different chromosomes and wireframe sphere is the nucleus.

My results are consistent with a topo-II axis being required for axial chromosome compaction in agreement with a recent study that found topo-II to contribute to axial chromosome compaction (Samejima et al.; 2012) using varying concentrations of topo-II inhibitors.

Often, the complexity and dynamics of biological systems hinder the ability to use intuition for interpretation. In the example of chromosome axis formation, intuition might lead to assuming that a scaffold is preassembled and the chromatin organized relative to it. The temporal staining pattern of topo-II during prophase (Figure III.5A) is inconsistent with this idea. Instead, it suggests that topo-II acts on a local scale to constrain the chromatin and facilitate the assembly of well-formed chromosomes. To test whether the hypothesis of condensation as a local phenomenon is physically plausible, we generated a computational simulation of chromosome condensation. We model the chromatin as a freely jointed chain of rigid beads (Wong et al., 2012). After initialization, we subject the chromatin to two rules which we successively

enforce: Constraining the bending angle of the joints, which could reflect the role of topo-II, and allowing beads to bind to one another more strongly when the axial distance is smaller between beads, which reflects the main condensation activity. We find that these two rules are sufficient to form linear chromosomes (Figure III.10D). Thus, our simulations illustrate that it is not necessary for proteins to generate an independent scaffold, but that action at a local scale is sufficient to establish long-range chromosome axes. Furthermore, axes need not be preassembled, and more likely are generated during the assembly process (Figure III.5A and Figure III.11A-11B). In addition, the simulations suggest that the mechanism of chromosome condensation could limit the stable chromosome length.

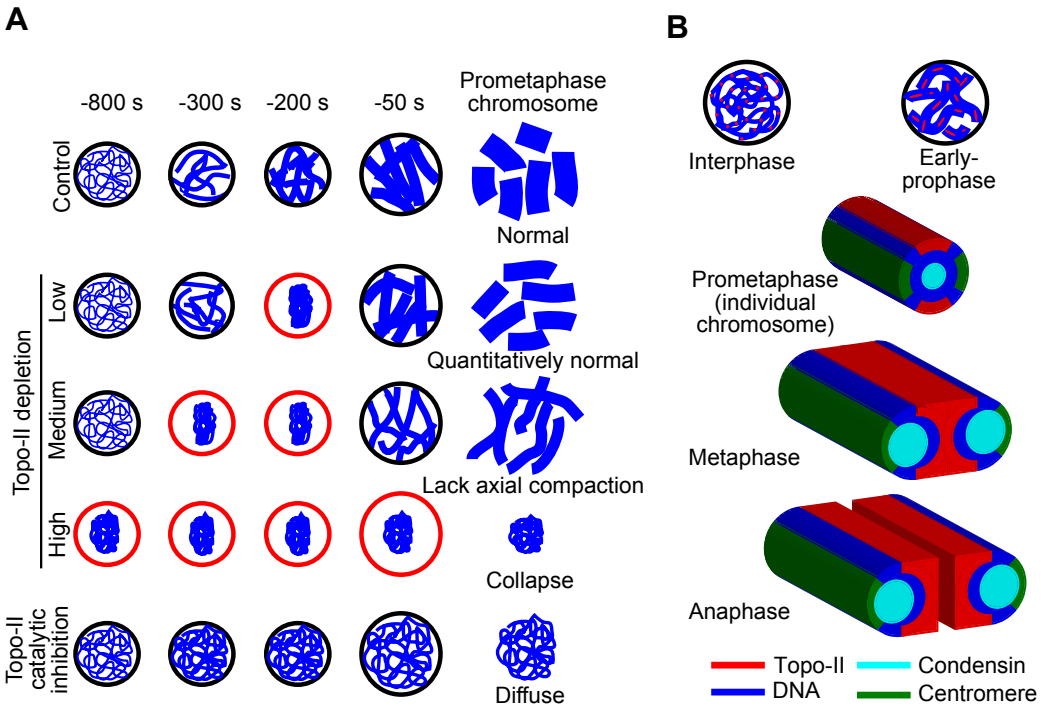

Figure III.11 - Chromosome condensation model. (A) A schematic representation of chromosome condensation defects in mitosis in graded topo-II depletion, low ~25%, medium ~70% and high ~95% depletion, and in topo-II catalytic inhibition. Red-circle nuclei show PCC stages. **(B)** Condensation

model. Three-dimensional schematic representation of topo-II, condensin and centromeres spatial organization during mitosis, prometaphase (individual chromosome), metaphase and anaphase, in *C. elegans.* An interphase nucleus shows topo-II localize as foci whereas in early-prophase a small topo-II structure is being assembled. A linear topo-II axes are shown in prometaphase, metaphase and anaphase.

III.5 Discussion

Studies of mitotic chromosome protein composition revealed roughly equal amounts of histone and non-histone proteins (Adolph et al., 1977; Adolphs et al., 1977; Paulson and Laemmli, 1977). Electron microscopy of histone depleted metaphase chromosomes clearly showed that chromosomes are composed of DNA loops that are anchored to a proteinaceous axis (Paulson and Laemmli, 1977). This proteinaceous axis, referred to as 'the chromosome scaffold', was shown to be rich in topo-II (Earnshaw et al., 1985; Lewis and Laemmli, 1982). Disparate results in various model systems have provided evidence both for and against topo-II scaffold function (Adachi et al., 1991; Andreassen et al., 1997; Christensen et al., 2002; Earnshaw et al., 1985; Hirano and Mitchison, 1993; Hizume et al., 2007; Tavormina et al., 2002). These include localization and dynamics studies as well as loss of function and small molecule inhibition. In sum, the precise role of this major chromosome component has been debated for several decades.

Here I have shown that the *C. elegans* topo-II protein functions as both a structural protein and enzymatic decatenase in mitotic chromosome assembly. Chemical inhibition of topo-II function resulted in a distinct phenotype compared to removal of the protein by RNAi (Figure III.3A-3C). Supporting the hypothesis that topo-II plays a non-enzymatic role in chromosome condensation. Localization studies revealed that topo-II localized to a linear axis that was physically independent from centromere axis formation (Figure III. 5, 7 and Figure III.8A-8C). Based on these results, we generated a computer simulation to reveal that independent, short-range activities confining the bending angles and movement of chromatin was sufficient to generate a linear arrangement (Figure III.10D). Therefore, I propose that topo-II does indeed form a chromosome axis whose activity is critical for chromosome assembly in mitosis. I also note that my data are inconsistent with a topo-II scaffold in the classical sense.

My results confirm the proposed role for topo-II in constraining chromosome length. Previous studies used catalytic inhibitors and thus concluded that length regulation is via decatenase function. To treat *C. elegans* embryos with topo-II inhibitors, I am required to inject drug into the gonads and await fertilization of treated embryos. Due to this technical challenge, I was unable to generate a dose response curve with inhibitors and, therefore, determine if chromosome length regulation was due to catalytic or non-catalytic mechanisms. Generally speaking, inhibition of enzymes (such as kinases) results in a threshold and not graded dose response curve (Thurmond et al., 2001). In graded RNAi depletions of topo-II, I saw a linear response (albeit over a limited dynamic range) in chromosome length relation to topo-II abundance. These data are consistent with a structural based mechanism, however, I can not rule out catalytic function in chromosome length regulation.

My results suggest that the topo-II structural role is independent of catalytic activity, however, it is important to point out that these two functions are almost certainly linked. Future mutational analysis in *C. elegans* may help to better decipher these mechanisms. My analysis should also be carefully considered in the context of the holocentric *C. elegans* chromosomes. Centromeres in *C. elegans* form an axis on each chromatid and it is conceivable (if not probable) that the functions I report for topo-II axis formation are unique to centromere regions of chromosomes. In vertebrates (not holocentric), topo-II is known to be localized to chromosome arms in a punctate manner whereas at centromeres there is a strong concentration. Therefore, my results possibly reveal an important mechanism in chromosome assembly and almost certainly reflect a centromere specific chromatin structure critical for cell division.

Acknowledgments:

I thank Joël Ryan, Abbas Padeganeh, Anne-Marie Ladouceur, as well as all Maddox lab members for helpful discussion and for critical reading of this manuscript. P.S.M. is the Canada Research Chair in Cell Division and Chromosomal Organization. This work was supported by a research grant from the CIHR (MOP-106548).

Chapter IV

Ribonucleotide reductase is involved in nucleosome stability

Ribonucleotide reductase is involved in nucleosome stability.

Rajesh Ranjan[1, 2], and Paul S. Maddox[1-5]

[1]Systems biology option in the graduate program in Molecular Biology, Université de Montréal

[2]Institute for Research in Immunology and Cancer (IRIC), Université de Montréal

[3]Department of Pathology and Cell Biology, Université de Montréal

[4]Current Address: Department of Biology, University of North Carolina at Chapel Hill

[5]To whom correspondence should be addressed

Paul S. Maddox

Department of Biology, University of North Carolina at Chapel Hill

Campus Box #3280

Chapel Hill, NC 27599-3280

USA

IV.1 Abstract

Assembly of mitotic chromosomes is a dynamic event occurring rapidly prior to each cell division. Given the complexity of this process, genetic and biochemical approaches have identified factors involved in the assembly, notably nucleosome assembly factors, histones, the condensin complex and topoisomerase II. Chromosome assembly begins after DNA replication in S-phase as new nucleosomes are assembled on replicated chromatids. Ribonucleotide reductase (RNR) is an enzyme that catalyzes deoxyribonucleotide (dNTP) biosynthesis from ribonucleotides, and hence is required for DNA replication (Jordan and Reichard, 1998; Nordlund and Reichard, 2006). It has no known role in nucleosome stabilization or chromatin assembly. Surprisingly, when RNR was depleted by RNAi in *C. elegans* embryos, the bulk of the nucleosomal GFP-H2B was dissociated (~70%) and remained diffused throughout mitosis. In contrast, inhibition of DNA replication, by depleting DNA polymerase or primase resulted in a quantitatively distinct phenotype, wherein GFP-H2B remained chromatin associated. Chromosomes also formed after replication inhibition using a small molecule inhibitor, methyl methane sulphonate (MMS). These results indicate that independent of its catalytic function, RNR acts to stabilize nucleosomes and fulfills a structural role for chromosome formation. Interestingly, graded RNR depletion showed that it is required stoichiometrically, consistent with a structural role. In sum, I distinguish and define structural and catalytic functions of RNR *in vivo*. I conclude that RNR functions to stabilize nucleosomes, which is a prerequisite step for chromatin assembly and chromosome formation in *C. elegans*.

IV.2 Introduction

DNA replication is a fundamental process for all livings organisms and occurs during S-phase of the cell cycle. DNA biosynthesis requires DNA building blocks called deoxyribonucleotides, dNTPs. Ribonucleotide reductases (RNRs) catalyzes the formation of the DNA building blocks needed for DNA replication as well as for DNA repair; the mechanism involves substitution of the 2'OH of a ribonucleotide with hydrogen (Hofer et al., 2012; Jordan and Reichard, 1998; Nordlund and Reichard, 2006). In the nucleus, dNTP pools need to be precisely balanced, since mutation rates increase when dNTP levels are unbalanced, and RNR is the key player in this homeostasis (Chabes et al., 2003; Kumar et al., 2011; Mathews, 2006; Weinberg et al., 1981). Ribonucleotide reductases are grouped into three major classes based on the mechanisms they use for radical generation (Jordan and Reichard, 1998; Nordlund and Reichard, 2006). In spite of differences in the sequences of the three RNRs classes, basic structural features are largely similar, indicating a common evolutionary origin.

DNA replication coupled with nucleosome assembly is critical for the maintenance of genome stability in all organisms. Nucleosomes consist of ~145 base pairs of DNA wrapped around a core histone octamer composed of one histone $(H3\text{-}H4)_2$ tetramer and two histone H2A-H2B dimers (Luger et al., 1997). Nucleosomes are assembled following DNA replication during S-phase in a process called replication-coupled nucleosome assembly (McKnight and Miller, 1977; Stillman, 1986). Nucleosomes need to be disassembled during replication and reassembled after DNA replication, which is tightly regulated by histone chaperones at different steps (Burgess and Zhang, 2013; Tagami et al., 2004). Several histone chaperones participate in distinct steps of nucleosome assembly such as Nap1 (nucleosome assembly protein 1), which helps to shuttle histones from the cytoplasm to the nucleus (Burgess and Zhang, 2013; Campos et al., 2010; Mosammaparast et al., 2002). NASP (nuclear autoantigenic sperm protein) modulates the supply of histones (Burgess and Zhang, 2013; Cook et al., 2011; Groth et al., 2007). Asf1 (anti-silencing factor 1) regulates the enzymatic activity of histone-modifying enzymes that bridge interactions between

histones and histone-modifying enzymes, while CAF-1 (chromatin assembly factor 1) and Rtt106 support nucleosome assembly (Burgess and Zhang, 2013; Han et al., 2007; Parthun et al., 1996).

It has been shown earlier that there is some interconnection among replication machinery and nucleosome assembly machinery. For instance, histone chaperones have also been shown to interact with the DNA replication machinery to facilitate nucleosome assembly. For example, CAF-1 interacts with PCNA (proliferating cell nuclear antigen), and ASF1 interacts with the replicative helicase MCM in human and interacts with replication factor C of the PCNA loading complex, in budding yeast (Franco et al., 2005; Groth et al., 2007; Moggs et al., 2000; Shibahara and Stillman, 1999; Zhang et al., 2000). The histone chaperone FACT (facilitate chromatin transcription) physically interacts with DNA polymerase and MCM (Tan et al., 2006; Wittmeyer et al., 1999). These results suggest that some of the replication factors could have further role in chromatin organization.

The role of replication-associated proteins in chromatin organization has not yet been elucidated. Here I show that the dNTP biosynthesis enzyme ribonucleotide reductase (RNR) acts as a nucleosome-stabilizing factor in *C. elegans*.

IV.3 Materials and Methods

IV.3.1 RNA interference

In order to perform RNA interference (RNAi), TH32 worms at L4 stage were allowed to feed on bacterial strains that express dsRNA against RNR-2. To achieve RNR depletion, young adult worms were incubated on RNR dsRNA expressing bacterial plates for 48 hours at 20°C before imaging.

IV.3.2 Ribonucleotide reductase (RNR) graded depletion

RNR was depleted to various extents using bacterial feeding for various time periods. To achieve high RNR depletion, young adult worms were incubated on RNR dsRNA expressing bacterial plates for 48 hours at 20°C before imaging. To achieve medium RNR depletion young adult worms were incubated on RNR dsRNA expressing bacterial plates for 24 to 36 hours at 20°C before imaging. To achieve low RNR depletion young adult worms were incubated on RNR dsRNA expressing bacterial plates for 12 hours at 20°C before imaging.

IV.3.3 Drugs

To inhibit catalytic activity of RNR *in vivo*, the small molecule hydroxyurea (HU) was injected into the young adult gonad of TH32 worms at 0.5 mM. Worms were then incubated for 60 to 100 minutes prior to imaging. To inhibit DNA replication *in vivo*, the small molecule methyl methane sulfonate (MMS) was injected into the young adult gonad of TH32 worms at 0.01% concentration. Worms were then incubated for 1 to 5 hours prior to imaging.

IV.3.5 Worm strains

The TH32 *C. elegans* strain, which co-expresses GFP::histone H2B and GFP::γ-tubulin, was used for live and fixed-cell imaging. The N2 strain was used as a wild type and was used for biochemical assays as well as fixed-cell imaging.

IV.3.6 Immunofluorescence

Immunofluorescence was carried out in fixed cell as described in the chapter II (see materials and methods).

IV.3.7 Fixed Imaging

Fixed-cell imaging was performed as described previously in the chapter II (see materials and methods).

IV.3.8 Live Imaging

C. elegans early embryos were live imaged as described earlier in the chapter II (see materials and methods).

IV.3.9 Quantitative area intensity assay

The previously described fluorescence intensity based assay was used for quantitative analysis of chromosome condensation in time-lapse images (Chapter II, Materials and Methods) (Maddox et al., 2006).

IV.3.10 Quantification of nucleosomes

For quantitative analyses of nucleosomes on RNR depleted chromatin, the sum intensity of GFP-H2B signal on metaphase chromosomes were quantified; to sum the total amount of stably assembled GFP-H2B in nucleosomes. Background intensity has subtracted to get absolute intensity coming from nucleosomal GFP-H2B. To do so, maximum intensity projections of z-stacks of nine images were generated for metaphase, and a square of 50x80 pixels fitting to the metaphase was selected as the region of interest (ROI). Then, the sum intensity within the ROI was generated at each metaphase using NIS-elements software, which serves as a quantitative readout of stably assembled nucleosome.

IV.4 Results

IV.4.1 Ribonucleotide reductase depletion results in diffuse GFP-histone H2B in mitosis

Nucleosome assembly is the first step in chromatin assembly. Nucleosome assembly is couple to DNA replication, and, replication factors could play a role in nucleosome assembly. To test this hypothesis, I depleted replication-associated proteins in TH-32 worm embryos expressing GFP-H2B and analyzed condensation by time-lapse imaging. Interestingly, when I depleted RNR-2 (one of the subunits of the ribonucleotide reductase complex), I observed two defects during mitosis. First, GFP-histone H2B remained diffuse in prophase. Second, after nuclear envelope breakdown (NEBD) the GFP-H2B signal decreased to background levels (Figure IV.1A-B). These results suggest that GFP-H2B dissociated from DNA. Hydroxyurea (HU) inhibits RNR catalytic function by scavenging the tyrosyl free radicals, which generate at RNR-2 tyrosine residue at the active site. HU treatment to the worm results in almost similar phenotype as in RNR depletion, which could be due to conformation changes in the RNR complex.

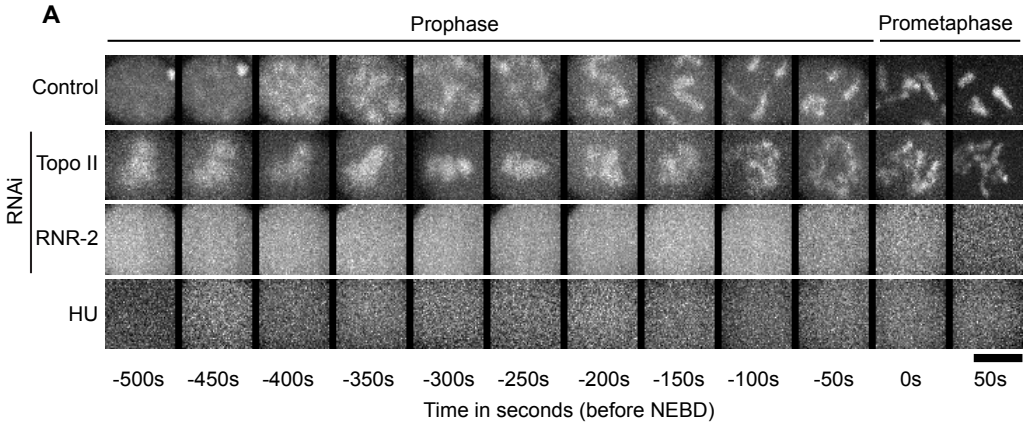

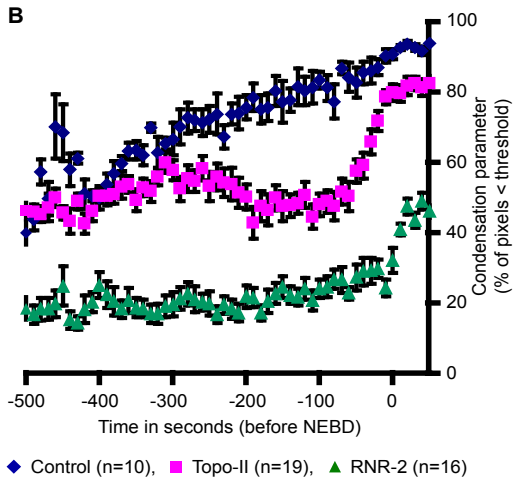

Figure IV.1 – RNR-2 depletion results in diffuse chromatin and GFP-H2B. The TH32 *C. elegans* early embryo (One-cell embryo), co-expressing GFP-Histone H2B and GFP-γ tubulin, was used for time-lapse imaging. **(A)** A 50x50 pixel square region of the male pronucleus is shown as time-lapse movies at 50-second intervals before nuclear envelope break down (NEBD, 0 sec). A montage is made for the control, topo-II depletion (positive control), RNR-2 depletion and RNR catalytic inhibition (by HU). Montages show chromosome condensation profiles at different mitotic stages; prophase (-500s to -50s), NEBD (0s), and prometaphase (50s). Scale bar = 5μm. **(B)** Quantitative analysis of chromosome condensation in mitosis (-500s to 50s) using a fluorescence area based assay (Maddox et al., 2006), in control (black), RNR-2 depleted (green) and topo-II depleted (pink). A flat line in RNR-2 depleted embryos in prophase shows that chromatin remains diffuse. The condensation parameter is a percentage of pixels below 35% threshold intensity. Bar show the standard error of the mean; n, control = 10, topo-II = 19, and RNR-2 = 16.

One could postulate that GFP-H2B is overexpressed in the RNR depletion background, and excess GFP-H2B remains diffuse. To test this hypothesis, I co-

stained chromatin with DAPI and anti-H2B antibody. Anti-H2B antibody did not stain the chromosomes in prometaphase, indicating that histones, or at least histone H2Bs had dissociated from nucleosomes. DAPI staining showed that prophase chromatin remained diffuse after RNR depletion (Figure IV.2). In sum, these results suggest that RNR is required for nucleosome integrity.

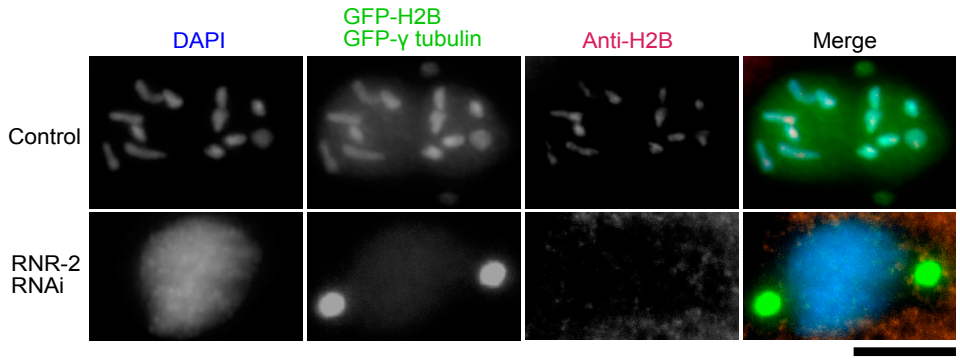

Figure IV.2 – **H2B is not localized to RNR-2 depleted chromosomes.** One-cell C. elegans embryos co-expressing GFP-H2B and GFP-γ-tubulin fixed in methanol, were stained with anti-H2B antibody and DAPI. The prometaphase chromosomes were imaged. Imaris software was used to reconstruct images from deconvolved Z-stacks (see materials and methods). Blue = chromosome, red = histone H2B, and green = GFP-H2B and GFP-gamma tubulin. Scale bar = 1μM.

IV.4.2 DNA replication inhibition results in a quantitatively distinct phenotype

RNR catalyzes the formation of raw material for DNA replication. Therefore, I speculated that RNR depletion could block DNA replication, and, one could argue that the RNR depletion phenotype is the result of DNA replication defects. To test this

hypothesis I inhibited DNA replication by various means; such as RNAi depletion of DNA polymerase alpha (Pol-α), DNA polymerase delta (Pol-δ), primase subunit B (Pri-1) and primase subunit D (Div-1), and with the small molecule inhibitor MMS (methyl methane sulphonate). If the RNR depletion phenotype were due to replication defects then I would expect to see similar phenotypes after inhibiting replication by other means. Surprisingly, in contrast to RNR depleted embryos where chromosomes did not form, unreplicated chromatin assembles and forms chromosomes upon mitotic entry. Similarly, chromosomes formed after inhibiting replication with the small molecule inhibitor MMS (Figure IV.3). To test the extent of replication inhibition, I conducted quantitative analyses of stably associated GFP-H2B in nucleosomes at metaphase and results showed a nearly 75-80% decrease in replication (Figure IV.4B).

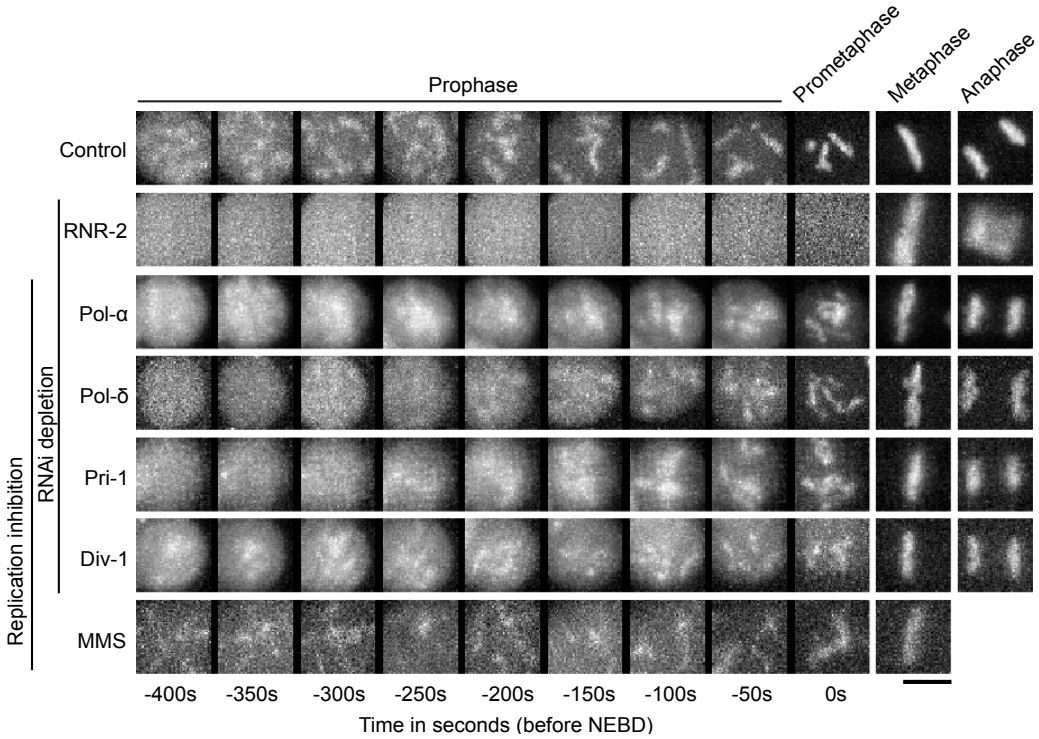

Figure IV.3 – Replication inhibition results in a distinct phenotype than RNR depletion. The TH32 *C. elegans* early embryo (One-cell embryo), co-expressing GFP-Histone H2B and GFP-γ tubulin, is used for time-lapse imaging. A 50x50 pixel square region is cut from male pronucleus time-lapse movies at 50-second intervals before nuclear envelope break down (NEBD, 0 sec). A montage is made for the control, RNR-2 depletion, and Pol-alpha, pol-delta, Pri-1 and Div-1 depletion (inhibits DNA replication), small-molecule inhibition of replication (by MMS). Montages show chromosome condensation profiles at different mitotic stages; prophase (-500s to -50s), prometaphase (0s), metaphase and anaphase. Scale bar = 5μm.

IV.4.3 Graded RNR depletion is consistent with a stoichiometric function

A structural protein would be expected to be required stoichiometrically, assuming a structural protein would stably associate with the target. To test this hypothesis, I quantified stably assembled GFP-H2B in nucleosomes at metaphase, assuming unassembled free GFP-H2B would diffuse following NEBD after RNR depletion. My quantitative analysis showed that the amount of stably associated GFP-H2B in nucleosomes at metaphase successively decreased to ~25% as RNR depletion increased to a maximum (assuming maximum ~75-80% depletion with this method) (Figure IV.4A). Ideally, the level of stable nucleosomes at metaphase should not go below 50%, even if DNA replication is completely inhibited. After replication inhibition, by depleting DNA polymerase or primase subunits, the amount of stable nucleosomes was ~60% (Figure IV.4B).

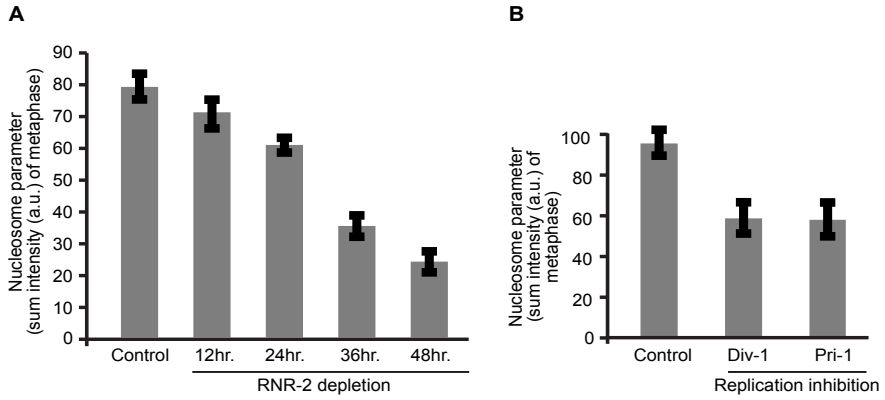

Figure IV.4 – RNR is required stoichiometrically during mitosis. RNR-2 is depleted to various levels using RNAi method (see materials and methods), and then imaged. Quantitative analysis of graded RNR-2 depletion using NIS-element software. Amount of stably assembled GFP-H2B in the nucleosome on metaphase has been determined by measuring the sum intensity of GFP-H2B within the region of interest. Nucleosome parameter is the sum intensity of GFP-H2B on metaphase above background. **(A)** Graph is made from control (n = 16) and RNR-2 depletion for 12 hours. (n = 10), 24 hours. (n = 22), 36 hours. (n = 13) and 48 hours. (n = 11) hours. **(B)** Graph is made from control (n = 6) and replication inhibition, by depleting Div-1 (n = 7) and Pri-1 (n = 6) subunit of DNA polymerase for 48 hours. Error bar is the standard error of the mean.

These results indicate that RNR functions in a stoichiometric fashion, which supports the hypothesis that it is involved in nucleosome stability.

IV.5 Discussion

Ribonucleotide reductase is present in all living organisms and has an evolutionarily conserved catalytic function. The majority of work has demonstrated that it is required for production of deoxyribonucleotides (dNTPs) from ribonucleotides (Hofer et al., 2012; Jordan and Reichard, 1998; Nordlund and Reichard, 2006). Substantial work has showed that RNR is overexpressed during DNA repair to provide the extra dNTPs needed to repair DNA. In prokaryotes, a number of species have more than one ribonucleotide reductase homolog with unknown function. These studies suggest that RNR could have other roles in mitosis (Jordan and Reichard, 1998). In my study, RNR depletion and H2B immunostaining revealed that core histone H2B remained dissociated during mitosis. Quantitative analysis of chromosomes after graded RNR-2 depletion support the hypothesis that it has a structural role in stabilizing nucleosomes. In sum, I have discovered a novel function for ribonucleotide reductase; however, more needs to be done to uncover the underlying molecular mechanism.

Chapter V

Discussion and future perspectives

There is a long-standing question about how genomic DNA is packaged into a mitotic chromosome. It has long been assumed that DNA is wrapped around histones, forming nucleosomes, followed by a nucleosome fiber folded into a 30 nm chromatin fiber before higher order chromatin organization; the “hierarchical helical folding” model. This model suggests that the 30 nm chromatin fiber is folded progressively into ~100 nm and then ~200 nm to form the final ~700 nm chromatids (Belmont and Bruce, 1994; Finch and Klug, 1976; Tumbar et al., 1999). However, the formation of 30 nm chromatin fibers remains controversial because it has never been observed in intact eukaryotic cells (Eltsov et al., 2008; Maeshima et al., 2010; Nishino et al., 2012; Joti et al., 2012).

To visualize mitotic chromosomes, cryoelectron microscopy (cryo-EM) has been used to study and understand the higher-order structure of human mitotic chromosomes. However, this technique did not detect higher order structures such as 30nm chromatin fiber in hydrated human mitotic cells (Eltsov et al., 2008). To visualize mitotic chromosome structure in solution, small-angle X-ray scattering (SAXS) has been performed. In general, scattering at small angles revealed periodic structures within the non-crystalline materials (Roe R-J, 2000). Consistent with observations from Cryo-EM, SAXS did not detect structural features larger than 11nm, indicating that mitotic chromatin compacts with a homogeneous grainy texture of nucleosome fibers (Maeshima et al., 2010; Nishino et al., 2012; Joti et al., 2012). In sum, these results strongly suggest that, the “beads on a string” nucleosomal fiber does not assemble into 30-nm fiber; rather it exists in a highly disordered and integrated state; the “fractal” model.

How nucleosomal fibers transition into mitotic chromosomes remains elusive. Mechanical micromanipulation studies of a vertebrate mitotic chromosome revealed that mitotic chromosomes are a composite network of DNA and proteinaceous links (Michaelis et al., 1997; Poirier and Marko, 2002; Sundin and Varshavsky, 1980). Therefore, a protein based scaffold model has been hypothesized for mitotic chromosome assembly. However, immunostaining of fixed vertebrate chromosomes revealed no evidence for a contiguous protein scaffold; rather an axis-like enrichment

of condensation factors has been observed (Hudson et al., 2008; Maeshima and Laemmli, 2003; Samejima et al., 2012). Also, live cell imaging of fluorescently tagged condensin and topo II does not support an independent protein scaffold models (Christensen et al., 2002; Gerlich et al., 2006; Hirota et al., 2004; Tavormina et al., 2002). Therefore, it is conceivable that this axis-like proteineous structure functions as a broad network of protein-mediated interactions using DNA binding to compact the chromosomes, instead of forming an independent protein-scaffold.

In keeping with this line of thinking, I propose that topo II functions as a local short-range scaffold, which is in contrast to the preassembled protein scaffold hypothesis. It has long been unclear whether topo II performs a scaffold function. It has been assumed that topo II mediated chromosome condensation is due to its decatenation activity, which is essential for the primary organization of chromatin and subsequent condensation process. My *in vivo* studies, using live cell imaging assays and small molecule inhibitors, immunofluorescence, and condensation simulation predict a scaffold function for topo II. My assays distinguish between the enzymatic and structural functions of topo II, however, it is probable that both these functions are tightly linked.

I also investigated how condensin, topo II and CENP-A coordinate their functions during mitotic chromosome assembly in *C. elegans*. My results suggest that these factors function independently with distinct molecular mechanisms. My super-resolution analysis of 3D reconstructed images revealed that topo-II, condensin and CENP-A axes are physically distinct by 75-300 nm on metaphase chromosomes. Also, these factors function in a temporally independent manner during the cell cycle. In sum, I conclude that topo II, condensin and CENP-A function in a spatiotemporally independent fashion, and in a coordinated manner to ensure proper mitotic chromosome assembly and faithful chromosome segregation into daughter cells.

Nucleosomes are the basic structural unit of chromosomes; and must be assembled prior to forming mitotic chromosomes. In my study, I found that a factor that involved in dNTP biosynthesis, ribonucleotide reductase (RNR), is required for nucleosome

stability and subsequent chromatin assembly. Depletion of RNR resulted in almost complete failure of chromatin assembly and the dissociation of GFP-H2Bs from the nucleosomes. This suggests that RNR acts as a nucleosome-stabilizing factor. I studies revealed that some of the replication-associated proteins, RNR and RPA-1, are also involved in mitotic chromosome assembly; however, the underlying molecular mechanism still needs to be investigated.

Chromosome condensation is a highly dynamic process, and must happen in a timely fashion. The lack of chronological sequences could lead to genomic instability. Therefore, condensation factors are temporally regulated during the cell cycle (Bilodeau and Cote, 2012). For instance, condensins are cell cycle regulated; when the cell enters G1, condensins dissociates from chromosomes. During G2 condensin II accumulates throughout the genome, while condensin I remains excluded from the nucleus (Bilodeau and Cote, 2012; Liu et al., 2010). After NEBD, condensin I has access to the chromosome and associates with it. Topo II chromosomal concentration is at its peak in interphase, which subsequently decreases to a minimum following mitosis (Swedlow et al., 1993). These observations indicate that association and dissociation of condensation factors, from the chromosomes, are tightly regulated during mitosis to ensure timely condensation.

My studies revealed that the depletion of a few transmembrane proteins, ABCX-1 and W02D9.2, results in delayed chromosome condensation, which indicates that these proteins probably regulate transport of yet unknown condensation factors required for timely prophase chromosome condensation. Further investigation of these proteins would certainly lead to improving our understanding about prophase chromosome condensation.

Altogether, my studies opened the door to consider that proteins from different families are involved in mitotic chromosome assembly. These proteins seem to function in a spatiotemporally independent manner, with distinct molecular mechanisms.

Future perspectives

In higher eukaryotes mitotic chromosomes compact 10,000- to 20,000-fold, by the ratio of the DNA length to metaphase chromosome length (Belmont, 2002; Li et al., 1998). During each cell cycle, chromosome condensation must be precisely accurate and occur in a timely fashion. Any subtle defect, either in timing of chromosome condensation or physical resolution of the chromosome results in genomic instability, aneuploidy and segregation defects, a leading cause of various disease states including birth defects and cancerous transformation (Cimini et al., 2002; Weaver et al., 2007). Therefore, understanding underlying molecular mechanisms of chromosome condensation would provide new insight into disease mechanisms and would allow the identification of new drug targets.

My *in vivo* screening has revealed several novel proteins required for mitotic chromosome assembly in *C. elegans*. A systematic approach to this problem would offer a powerful way to find more novel functional proteins involved in mitotic chromosome assembly. For instance, Immunoprecipitation with antibodies against known and those yet to be discovered proteins, combined with mass-spectrometry could delineate novel proteins and protein complexes involved in the mitotic chromosome assembly.

Our fluorescence area based quantitative assay reports temporal and relative disturbances in condensation; however, it does not report the state of local DNA compaction. Therefore, in order to define the molecular mechanisms of such a complex dynamic process, we must understand physical states of the intermediates leading to packaged chromosomes. To do so, we need to develop an assay that could quantify the condensation in 3D image pixel (voxel). The GFP-histone fluorescence intensity per voxel would reflect the local density of nucleosomes, and thus the local chromosome compaction. Importantly, the assay can detect multiple condensation states within a single image, which will create a quantitative framework upon which we can generate the molecular mechanisms of chromosome condensation.

In sum, the outcome of these future experiments will serve as a basis for the development of detailed structural and functional interaction maps of key factors. Mapping all protein interactions, both known, and those yet to be discovered would give us a better understanding of underlying molecular mechanisms and architecture of chromosome assembly. With the technological advancements in last two decades and in the next few years it now appears possible that the molecular architecture of chromosomes will soon be understood at a previously unimagined level of detail.

Chapter VI

Bibliography

1. Abe, S., Nagasaka, K., Hirayama, Y., Kozuka-Hata, H., Oyama, M., Aoyagi, Y., Obuse, C., and Hirota, T. (2011). The initial phase of chromosome condensation requires Cdk1-mediated phosphorylation of the CAP-D3 subunit of condensin II. Genes Dev *25*, 863-874.
2. Adachi, Y., Kas, E., and Laemmli, U.K. (1989). Preferential, cooperative binding of DNA topoisomerase II to scaffold-associated regions. EMBO J *8*, 3997-4006.
3. Adachi, Y., Luke, M., and Laemmli, U.K. (1991). Chromosome assembly in vitro: topoisomerase II is required for condensation. Cell *64*, 137-148.
4. Adolph, K.W., Cheng, S.M., and Laemmli, U.K. (1977). Role of nonhistone proteins in metaphase chromosome structure. Cell *12*, 805-816.
5. Adolphs, K.W., Cheng, S.M., Paulson, J.R., and Laemmli, U.K. (1977). Isolation of a protein scaffold from mitotic HeLa cell chromosomes. Proc Natl Acad Sci U S A *74*, 4937-4941.
6. Akey, C.W., and Luger, K. (2003). Histone chaperones and nucleosome assembly. Curr Opin Struct Biol *13*, 6-14.
7. Andersen, J.S., Wilkinson, C.J., Mayor, T., Mortensen, P., Nigg, E.A., and Mann, M. (2003). Proteomic characterization of the human centrosome by protein correlation profiling. Nature *426*, 570-574.
8. Anderson, D.E., Losada, A., Erickson, H.P., and Hirano, T. (2002). Condensin and cohesin display different arm conformations with characteristic hinge angles. J Cell Biol *156*, 419-424.
9. Andreassen, P.R., Lacroix, F.B., and Margolis, R.L. (1997). Chromosomes with two intact axial cores are induced by G2 checkpoint override: evidence that DNA decatenation is not required to template the chromosome structure. J Cell Biol *136*, 29-43.
10. Antonio, C., Ferby, I., Wilhelm, H., Jones, M., Karsenti, E., Nebreda, A.R., and Vernos, I. (2000). Xkid, a chromokinesin required for chromosome alignment on the metaphase plate. Cell *102*, 425-435.

11. Aragon, L., Martinez-Perez, E., and Merkenschlager, M. (2013). Condensin, cohesin and the control of chromatin states. Curr Opin Genet Dev *23*, 204-211.
12. Baxter, J., Sen, N., Martinez, V.L., De Carandini, M.E., Schvartzman, J.B., Diffley, J.F., and Aragon, L. (2011). Positive supercoiling of mitotic DNA drives decatenation by topoisomerase II in eukaryotes. Science *331*, 1328-1332.
13. Belmont, A.S. (2002). Mitotic chromosome scaffold structure: new approaches to an old controversy. Proc Natl Acad Sci U S A *99*, 15855-15857.
14. Berger, J.M., Gamblin, S.J., Harrison, S.C., and Wang, J.C. (1996). Structure and mechanism of DNA topoisomerase II. Nature *379*, 225-232.
15. Berrios, M., Filson, A.J., Blobel, G., and Fisher, P.A. (1983). A 174-kilodalton ATPase/dATPase polypeptide and a glycoprotein of apparently identical molecular weight are common but distinct components of higher eukaryotic nuclear structural protein subfractions. J Biol Chem *258*, 13384-13390.
16. Bohn, A.A., Forsyth, C.S., Kerkvliet, N.I., and Frank, A.A. (1997). Immunologic effects of cocaine in prenatally exposed rats and mice. Toxicol Lett *91*, 47-55.
17. Bojanowski, K., Maniotis, A.J., Plisov, S., Larsen, A.K., and Ingber, D.E. (1998). DNA topoisomerase II can drive changes in higher order chromosome architecture without enzymatically modifying DNA. J Cell Biochem *69*, 127-142.
18. Brinkley, B.R., Zinkowski, R.P., Mollon, W.L., Davis, F.M., Pisegna, M.A., Pershouse, M., and Rao, P.N. (1988). Movement and segregation of kinetochores experimentally detached from mammalian chromosomes. Nature *336*, 251-254.
19. Bulacu, M., and van der Giessen, E. (2007). Molecular-dynamics simulation study of the glass transition in amorphous polymers with

controlled chain stiffness. Phys Rev E Stat Nonlin Soft Matter Phys *76*, 011807.

20. Burgess, R.J., and Zhang, Z. (2013). Histone chaperones in nucleosome assembly and human disease. Nat Struct Mol Biol *20*, 14-22.
21. Campos, E.I., Fillingham, J., Li, G., Zheng, H., Voigt, P., Kuo, W.H., Seepany, H., Gao, Z., Day, L.A., Greenblatt, J.F.*, et al.* (2010). The program for processing newly synthesized histones H3.1 and H4. Nat Struct Mol Biol *17*, 1343-1351.
22. Chabes, A., Georgieva, B., Domkin, V., Zhao, X., Rothstein, R., and Thelander, L. (2003). Survival of DNA damage in yeast directly depends on increased dNTP levels allowed by relaxed feedback inhibition of ribonucleotide reductase. Cell *112*, 391-401.
23. Champoux, J.J., and Dulbecco, R. (1972). An activity from mammalian cells that untwists superhelical DNA--a possible swivel for DNA replication (polyoma-ethidium bromide-mouse-embryo cells-dye binding assay). Proc Natl Acad Sci U S A *69*, 143-146.
24. Charbin, A., Bouchoux, C., and Uhlmann, F. (2014). Condensin aids sister chromatid decatenation by topoisomerase II. Nucleic Acids Res *42*, 340-348.
25. Charron, M., and Hancock, R. (1990). DNA topoisomerase II is required for formation of mitotic chromosomes in Chinese hamster ovary cells: studies using the inhibitor 4'-demethylepipodophyllotoxin 9-(4,6-O-thenylidene-beta-D-glucopyranoside). Biochemistry *29*, 9531-9537.
26. Cheeseman, I.M., Niessen, S., Anderson, S., Hyndman, F., Yates, J.R., 3rd, Oegema, K., and Desai, A. (2004). A conserved protein network controls assembly of the outer kinetochore and its ability to sustain tension. Genes Dev *18*, 2255-2268.
27. Chen, G.L., Yang, L., Rowe, T.C., Halligan, B.D., Tewey, K.M., and Liu, L.F. (1984). Nonintercalative antitumor drugs interfere with the breakage-reunion reaction of mammalian DNA topoisomerase II. J Biol Chem *259*, 13560-13566.

28. Christensen, M.O., Larsen, M.K., Barthelmes, H.U., Hock, R., Andersen, C.L., Kjeldsen, E., Knudsen, B.R., Westergaard, O., Boege, F., and Mielke, C. (2002). Dynamics of human DNA topoisomerases IIalpha and IIbeta in living cells. J Cell Biol *157*, 31-44.
29. Churchman, L.S., Okten, Z., Rock, R.S., Dawson, J.F., and Spudich, J.A. (2005). Single molecule high-resolution colocalization of Cy3 and Cy5 attached to macromolecules measures intramolecular distances through time. Proc Natl Acad Sci U S A *102*, 1419-1423.
30. Cimini, D., Fioravanti, D., Salmon, E.D., and Degrassi, F. (2002). Merotelic kinetochore orientation versus chromosome mono-orientation in the origin of lagging chromosomes in human primary cells. J Cell Sci *115*, 507-515.
31. Cook, A.J., Gurard-Levin, Z.A., Vassias, I., and Almouzni, G. (2011). A specific function for the histone chaperone NASP to fine-tune a reservoir of soluble H3-H4 in the histone supply chain. Mol Cell *44*, 918-927.
32. Cortes, F., Pastor, N., Mateos, S., and Dominguez, I. (2003). Roles of DNA topoisomerases in chromosome segregation and mitosis. Mutat Res *543*, 59-66.
33. Cuvier, O., and Hirano, T. (2003). A role of topoisomerase II in linking DNA replication to chromosome condensation. J Cell Biol *160*, 645-655.
34. Cuylen, S., Metz, J., and Haering, C.H. Condensin structures chromosomal DNA through topological links. Nat Struct Mol Biol *18*, 894-901.
35. Cuylen, S., Metz, J., and Haering, C.H. (2011). Condensin structures chromosomal DNA through topological links. Nat Struct Mol Biol *18*, 894-901.
36. Dejardin, J., and Kingston, R.E. (2009). Purification of proteins associated with specific genomic Loci. Cell *136*, 175-186.
37. Depew, R.E., Liu, L.F., and Wang, J.C. (1978). Interaction between DNA and Escherichia coli protein omega. Formation of a complex between single-stranded DNA and omega protein. J Biol Chem *253*, 511-518.

38. Desai, A., Rybina, S., Muller-Reichert, T., Shevchenko, A., Hyman, A., and Oegema, K. (2003). KNL-1 directs assembly of the microtubule-binding interface of the kinetochore in C. elegans. Genes Dev *17*, 2421-2435.
39. DiNardo, S., Voelkel, K., and Sternglanz, R. (1984). DNA topoisomerase II mutant of Saccharomyces cerevisiae: topoisomerase II is required for segregation of daughter molecules at the termination of DNA replication. Proc Natl Acad Sci U S A *81*, 2616-2620.
40. Dong, K.C., and Berger, J.M. (2007). Structural basis for gate-DNA recognition and bending by type IIA topoisomerases. Nature *450*, 1201-1205.
41. Downes, C.S., Mullinger, A.M., and Johnson, R.T. (1991). Inhibitors of DNA topoisomerase II prevent chromatid separation in mammalian cells but do not prevent exit from mitosis. Proc Natl Acad Sci U S A *88*, 8895-8899.
42. Drpic, D., Barisic, M., Pinheiro, D., and Maiato, H. (2013). Selective tracking of template DNA strands after induction of mitosis with unreplicated genomes (MUGs) in Drosophila S2 cells. Chromosome Res *21*, 329-337.
43. Earnshaw, W.C., Halligan, B., Cooke, C.A., Heck, M.M., and Liu, L.F. (1985). Topoisomerase II is a structural component of mitotic chromosome scaffolds. J Cell Biol *100*, 1706-1715.
44. Earnshaw, W.C., and Heck, M.M. (1985). Localization of topoisomerase II in mitotic chromosomes. J Cell Biol *100*, 1716-1725.
45. Eltsov, M., Maclellan, K.M., Maeshima, K., Frangakis, A.S., and Dubochet, J. (2008). Analysis of cryo-electron microscopy images does not support the existence of 30-nm chromatin fibers in mitotic chromosomes in situ. Proc Natl Acad Sci U S A *105*, 19732-19737.
46. Englund, P.T. (1978). The replication of kinetoplast DNA networks in Crithidia fasciculata. Cell *14*, 157-168.
47. Finch, J.T., and Klug, A. (1976). Solenoidal model for superstructure in chromatin. Proc Natl Acad Sci U S A *73*, 1897-1901.

48. Foster, L.J., De Hoog, C.L., and Mann, M. (2003). Unbiased quantitative proteomics of lipid rafts reveals high specificity for signaling factors. Proc Natl Acad Sci U S A *100*, 5813-5818.
49. Franco, A.A., Lam, W.M., Burgers, P.M., and Kaufman, P.D. (2005). Histone deposition protein Asf1 maintains DNA replisome integrity and interacts with replication factor C. Genes Dev *19*, 1365-1375.
50. Fussner, E., Ching, R.W., and Bazett-Jones, D.P. (2011). Living without 30nm chromatin fibers. Trends Biochem Sci *36*, 1-6.
51. Gasser, S.M., Laroche, T., Falquet, J., Boy de la Tour, E., and Laemmli, U.K. (1986). Metaphase chromosome structure. Involvement of topoisomerase II. J Mol Biol *188*, 613-629.
52. Gassmann, R., Henzing, A.J., and Earnshaw, W.C. (2005). Novel components of human mitotic chromosomes identified by proteomic analysis of the chromosome scaffold fraction. Chromosoma *113*, 385-397.
53. Gassmann, R., Vagnarelli, P., Hudson, D., and Earnshaw, W.C. (2004). Mitotic chromosome formation and the condensin paradox. Exp Cell Res *296*, 35-42.
54. Geiman, T.M., Sankpal, U.T., Robertson, A.K., Chen, Y., Mazumdar, M., Heale, J.T., Schmiesing, J.A., Kim, W., Yokomori, K., Zhao, Y*., et al.* (2004). Isolation and characterization of a novel DNA methyltransferase complex linking DNMT3B with components of the mitotic chromosome condensation machinery. Nucleic Acids Res *32*, 2716-2729.
55. Gellert, M., Mizuuchi, K., O'Dea, M.H., and Nash, H.A. (1976). DNA gyrase: an enzyme that introduces superhelical turns into DNA. Proc Natl Acad Sci U S A *73*, 3872-3876.
56. Gerlich, D., Hirota, T., Koch, B., Peters, J.M., and Ellenberg, J. (2006). Condensin I stabilizes chromosomes mechanically through a dynamic interaction in live cells. Curr Biol *16*, 333-344.
57. Gorbsky, G.J. (1994). Cell cycle progression and chromosome segregation in mammalian cells cultured in the presence of the topoisomerase II

inhibitors ICRF-187 [(+)-1,2-bis(3,5-dioxopiperazinyl-1-yl)propane; ADR-529] and ICRF-159 (Razoxane). Cancer Res *54*, 1042-1048.

58. Green, L.C., Kalitsis, P., Chang, T.M., Cipetic, M., Kim, J.H., Marshall, O., Turnbull, L., Whitchurch, C.B., Vagnarelli, P., Samejima, K.*, et al.* (2012). Contrasting roles of condensin I and condensin II in mitotic chromosome formation. J Cell Sci *125*, 1591-1604.
59. Groth, A., Corpet, A., Cook, A.J., Roche, D., Bartek, J., Lukas, J., and Almouzni, G. (2007). Regulation of replication fork progression through histone supply and demand. Science *318*, 1928-1931.
60. Guacci, V., Koshland, D., and Strunnikov, A. (1997). A direct link between sister chromatid cohesion and chromosome condensation revealed through the analysis of MCD1 in S. cerevisiae. Cell *91*, 47-57.
61. Ha, M.J., Yoon, J., Moon, E., Lee, Y.M., Kim, H.J., and Kim, W. (2000). Assignment of the kinesin family member 4 genes (KIF4A and KIF4B) to human chromosome bands Xq13.1 and 5q33.1 by in situ hybridization. Cytogenet Cell Genet *88*, 41-42.
62. Haering, C.H., Farcas, A.M., Arumugam, P., Metson, J., and Nasmyth, K. (2008). The cohesin ring concatenates sister DNA molecules. Nature *454*, 297-301.
63. Haering, C.H., Lowe, J., Hochwagen, A., and Nasmyth, K. (2002). Molecular architecture of SMC proteins and the yeast cohesin complex. Mol Cell *9*, 773-788.
64. Han, J., Zhou, H., Li, Z., Xu, R.M., and Zhang, Z. (2007). Acetylation of lysine 56 of histone H3 catalyzed by RTT109 and regulated by ASF1 is required for replisome integrity. J Biol Chem *282*, 28587-28596.
65. Hartman, P.S., and Herman, R.K. (1982). Radiation-sensitive mutants of Caenorhabditis elegans. Genetics *102*, 159-178.
66. Hayama, R., Bahng, S., Karasu, M.E., and Marians, K.J. (2013). The MukB-ParC interaction affects the intramolecular, not intermolecular, activities of topoisomerase IV. J Biol Chem *288*, 7653-7661.

67. Hayama, R., and Marians, K.J. (2010). Physical and functional interaction between the condensin MukB and the decatenase topoisomerase IV in Escherichia coli. Proc Natl Acad Sci U S A *107*, 18826-18831.
68. Hirano, T. Condensins: universal organizers of chromosomes with diverse functions. Genes Dev *26*, 1659-1678.
69. Hirano, T. (2005). SMC proteins and chromosome mechanics: from bacteria to humans. Philos Trans R Soc Lond B Biol Sci *360*, 507-514.
70. Hirano, T. (2006). At the heart of the chromosome: SMC proteins in action. Nat Rev Mol Cell Biol *7*, 311-322.
71. Hirano, T. (2010). How to separate entangled sisters: interplay between condensin and decatenase. Proc Natl Acad Sci U S A *107*, 18749-18750.
72. Hirano, T. (2012). Condensins: universal organizers of chromosomes with diverse functions. Genes Dev *26*, 1659-1678.
73. Hirano, T., Kobayashi, R., and Hirano, M. (1997). Condensins, chromosome condensation protein complexes containing XCAP-C, XCAP-E and a Xenopus homolog of the Drosophila Barren protein. Cell *89*, 511-521.
74. Hirano, T., and Mitchison, T.J. (1991). Cell cycle control of higher-order chromatin assembly around naked DNA in vitro. J Cell Biol *115*, 1479-1489.
75. Hirano, T., and Mitchison, T.J. (1993). Topoisomerase II does not play a scaffolding role in the organization of mitotic chromosomes assembled in Xenopus egg extracts. J Cell Biol *120*, 601-612.
76. Hirano, T., and Mitchison, T.J. (1994). A heterodimeric coiled-coil protein required for mitotic chromosome condensation in vitro. Cell *79*, 449-458.
77. Hirota, T., Gerlich, D., Koch, B., Ellenberg, J., and Peters, J.M. (2004). Distinct functions of condensin I and II in mitotic chromosome assembly. J Cell Sci *117*, 6435-6445.
78. Hizume, K., Araki, S., Yoshikawa, K., and Takeyasu, K. (2007). Topoisomerase II, scaffold component, promotes chromatin compaction in vitro in a linker-histone H1-dependent manner. Nucleic Acids Res *35*, 2787-2799.

79. Hizume, K., Yoshimura, S.H., and Takeyasu, K. (2005). Linker histone H1 per se can induce three-dimensional folding of chromatin fiber. Biochemistry *44*, 12978-12989.
80. Hofer, A., Crona, M., Logan, D.T., and Sjoberg, B.M. (2012). DNA building blocks: keeping control of manufacture. Crit Rev Biochem Mol Biol *47*, 50-63.
81. Holway, A.H., Hung, C., and Michael, W.M. (2005). Systematic, RNA-interference-mediated identification of mus-101 modifier genes in Caenorhabditis elegans. Genetics *169*, 1451-1460.
82. Holway, A.H., Kim, S.H., La Volpe, A., and Michael, W.M. (2006). Checkpoint silencing during the DNA damage response in Caenorhabditis elegans embryos. J Cell Biol *172*, 999-1008.
83. Hozier, J., Renz, M., and Nehls, P. (1977). The chromosome fiber: evidence for an ordered superstructure of nucleosomes. Chromosoma *62*, 301-317.
84. Huang, C.E., Milutinovich, M., and Koshland, D. (2005). Rings, bracelet or snaps: fashionable alternatives for Smc complexes. Philos Trans R Soc Lond B Biol Sci *360*, 537-542.
85. Hudson, D.F., Vagnarelli, P., Gassmann, R., and Earnshaw, W.C. (2003). Condensin is required for nonhistone protein assembly and structural integrity of vertebrate mitotic chromosomes. Dev Cell *5*, 323-336.
86. Johnson, M.K., and Wise, D.A. Distribution of kinetochore fragments during mitosis with unreplicated genomes. Cytoskeleton (Hoboken) *67*, 172-177.
87. Jordan, A., and Reichard, P. (1998). Ribonucleotide reductases. Annu Rev Biochem *67*, 71-98.
88. Joti, Y., Hikima, T., Nishino, Y., Kamada, F., Hihara, S., Takata, H., Ishikawa, T., and Maeshima, K. (2012). Chromosomes without a 30-nm chromatin fiber. Nucleus *3*, 404-410.
89. Kavenoff, R., and Ryder, O.A. (1976). Electron microscopy of membrane-associated folded chromosomes of Escherichia coli. Chromosoma *55*, 13-25.

90. Kepert, J.F., Mazurkiewicz, J., Heuvelman, G.L., Toth, K.F., and Rippe, K. (2005). NAP1 modulates binding of linker histone H1 to chromatin and induces an extended chromatin fiber conformation. J Biol Chem *280*, 34063-34072.
91. Kornberg, R.D. (1974). Chromatin structure: a repeating unit of histones and DNA. Science *184*, 868-871.
92. Kornberg, R.D., and Thomas, J.O. (1974). Chromatin structure; oligomers of the histones. Science *184*, 865-868.
93. Kumar, D., Abdulovic, A.L., Viberg, J., Nilsson, A.K., Kunkel, T.A., and Chabes, A. (2011). Mechanisms of mutagenesis in vivo due to imbalanced dNTP pools. Nucleic Acids Res *39*, 1360-1371.
94. Kurasawa, Y., Earnshaw, W.C., Mochizuki, Y., Dohmae, N., and Todokoro, K. (2004). Essential roles of KIF4 and its binding partner PRC1 in organized central spindle midzone formation. EMBO J *23*, 3237-3248.
95. Kwon, M., Morales-Mulia, S., Brust-Mascher, I., Rogers, G.C., Sharp, D.J., and Scholey, J.M. (2004). The chromokinesin, KLP3A, dives mitotic spindle pole separation during prometaphase and anaphase and facilitates chromatid motility. Mol Biol Cell *15*, 219-233.
96. Lai, S.K., Wong, C.H., Lee, Y.P., and Li, H.Y. (2011). Caspase-3-mediated degradation of condensin Cap-H regulates mitotic cell death. Cell Death Differ *18*, 996-1004.
97. Lee, Y.M., and Kim, W. (2003). Association of human kinesin superfamily protein member 4 with BRCA2-associated factor 35. Biochem J *374*, 497-503.
98. Levesque, A.A., and Compton, D.A. (2001). The chromokinesin Kid is necessary for chromosome arm orientation and oscillation, but not congression, on mitotic spindles. J Cell Biol *154*, 1135-1146.
99. Lewis, C.D., and Laemmli, U.K. (1982). Higher order metaphase chromosome structure: evidence for metalloprotein interactions. Cell *29*, 171-181.

100. Li, G., Sudlow, G., and Belmont, A.S. (1998). Interphase cell cycle dynamics of a late-replicating, heterochromatic homogeneously staining region: precise choreography of condensation/decondensation and nuclear positioning. J Cell Biol *140*, 975-989.
101. Li, Y., Stewart, N.K., Berger, A.J., Vos, S., Schoeffler, A.J., Berger, J.M., Chait, B.T., and Oakley, M.G. (2010). Escherichia coli condensin MukB stimulates topoisomerase IV activity by a direct physical interaction. Proc Natl Acad Sci U S A *107*, 18832-18837.
102. Liu, L.F., Depew, R.E., and Wang, J.C. (1976). Knotted single-stranded DNA rings: a novel topological isomer of circular single-stranded DNA formed by treatment with Escherichia coli omega protein. J Mol Biol *106*, 439-452.
103. Liu, W., Tanasa, B., Tyurina, O.V., Zhou, T.Y., Gassmann, R., Liu, W.T., Ohgi, K.A., Benner, C., Garcia-Bassets, I., Aggarwal, A.K.*, et al.* (2010). PHF8 mediates histone H4 lysine 20 demethylation events involved in cell cycle progression. Nature *466*, 508-512.
104. Lohka, M.J., and Masui, Y. (1984). Effects of Ca2+ ions on the formation of metaphase chromosomes and sperm pronuclei in cell-free preparations from unactivated Rana pipiens eggs. Dev Biol *103*, 434-442.
105. Luger, K., Mader, A.W., Richmond, R.K., Sargent, D.F., and Richmond, T.J. (1997). Crystal structure of the nucleosome core particle at 2.8 A resolution. Nature *389*, 251-260.
106. Maddox, P.S., Hyndman, F., Monen, J., Oegema, K., and Desai, A. (2007). Functional genomics identifies a Myb domain-containing protein family required for assembly of CENP-A chromatin. J Cell Biol *176*, 757-763.
107. Maddox, P.S., Oegema, K., Desai, A., and Cheeseman, I.M. (2004). "Holo"er than thou: chromosome segregation and kinetochore function in C. elegans. Chromosome Res *12*, 641-653.
108. Maddox, P.S., Portier, N., Desai, A., and Oegema, K. (2006). Molecular analysis of mitotic chromosome condensation using a quantitative time-

resolved fluorescence microscopy assay. Proc Natl Acad Sci U S A *103*, 15097-15102.

109. Maeshima, K., Hihara, S., and Eltsov, M. (2010). Chromatin structure: does the 30-nm fibre exist in vivo? Curr Opin Cell Biol *22*, 291-297.
110. Mathews, C.K. (2006). DNA precursor metabolism and genomic stability. FASEB J *20*, 1300-1314.
111. Mazumdar, M., and Misteli, T. (2005). Chromokinesins: multitalented players in mitosis. Trends Cell Biol *15*, 349-355.
112. Mazumdar, M., Sundareshan, S., and Misteli, T. (2004). Human chromokinesin KIF4A functions in chromosome condensation and segregation. J Cell Biol *166*, 613-620.
113. McKnight, S.L., and Miller, O.L., Jr. (1977). Electron microscopic analysis of chromatin replication in the cellular blastoderm Drosophila melanogaster embryo. Cell *12*, 795-804.
114. Melters, D.P., Paliulis, L.V., Korf, I.F., and Chan, S.W. Holocentric chromosomes: convergent evolution, meiotic adaptations, and genomic analysis. Chromosome Res *20*, 579-593.
115. Melters, D.P., Paliulis, L.V., Korf, I.F., and Chan, S.W. (2012). Holocentric chromosomes: convergent evolution, meiotic adaptations, and genomic analysis. Chromosome Res *20*, 579-593.
116. Michaelis, C., Ciosk, R., and Nasmyth, K. (1997). Cohesins: chromosomal proteins that prevent premature separation of sister chromatids. Cell *91*, 35-45.
117. Mirkovitch, J., Mirault, M.E., and Laemmli, U.K. (1984). Organization of the higher-order chromatin loop: specific DNA attachment sites on nuclear scaffold. Cell *39*, 223-232.
118. Misra, N.C., and Roberts, D.W. (1975). Inhibition by 4'-demethyl-epipodophyllotoxin 9-(4,6-O-2-thenylidene-beta-D-glucopyranoside) of human lymphoblast cultures in G2 phase of the cell cycle. Cancer Res *35*, 99-105.

119. Moggs, J.G., Grandi, P., Quivy, J.P., Jonsson, Z.O., Hubscher, U., Becker, P.B., and Almouzni, G. (2000). A CAF-1-PCNA-mediated chromatin assembly pathway triggered by sensing DNA damage. Mol Cell Biol *20*, 1206-1218.
120. Morrison, C., Henzing, A.J., Jensen, O.N., Osheroff, N., Dodson, H., Kandels-Lewis, S.E., Adams, R.R., and Earnshaw, W.C. (2002). Proteomic analysis of human metaphase chromosomes reveals topoisomerase II alpha as an Aurora B substrate. Nucleic Acids Res *30*, 5318-5327.
121. Mosammaparast, N., Ewart, C.S., and Pemberton, L.F. (2002). A role for nucleosome assembly protein 1 in the nuclear transport of histones H2A and H2B. EMBO J *21*, 6527-6538.
122. Murray, A.W., and Szostak, J.W. (1985). Chromosome segregation in mitosis and meiosis. Annu Rev Cell Biol *1*, 289-315.
123. Nakano, K., Balint, E., Ashcroft, M., and Vousden, K.H. (2000). A ribonucleotide reductase gene is a transcriptional target of p53 and p73. Oncogene *19*, 4283-4289.
124. Nasmyth, K. (2001). Disseminating the genome: joining, resolving, and separating sister chromatids during mitosis and meiosis. Annu Rev Genet *35*, 673-745.
125. Nasmyth, K. (2011). Cohesin: a catenase with separate entry and exit gates? Nat Cell Biol *13*, 1170-1177.
126. Nasmyth, K., and Haering, C.H. (2005). The structure and function of SMC and kleisin complexes. Annu Rev Biochem *74*, 595-648.
127. Norbury, C., and Nurse, P. (1992). Animal cell cycles and their control. Annu Rev Biochem *61*, 441-470.
128. Nordlund, P., and Reichard, P. (2006). Ribonucleotide reductases. Annu Rev Biochem *75*, 681-706.
129. O'Connell, C.B., Loncarek, J., Hergert, P., Kourtidis, A., Conklin, D.S., and Khodjakov, A. (2008). The spindle assembly checkpoint is satisfied in the absence of interkinetochore tension during mitosis with unreplicated genomes. J Cell Biol *183*, 29-36.

130. O'Connell, C.B., Loncarek, J., Kalab, P., and Khodjakov, A. (2009). Relative contributions of chromatin and kinetochores to mitotic spindle assembly. J Cell Biol *187*, 43-51.
131. Oegema, K., Savoian, M.S., Mitchison, T.J., and Field, C.M. (2000). Functional analysis of a human homologue of the Drosophila actin binding protein anillin suggests a role in cytokinesis. J Cell Biol *150*, 539-552.
132. Oh, S., Hahn, H., Torrey, T.A., Shin, H., Choi, W., Lee, Y.M., Morse, H.C., and Kim, W. (2000). Identification of the human homologue of mouse KIF4, a kinesin superfamily motor protein. Biochim Biophys Acta *1493*, 219-224.
133. Ohta, S., Bukowski-Wills, J.C., Sanchez-Pulido, L., Alves Fde, L., Wood, L., Chen, Z.A., Platani, M., Fischer, L., Hudson, D.F., Ponting, C.P.*, et al.* (2010a). The protein composition of mitotic chromosomes determined using multiclassifier combinatorial proteomics. Cell *142*, 810-821.
134. Ohta, S., Bukowski-Wills, J.C., Wood, L., de Lima Alves, F., Chen, Z., Rappsilber, J., and Earnshaw, W.C. (2010b). Proteomics of isolated mitotic chromosomes identifies the kinetochore protein Ska3/Rama1. Cold Spring Harb Symp Quant Biol *75*, 433-438.
135. Olins, A.L., and Olins, D.E. (1974). Spheroid chromatin units (v bodies). Science *183*, 330-332.
136. Ong, S.E., Blagoev, B., Kratchmarova, I., Kristensen, D.B., Steen, H., Pandey, A., and Mann, M. (2002). Stable isotope labeling by amino acids in cell culture, SILAC, as a simple and accurate approach to expression proteomics. Mol Cell Proteomics *1*, 376-386.
137. Ono, T., Fang, Y., Spector, D.L., and Hirano, T. (2004). Spatial and temporal regulation of Condensins I and II in mitotic chromosome assembly in human cells. Mol Biol Cell *15*, 3296-3308.
138. Ono, T., Losada, A., Hirano, M., Myers, M.P., Neuwald, A.F., and Hirano, T. (2003). Differential contributions of condensin I and condensin II to mitotic chromosome architecture in vertebrate cells. Cell *115*, 109-121.
139. Ono, T., Yamashita, D., and Hirano, T. (2013). Condensin II initiates sister chromatid resolution during S phase. J Cell Biol *200*, 429-441.

140. Oudet, P., Gross-Bellard, M., and Chambon, P. (1975). Electron microscopic and biochemical evidence that chromatin structure is a repeating unit. Cell *4*, 281-300.
141. Parthun, M.R., Widom, J., and Gottschling, D.E. (1996). The major cytoplasmic histone acetyltransferase in yeast: links to chromatin replication and histone metabolism. Cell *87*, 85-94.
142. Patino, B., Posada, M.L., Gonzalez-Jaen, M.T., and Vazquez, C. (1997). The course of pectin degradation by polygalacturonases from Fusarium oxysporum f. sp. radicis lycopersici. Microbios *91*, 47-54.
143. Paulson, J.R., and Laemmli, U.K. (1977). The structure of histone-depleted metaphase chromosomes. Cell *12*, 817-828.
144. Paweletz, N. (2001). Walther Flemming: pioneer of mitosis research. Nat Rev Mol Cell Biol *2*, 72-75.
145. Porter, A.C., and Farr, C.J. (2004). Topoisomerase II: untangling its contribution at the centromere. Chromosome Res *12*, 569-583.
146. Porter, I.M., McClelland, S.E., Khoudoli, G.A., Hunter, C.J., Andersen, J.S., McAinsh, A.D., Blow, J.J., and Swedlow, J.R. (2007). Bod1, a novel kinetochore protein required for chromosome biorientation. J Cell Biol *179*, 187-197.
147. Rattner, J.B., Hendzel, M.J., Furbee, C.S., Muller, M.T., and Bazett-Jones, D.P. (1996). Topoisomerase II alpha is associated with the mammalian centromere in a cell cycle- and species-specific manner and is required for proper centromere/kinetochore structure. J Cell Biol *134*, 1097-1107.
148. Redon, C., Pilch, D., Rogakou, E., Sedelnikova, O., Newrock, K., and Bonner, W. (2002). Histone H2A variants H2AX and H2AZ. Curr Opin Genet Dev *12*, 162-169.
149. Ribeiro, S.A., Gatlin, J.C., Dong, Y., Joglekar, A., Cameron, L., Hudson, D.F., Farr, C.J., McEwen, B.F., Salmon, E.D., Earnshaw, W.C.*, et al.* (2009). Condensin regulates the stiffness of vertebrate centromeres. Mol Biol Cell *20*, 2371-2380.

150. Ris, H., and Kubai, D.F. (1970). Chromosome structure. Annu Rev Genet *4*, 263-294.
151. Robinson, P.J., and Rhodes, D. (2006). Structure of the '30 nm' chromatin fibre: a key role for the linker histone. Curr Opin Struct Biol *16*, 336-343.
152. Roca, J., Ishida, R., Berger, J.M., Andoh, T., and Wang, J.C. (1994). Antitumor bisdioxopiperazines inhibit yeast DNA topoisomerase II by trapping the enzyme in the form of a closed protein clamp. Proc Natl Acad Sci U S A *91*, 1781-1785.
153. Roe R-J. (2000). Methods of X-Ray and Neutron Scattering in Polymer Science.
154. Saitoh, N., Goldberg, I.G., Wood, E.R., and Earnshaw, W.C. (1994). ScII: an abundant chromosome scaffold protein is a member of a family of putative ATPases with an unusual predicted tertiary structure. J Cell Biol *127*, 303-318.
155. Sakaguchi, A., and Kikuchi, A. (2004). Functional compatibility between isoform alpha and beta of type II DNA topoisomerase. J Cell Sci *117*, 1047-1054.
156. Samejima, K., Samejima, I., Vagnarelli, P., Ogawa, H., Vargiu, G., Kelly, D.A., de Lima Alves, F., Kerr, A., Green, L.C., Hudson, D.F.*, et al.* Mitotic chromosomes are compacted laterally by KIF4 and condensin and axially by topoisomerase IIalpha. J Cell Biol *199*, 755-770.
157. Samejima, K., Samejima, I., Vagnarelli, P., Ogawa, H., Vargiu, G., Kelly, D.A., de Lima Alves, F., Kerr, A., Green, L.C., Hudson, D.F.*, et al.* (2012). Mitotic chromosomes are compacted laterally by KIF4 and condensin and axially by topoisomerase IIalpha. J Cell Biol *199*, 755-770.
158. Schalch, T., Duda, S., Sargent, D.F., and Richmond, T.J. (2005). X-ray structure of a tetranucleosome and its implications for the chromatin fibre. Nature *436*, 138-141.
159. Schirmer, E.C., Florens, L., Guan, T., Yates, J.R., 3rd, and Gerace, L. (2003). Nuclear membrane proteins with potential disease links found by subtractive proteomics. Science *301*, 1380-1382.

160. Sekine, Y., Okada, Y., Noda, Y., Kondo, S., Aizawa, H., Takemura, R., and Hirokawa, N. (1994). A novel microtubule-based motor protein (KIF4) for organelle transports, whose expression is regulated developmentally. J Cell Biol *127*, 187-201.
161. Seydoux, G., and Dunn, M.A. (1997). Transcriptionally repressed germ cells lack a subpopulation of phosphorylated RNA polymerase II in early embryos of Caenorhabditis elegans and Drosophila melanogaster. Development *124*, 2191-2201.
162. Shamu, C.E., and Murray, A.W. (1992). Sister chromatid separation in frog egg extracts requires DNA topoisomerase II activity during anaphase. J Cell Biol *117*, 921-934.
163. Shibahara, K., and Stillman, B. (1999). Replication-dependent marking of DNA by PCNA facilitates CAF-1-coupled inheritance of chromatin. Cell *96*, 575-585.
164. Shintomi, K., and Hirano, T. (2011). The relative ratio of condensin I to II determines chromosome shapes. Genes Dev *25*, 1464-1469.
165. Spence, J.M., Phua, H.H., Mills, W., Carpenter, A.J., Porter, A.C., and Farr, C.J. (2007). Depletion of topoisomerase IIalpha leads to shortening of the metaphase interkinetochore distance and abnormal persistence of PICH-coated anaphase threads. J Cell Sci *120*, 3952-3964.
166. Stanvitch, G., and Moore, L.L. (2008). cin-4, a gene with homology to topoisomerase II, is required for centromere resolution by cohesin removal from sister kinetochores during mitosis. Genetics *178*, 83-97.
167. Stillman, B. (1986). Chromatin assembly during SV40 DNA replication in vitro. Cell *45*, 555-565.
168. Sun, J., and Chung, K.F. (1997). Airway inflammation despite loss of bronchial hyper-responsiveness after multiple ozone exposures. Respir Med *91*, 47-55.
169. Swedlow, J.R., and Hirano, T. (2003). The making of the mitotic chromosome: modern insights into classical questions. Mol Cell *11*, 557-569.

170. Swedlow, J.R., Sedat, J.W., and Agard, D.A. (1993). Multiple chromosomal populations of topoisomerase II detected in vivo by time-lapse, three-dimensional wide-field microscopy. Cell *73*, 97-108.
171. Tagami, H., Ray-Gallet, D., Almouzni, G., and Nakatani, Y. (2004). Histone H3.1 and H3.3 complexes mediate nucleosome assembly pathways dependent or independent of DNA synthesis. Cell *116*, 51-61.
172. Takata, H., Uchiyama, S., Nakamura, N., Nakashima, S., Kobayashi, S., Sone, T., Kimura, S., Lahmers, S., Granzier, H., Labeit, S.*, et al.* (2007). A comparative proteome analysis of human metaphase chromosomes isolated from two different cell lines reveals a set of conserved chromosome-associated proteins. Genes Cells *12*, 269-284.
173. Tan, B.C., Chien, C.T., Hirose, S., and Lee, S.C. (2006). Functional cooperation between FACT and MCM helicase facilitates initiation of chromatin DNA replication. EMBO J *25*, 3975-3985.
174. Tanabe, K., Ikegami, Y., Ishida, R., and Andoh, T. (1991). Inhibition of topoisomerase II by antitumor agents bis(2,6-dioxopiperazine) derivatives. Cancer Res *51*, 4903-4908.
175. Tanaka, H., Arakawa, H., Yamaguchi, T., Shiraishi, K., Fukuda, S., Matsui, K., Takei, Y., and Nakamura, Y. (2000). A ribonucleotide reductase gene involved in a p53-dependent cell-cycle checkpoint for DNA damage. Nature *404*, 42-49.
176. Tavormina, P.A., Come, M.G., Hudson, J.R., Mo, Y.Y., Beck, W.T., and Gorbsky, G.J. (2002). Rapid exchange of mammalian topoisomerase II alpha at kinetochores and chromosome arms in mitosis. J Cell Biol *158*, 23-29.
177. Thadani, R., Uhlmann, F., and Heeger, S. (2012). Condensin, chromatin crossbarring and chromosome condensation. Curr Biol *22*, R1012-1021.
178. Theurkauf, W.E., and Hawley, R.S. (1992). Meiotic spindle assembly in Drosophila females: behavior of nonexchange chromosomes and the effects of mutations in the nod kinesin-like protein. J Cell Biol *116*, 1167-1180.

179. Thurmond, R.L., Wadsworth, S.A., Schafer, P.H., Zivin, R.A., and Siekierka, J.J. (2001). Kinetics of small molecule inhibitor binding to p38 kinase. Eur J Biochem *268*, 5747-5754.
180. Tokai, N., Fujimoto-Nishiyama, A., Toyoshima, Y., Yonemura, S., Tsukita, S., Inoue, J., and Yamamota, T. (1996). Kid, a novel kinesin-like DNA binding protein, is localized to chromosomes and the mitotic spindle. EMBO J *15*, 457-467.
181. Tremethick, D.J. (2007). Higher-order structures of chromatin: the elusive 30 nm fiber. Cell *128*, 651-654.
182. Uchiyama, S., Kobayashi, S., Takata, H., Ishihara, T., Hori, N., Higashi, T., Hayashihara, K., Sone, T., Higo, D., Nirasawa, T*., et al.* (2005). Proteome analysis of human metaphase chromosomes. J Biol Chem *280*, 16994-17004.
183. Uemura, T., Ohkura, H., Adachi, Y., Morino, K., Shiozaki, K., and Yanagida, M. (1987). DNA topoisomerase II is required for condensation and separation of mitotic chromosomes in S. pombe. Cell *50*, 917-925.
184. Vernos, I., and Karsenti, E. (1996). Motors involved in spindle assembly and chromosome segregation. Curr Opin Cell Biol *8*, 4-9.
185. Wang, J.C. (1971). Interaction between DNA and an Escherichia coli protein omega. J Mol Biol *55*, 523-533.
186. Wang, J.C. (2002). Cellular roles of DNA topoisomerases: a molecular perspective. Nat Rev Mol Cell Biol *3*, 430-440.
187. Wang, S.Z., and Adler, R. (1995). Chromokinesin: a DNA-binding, kinesin-like nuclear protein. J Cell Biol *128*, 761-768.
188. Weaver, B.A., Silk, A.D., Montagna, C., Verdier-Pinard, P., and Cleveland, D.W. (2007). Aneuploidy acts both oncogenically and as a tumor suppressor. Cancer Cell *11*, 25-36.
189. Weinberg, G., Ullman, B., and Martin, D.W., Jr. (1981). Mutator phenotypes in mammalian cell mutants with distinct biochemical defects and abnormal deoxyribonucleoside triphosphate pools. Proc Natl Acad Sci U S A *78*, 2447-2451.

190. Wise, D.A., and Brinkley, B.R. (1997). Mitosis in cells with unreplicated genomes (MUGs): spindle assembly and behavior of centromere fragments. Cell Motil Cytoskeleton *36*, 291-302.
191. Wittmeyer, J., Joss, L., and Formosa, T. (1999). Spt16 and Pob3 of Saccharomyces cerevisiae form an essential, abundant heterodimer that is nuclear, chromatin-associated, and copurifies with DNA polymerase alpha. Biochemistry *38*, 8961-8971.
192. Wong, H., Marie-Nelly, H., Herbert, S., Carrivain, P., Blanc, H., Koszul, R., Fabre, E., and Zimmer, C. A predictive computational model of the dynamic 3D interphase yeast nucleus. Curr Biol *22*, 1881-1890.
193. Wong, H., Marie-Nelly, H., Herbert, S., Carrivain, P., Blanc, H., Koszul, R., Fabre, E., and Zimmer, C. (2012). A predictive computational model of the dynamic 3D interphase yeast nucleus. Curr Biol *22*, 1881-1890.
194. Wray, W., and Stubblefield, E. (1970). A new method for the rapid isolation of chromosomes, mitotic apparatus, or nuclei from mammalian fibroblasts at near neutral pH. Exp Cell Res *59*, 469-478.
195. Zhang, P., Knowles, B.A., Goldstein, L.S., and Hawley, R.S. (1990). A kinesin-like protein required for distributive chromosome segregation in Drosophila. Cell *62*, 1053-1062.
196. Zhang, Z., Shibahara, K., and Stillman, B. (2000). PCNA connects DNA replication to epigenetic inheritance in yeast. Nature *408*, 221-225.